TU Delft

Rijkswaterstaat
Ministerie van Infrastructuur en Waterstaat

Assessing the Quality of LiDAR Infrastructure Point Clouds

T.A.W. Donkers

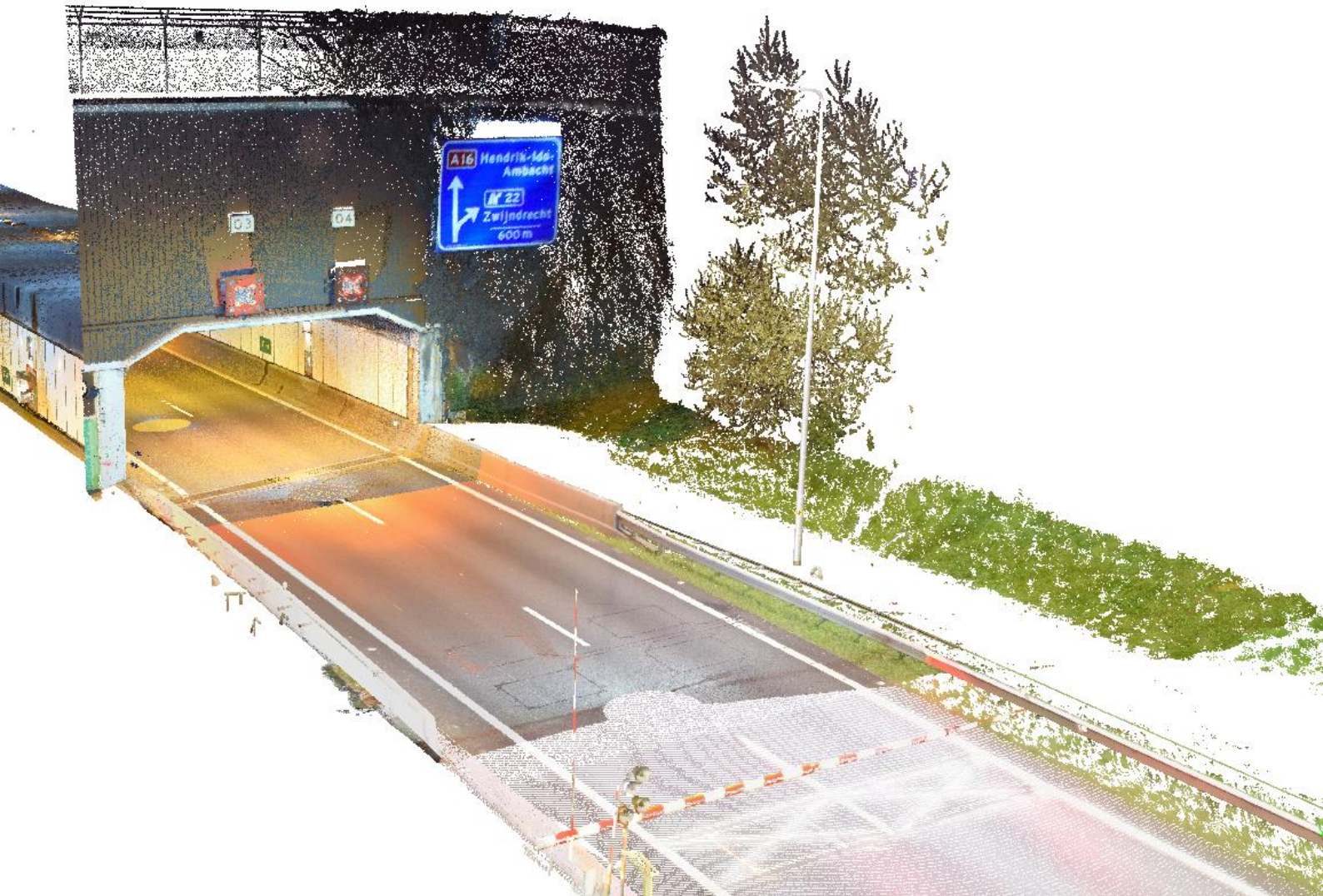

Assessing the Quality of LiDAR Infrastructure Point Clouds

by

T.A.W. Donkers

to obtain the degree of Master of Science
at the Delft University of Technology

Student number: 5409462
Project duration: February 12, 2024 - July 4, 2024

Thesis committee:

Dr. R.C. Lindenbergh	TU Delft, Optical and Laser Remote Sensing
Ir. D.H. van der Heide	Rijkswaterstaat, Advies en Toetsing Geodata
Ing. D. Sparla	Rijkswaterstaat, Advies en Toetsing Geodata
Dr.ir. A.A. Verhagen	TU Delft, Mathematical Geodesy and Positioning

TU Delft

Rijkswaterstaat
Ministerie van Infrastructuur en Waterstaat

Abstract

LIght Detection And Ranging (LiDAR) imaging technology has advanced over the past two decades, being used for applications such as Digital Terrain Models (DTM) and Building Integration Modeling (BIM) integration. The resulting products, point clouds, serve diverse purposes, each demanding specific quality standards. Failing to meet the standards risks rendering the data ineffective or even unusable. Contractors, including Rijkswaterstaat, therefore, specify adherence to set requirements or standards. Current manual sampling for assessing the quality highlights the need for an automated tool.

This study proposes a workflow for automating quality validation of LiDAR infrastructure point clouds. The workflow assesses point cloud quality based on three primary components: coverage, relative accuracy, and absolute accuracy. The methodology includes:

- *Point Cloud Density assessment*: involves analyzing 2D horizontal cells and partial-3D spaces to ensure compliance with density requirements.
- *Overlapping Regions Alignment*: identifies and compares surfaces in overlapping areas of point clouds to determine relative accuracy.
- *Benchmark alignment*: extracts points corresponding to spherical targets, estimates the center coordinates, and evaluates adherence to absolute accuracy standards.

Quality assessments were conducted on static, mobile, and airborne point clouds. The static point cloud analysis revealed non-compliance with density requirements in 2D, with approximately half the points failing to meet standards. In 3D analysis, compliance was observed for 1 m^2 horizontal cells, but individual 1-meter sections often fell short upon closer inspection. These findings highlight the need for tailored quality standards: detailed 3D analysis is crucial for complex environments like tunnels, while road environments can be effectively evaluated in 2D. Relative accuracy assessments for static and mobile datasets showed compliance with scanner specifications, with RMSE values meeting the specified requirements. Absolute accuracy assessments on static point clouds met requirements with minimal deviations in both XY and Z directions.

Recommendations include defining density requirements for different environments, establishing acceptance criteria, and defining allowable deviations for all requirements.

Preface

Completing this master's thesis signifies the end of my student journey. It started with uncertainty about what I wanted to do and ended with a found passion and excitement to start working as a professional. Overall, it has been an experience, during which I not only gained extensive knowledge but also experienced significant personal growth.

I could not have completed my graduation project without the help of several people. First, I want to give a huge thank you to Daan van der Heide and Daisy Sparla from Rijkswaterstaat. The guidance and support over the past months have been incredible. Our weekly meetings and their feedback were essential in shaping the report. I also want to thank my TU Delft supervisors, Roderik Lindenbergh and Sandra Verhagen. The support and advice throughout the entire process, especially in the final months when things became clearer, were invaluable.

Special thanks to Ingrid Alkemade from Rijkswaterstaat for the early conversations about the AHN specifications that helped me get started, and to Jantien Stoter from TU Delft for her guidance. I also appreciate all my colleagues at Rijkswaterstaat who helped out and introduced me to the world of geo-data and point clouds.

Thanks to my friends at TU Delft for keeping my spirits up during the long hours of writing. Finally, I want to thank my family, especially my mom, for their continuous support throughout the process.

I could not have written the report without all of you. I am proud of what I have achieved and hope you enjoy reading it.

Tessy Donkers
Delft, July 2024

Contents

List of Figures

List of Tables

Acronyms

1 Introduction

This study focuses on assessing the quality of LiDAR infrastructure points clouds. The problem is described in Section 1.1. Following that, Section 1.2 presents the research questions. Section 1.3 delimits the boundaries of the study. Finally, to assist readers, Section 1.4 provides a guide to navigating the study.

1.1 Problem Description

Over the past two decades, the acquisition of real-world scenes through 3D scanning has been an advancing practice. One such advanced imaging technology is *LIght Detection And Ranging (LiDAR)*, capable of generating large quantities of 3D data.

1.1.1 Introduction to LiDAR and Point Clouds

LiDAR is a remote sensing technology that employs laser beams to measure distances to objects. The fundamental principle of LiDAR involves emitting a laser signal from a measuring instrument towards a surface. The signal reflects off the surface and is detected once more by the instrument (Vosselman and Maas, 2010). The resulting data product is a densely spaced network of highly accurate points, often called a point cloud. A *Point Cloud* comprises a collection of data points in a three-dimensional coordinate system and represents an object's or scene's external surface (Q. Wang et al., 2020). The points are not limited to the coordinates (x,y,z) but often include other attributes such as color and intensity.

Point clouds are particularly useful in creating representations of the surrounding environment, which can be used to gain insights into the infrastructure and topography. For instance, the Netherlands has demonstrated the potential of the technology through national projects like the Actueel Hoogtebestand Nederland (AHN) and the SpoorInBeeld project by Prorail. The AHN project utilizes point cloud data to create detailed maps of the topography of the Netherlands and aids in various purposes such as assessing the water level and creating specifications for major maintenance, enforcement, and change detection (AHN, 2023b). Similarly, the SpoorInBeeld project from Prorail leverages point cloud data to map the railway network of the Netherlands, which helps in informed planning and efficient maintenance (Prorail, 2022).

1.1.2 3D Geo-datafundament Rijkswaterstaat

Point clouds as data sources are gaining importance within organizations transitioning towards more data-driven environments. For instance, Rijkswaterstaat (RWS), the Dutch governmental agency responsible for managing and maintaining the infrastructure of the Netherlands (including roads, bridges, and waterways), is increasingly becoming a data-driven organization (Rijkswaterstaat, n.d.-a). Currently, the Netherlands is facing an urgent and complex challenge related to replacing and renovating outdated structures. RWS plays a pivotal role in ensuring the safety, accessibility, and sustainability of the vital transportation networks and water resources of the country, where data plays a key role in the process.

Rijkswaterstaat produces a significant amount of geo-data, which almost always occurs in collaboration with other governmental bodies and third parties. However, the ability to share and combine all data is often not feasible due to the lack of standards and agreements regarding the availability and accessibility of geo-data. When dealing with geospatial data, particularly point clouds, differences can arise from various factors such as the software used, exchange formats, coordinate systems, and attributes. Toward that objective, national policy, referred to as the *3D Geo-datafundament*, is currently being developed (Rijkswaterstaat CIV, 2023). With the 3D Geo-datafundament in place, RWS will base the data on the geo-basic registration with added proprietary information instead of separate processes, as shown in Figure 1.1 (right), and expresses ownership of the data.

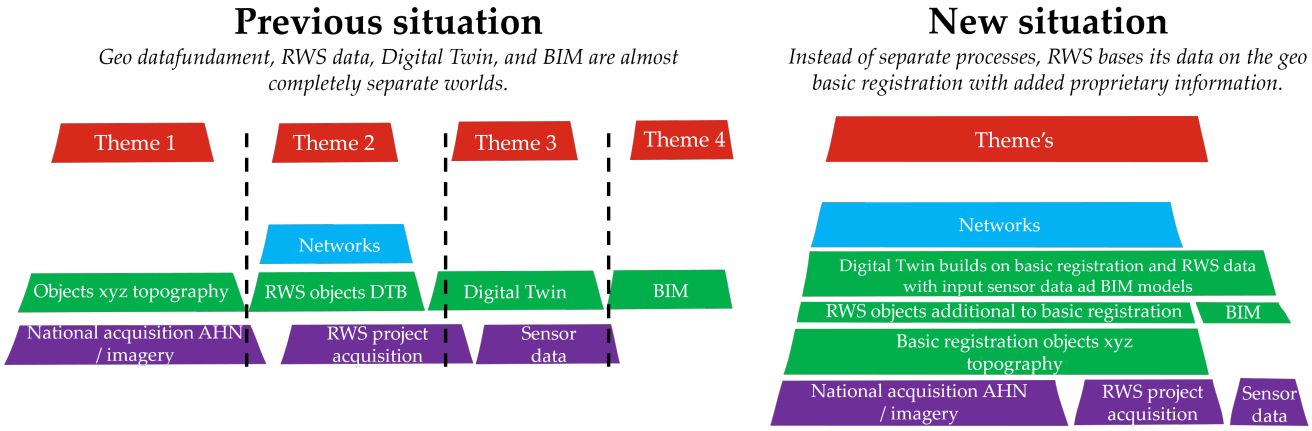

Figure 1.1. *Previous and new situation regarding 3D Geo-datafundament, based on (Rijkswaterstaat CIV, 2023)*

Within the 3D Geo-datafundament, point clouds are incorporated and serve various purposes. Currently, point clouds are utilized for clearance measurements for highway infrastructures (Doorrijprofielen) (DRP), contribute to the Digitaal Topografisch Bestand (DTB), aid in generating Digital Terrain Models (DTM)[1] are integrated into Building Information Modeling (BIM) models, and are fundamental in the development of Digital Twins[2].

[1] DRP, DTB, and DTM are introduced in Subsection 2.3.4.

[2] BIM models and Digital Twins are more commonly associated with building construction rather than infrastructure; therefore will not be incorporated within the study.

1.1.3 Research Objective

Point clouds can be employed for different objectives, each requiring different approaches. For instance, while BIM models need highly detailed point clouds for precise representations, DRP prioritizes clearance height, making the overall details of the point cloud less of interest. The quality requirements, therefore, depend on the intended use of the point cloud, and failing to meet the standards could render the data ineffective or even unusable for the intended purpose. Consequently, contractors (such as RWS) outline expectations and standards that subcontractors are required to meet.

RWS has recently released a set of product requirements outlining requirements for point cloud data, as detailed in (Rijkswaterstaat, 2023). Subcontractors must provide a detailed report justifying how the delivered data aligns with the specified requirements. RWS understands the importance of independently verifying the quality of the delivered data. Currently, data verification by the client is done by manually random sampling the point cloud and assessing adherence to the requirements. A tool which streamlines the verification process and ensures a consistent quality assessment would be beneficial as automating the process saves time and resources and enhances confidence in the accuracy and reliability of the data. Based on the result of the automation tool, the initial requirements, as detailed by RWS, shall be reviewed, and subsequent recommendations will be provided where necessary.

The following research objective is formulated:

The study develops a workflow for automatically validating the overall quality of LiDAR infrastructure point clouds and subsequently provides recommendations regarding the requirements.

1.2 Research Questions

The main question for the study is defined as:

> **How to assess the quality of LiDAR point clouds acquired for infrastructure projects?**

The study will be supported by the following sub-questions:

1. *What components contribute to the quality of a point cloud?*

The term quality is subjective, leading to varied interpretations and interchangeable use of the terms. Therefore, definitions and criteria for evaluating the quality of point clouds must be clearly defined to ensure objectivity.

2. *What quality standards are specified during the acquisition of openly available national point cloud datasets?*

Investigating existing quality standards provides insights regarding the use of quality components within different project objectives. Comparing multiple requirements makes it possible to discern which accuracy criteria are given greater priority or which criteria are not required at all.

3. *What workflow can be used for the assessment of quality components?*

Research is conducted on the existing methods for validating point clouds to gain an understanding of the current state-of-the-art. Subsequently, a workflow is developed to implement the validation of the primary quality components.

4. *What variations are present in the outcomes of the quality assessment for infrastructure point clouds acquired through different acquisition methods?*

Point clouds can be acquired through various methods, leading to distinct end products. The anticipation is that the evaluation of quality components will differ among the methods. Therefore, the approach will be applied to static, mobile, and airborne point clouds wherever possible. Understanding the differences offers an understanding of the constraints and prerequisites of each method.

5. *How should the requirements be specified for point clouds to validate the quality?*

After the validation procedure is implemented, recommendations will be provided for potential new or revised requirements to validate the quality.

1.3 Scope

The study focuses solely on point clouds that include "dry" infrastructure, in particular roads and tunnels[3]. Furthermore, only point clouds produced by LiDAR scanners are investigated. Methods that can also produce point clouds, such as photogrammetry and acoustic echosounders, are not within the scope of the research. Only the most used configurations are investigated, including static, mobile, and airborne. LiDAR point clouds from spaceborne configurations are not considered within the research.

The study focuses on point clouds as a final product delivered to the contractor. However, examining the original data is necessary for some analysis steps. The necessary data has been made exclusively available for the research.

1.4 Reading Guide

Chapter 2 presents background information, which includes an introduction to the laser scanning configurations, definitions, quality standards, state-of-the-art existing methods, and fundamental principles. Chapter 3 introduces the project and gives a description of the point cloud datasets used in the research. Chapter 4 details the methodology for assessing the quality of point clouds. Chapter 5 presents the results for each quality component. Chapter 6 discusses the limitations of the research. Finally, Chapter 7 concludes the research by answering the research questions as presented in Section 1.2. In addition, recommendations for potential future research are provided.

[3] An example of "wet" infrastructure are water-related structures such as dams or canals.

2 Background and State-of-the-art

Section 2.1 introduces laser scanning and point clouds. Section 2.2 establishes the definitions of quality, accuracy, errors, and quality components associated with point clouds. Section 2.3 delves into the quality standards of point clouds at both the European and national levels. Section 2.4 explores current relevant research regarding quality assessment. Finally, Section 2.5 presents fundamental principles used in quality assessments.

2.1 Laser Scanning and Point Clouds

A LiDAR scanner can be deployed in three main configurations: Terrestrial Laser Scanning (TLS), Mobile Laser Scanning (MLS), and Airborne Laser Scanning (ALS) (Benedek et al., 2021). The *error budget*, the allocation of potential errors that can arise throughout the scanning process, depends on the configuration of laser scanning. To interpret the quality, it is paramount to understand the origin of the errors.

2.1.1 Terrestrial Laser Scanning (TLS)

Terrestrial Laser Scanning (TLS) makes use of a stationary LiDAR scanner positioned at a fixed location and mounted on a stable platform like a tripod. Depending on the type of scanning system, the scanner rotates around both the mounting and vertical axis to provide seamless and total coverage of all directions as shown in Figure 2.1[4] (Lemmens, 2011).

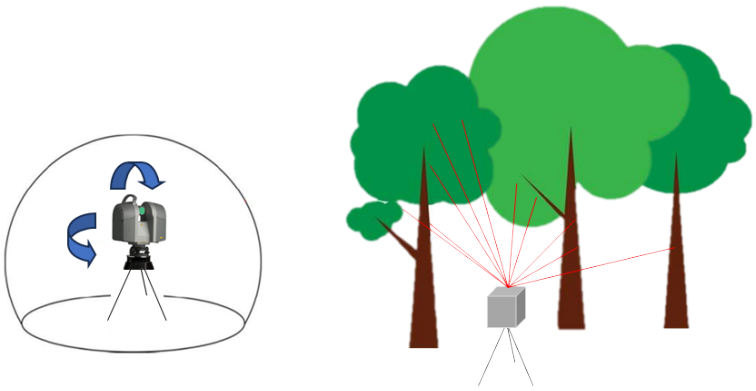

Figure 2.1. *TLS Trimble TX8-II laser scanner (Trimle, n.d.)*

[4]The laser scanners visualized in Figures 2.1, 2.2 and 2.3 are used in the project as mentioned in Chapter 3 Data.

Typically, static configurations are employed only where the environment needs to be surveyed with much detail. This is because the scanning is slow, and multiple stationary setups are needed to cover the desired extent. This is caused by the limitations of the requirement, as the point density gradually decreases further from the scanner set-up due to the attenuation of laser energy over distance and the geometry of the scanner as described in (Lindenbergh et al., 2005)[5]. A dense point cloud will be formed only in close proximity to the scanner. Also, the view of the scanner might be obstructed by objects and will result in occlusion.

Generally, the error budget of laser scanners comprises various factors. One factor is the calibration of the instrument. Environmental conditions (e.g., light, humidity, temperature) and properties of the scanned surface (e.g., roughness, reflectivity, color) also impact LiDAR performance (Soudarissanane et al., 2007). Additionally, errors in data processing, including noise filtering and point cloud registration, as well as inaccuracies in survey control points used for georeferencing, are considerations for ensuring the validity of the point cloud.

With TLS, the instrument remains in a static position, allowing for the use of pre-measured fixed reference points and removing the need to adjust the instrument for motion in free space. Additionally, it is possible to work in a local coordinate system, eliminating the need for transformation within the measurement area.

2.1.2 Mobile Laser Scanning (MLS)

Mobile Laser Scanning (MLS) uses sensors mounted on mobile platforms such as cars, trains, or vessels to capture data while moving. Integrated with the LiDAR sensor is a Global Navigation Satellite System (GNSS) receiver, which provides precise positioning information, and an Inertial Measurement Unit (IMU), which measures the motion and orientation of the scanner in terms of the pitch, roll, and yaw as shown in Figure 2.2 (Vosselman and Maas, 2010). By combining data from both the GNSS receiver and the IMU, the Position and Orientation System (POS) system provides continuous and accurate information about the position and orientation of the MLS system as it moves through the environment. Such information is crucial for geo-referencing the collected LiDAR data and ensuring accuracy and alignment with real-world coordinates.

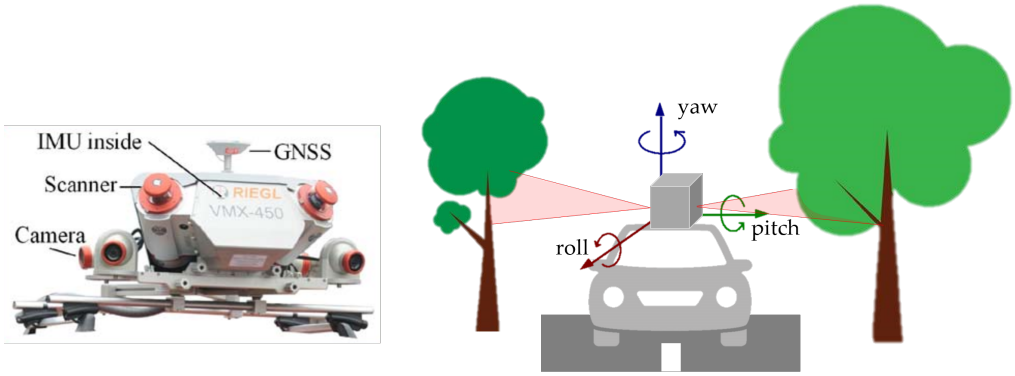

Figure 2.2. *MLS Riegl VMX 450 scanner (Yu et al., 2015)*

[5](Lindenbergh et al., 2005) provides an accuracy analysis of a panoramic high precision laser scanner and introduces the point density as a function of the scan parameters.

Additionally, MLS systems often incorporate cameras to capture visual imagery to complement the LiDAR data. With this surveying technique, point densities of more than 2500 points per m^2 can be achieved, depending on the vehicle speed and the type of scanner.

MLS data quality may vary based on factors such as vehicle speed and trajectory. Motion-induces errors might be caused by the vehicle vibrations, acceleration, and rotations. Objects obstructing the line of sight of the sensor, such as other moving vehicles, can result in incomplete or inaccurate scans. In order to survey the area sufficiently, multiple lanes are therefore driven (if available). By driving in multiple lanes, the survey vehicle covers a wider area during each pass, which results in more data points being collected over the same area than driving in a single lane.

2.1.3 Airborne Laser Scanning (ALS)

Airborne Laser Scanning (ALS) involves mounting sensors on aerial platforms such as aircraft, helicopters, or drones. Aerial surveying is often applied when large-scale point clouds need to be measured, as wide coverage and relatively rapid data acquisition are offered. Similar to MLS, ALS includes a laser scanner, GNSS receiver for accurate positioning, and an IMU for measuring the aircraft's motion and orientation as shown in Figure 2.3 (Vosselman and Maas, 2010).

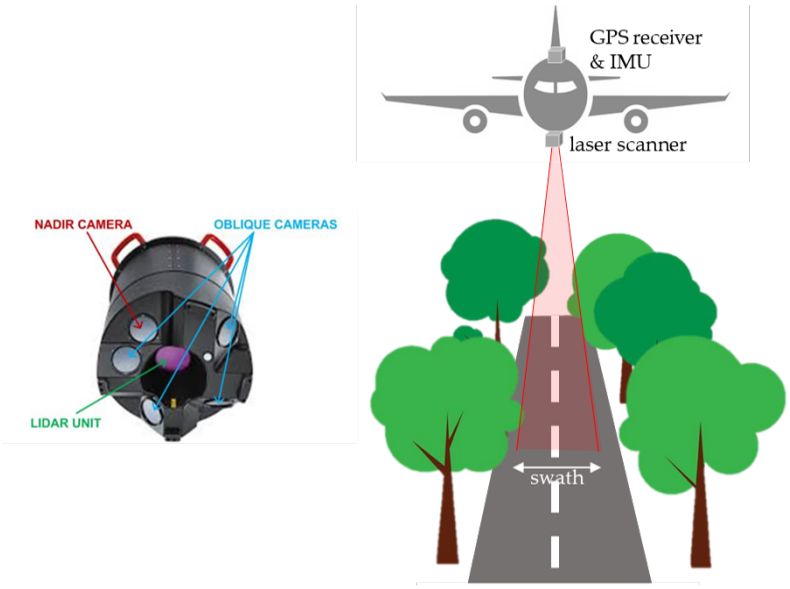

Figure 2.3. *ALS Leica Citymapper (Toschi et al., 2018)*

Significant sources of error are related to the positioning and orientation of the aircraft carrying the equipment. Variations in GNSS positioning and the aircraft's pitch, roll, and yaw can cause disruptions in the positioning of the points. Additionally, environmental conditions and terrain variations add more to the error budget due to the large distance from the surface. Adverse weather conditions such as fog, rain, or snow can degrade laser beam quality and attenuate laser pulses, leading to inaccuracies in range measurements. Terrain relief effects, such as surface elevation and vegetation cover variations, can also impact laser penetration and surface reflection properties.

2.1.4 Point Clouds

The data obtained from scanning with a LiDAR system is typically stored as a *point cloud*. Each point within a point cloud corresponds to a location in a three-dimensional coordinate system, forming a densely spaced network (Q. Wang et al., 2020).

Registration, the alignment of multiple scans to create one seamless point cloud, is an essential process when working with point clouds. Within the study, a distinction is made between point clouds relating to the registration:

- *Composite processed point cloud*: The point cloud is the final product as delivered by the subcontractor. All processed scanned point clouds are registered into one file encapsulating the entirety of the project area as shown in Figure 2.4a (left).
- *Original scanned point cloud*: Consists of the data captured during scanning of each separate scanner. For stationary point clouds, this entails the data collection from each stationary measurement setup, while for mobile point clouds, it involves data acquisition from each lane from distinct vehicles. The original data has not been registered yet and still contains artifacts such as outliers, as shown in Figure 2.4b. Normally, such data is not provided to the contractor.

(a) *Static composite point cloud* (b) *Static original scanned point cloud*

Figure 2.4. *Visualisation composite and original point cloud*

2.2 Definitions

Clear definitions regarding quality and accuracy are established. The following subsection provides a brief introduction to errors of point clouds. Finally, user requirements for evaluating the quality of a point cloud are defined.

2.2.1 Definition of Quality and Accuracy

Since the term quality means different things to different people and is relative to the specific process (Harvey and Green, 1993), it is important to establish clear definitions. When talking in the context of point clouds, the *quality* signifies the degree to which data meets the requirements and can be interpreted as reliable.

It is crucial to acknowledge that measurements contain inaccuracies due to limitations such as the scanner technology. According to (Tiberius et al., 2021), the term *accuracy* refers to the degree to which the result of a measurement matches the correct value or a standard. In other words, the degree of closeness of a measurement to the actual truth.

The term accuracy is commonly categorized into absolute and relative accuracy and is visualized in Figure 2.5. *Absolute accuracy* can be assessed by comparing the data with ground-surveyed checkpoints to reflect the degree of closeness between the obtained result and the actual value. A high absolute accuracy for geospatial data means that the coordinates are very close to their true positions on Earth's surface. *Relative accuracy* in a point cloud assesses the precision of point positions relative to each other or a known reference, irrespective of position, scale, or rotation. High relative accuracy indicates points are correctly positioned relative to the entire dataset (Njambi, 2021). For instance, it ensures consistent distances between points in the point cloud and reality, even with consistent errors in position, scale, or rotation.

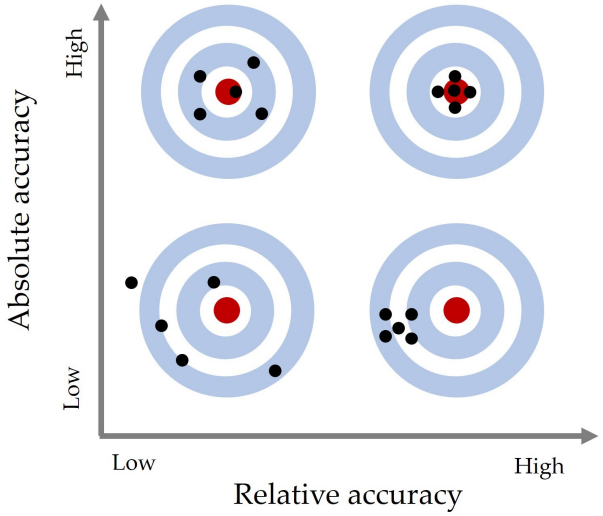

Figure 2.5. *Relative and absolute accuracy*

Accuracy alone does not fully capture the quality of a measurement. *Precision*, on the other hand, accounts for the variation or scatter in the measured values, reflecting the degree of repeatability of measurements under unchanged conditions. Thus, precision focuses on the consistency of measurements within a single dataset or instrument. Precision and relative accuracy are closely related but are not to be used interchangeably.

2.2.2 Introduction to Errors of Point Clouds

Inaccuracies or errors are inevitable within measurements. Errors broadly fall into two categories: random and systematic errors, shown in Figure 2.6. *Random (stochastic) errors* are due to unpredictable factors such as instrument noise and atmospheric conditions and mainly affect the precision. These errors are often referred to as *noise* as they distort the true signal. Random errors appear as erratic random deviations in the spatial arrangement of objects within the point cloud dataset and are not consistently biased.

Systematic errors represent consistent or proportional differences and follow a predictable pattern called *bias*. In contrast, systematic errors primarily affect the accuracy of the measurement (Christodoulides and Christodoulides, 2017). In a point cloud affected by systematic errors, all measurements are consistently shifted or skewed in a particular direction or exhibit a uniform offset from the true positions. Examples of systematic error are due to a laser sensor not being properly calibrated.

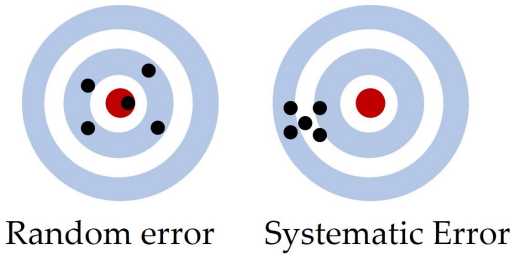

Figure 2.6. *Random and systematic errors*

The *empirical*[6] *standard deviation* (*std*), denoted by σ, is a numerical measure of the overall uncertainty within a dataset, which encompasses both random and systematic errors (Tiberius et al., 2021). In addition, the std can be further categorized into stochastic deviation, which accounts for uncertainty due to random errors, and systematic deviation, which measures consistent biases in measurements. Essentially, the std quantifies the extent to which individual measurements deviate from the mean value. A small std represents little uncertainty and, consequently, a high precision.

[6]Directly from observations rather than from a theoretical model.

2.2.3 User Requirements specific to Point Clouds

Based on, among others, (Kjorsvik, 2022) and (Winiwarter et al., 2021), (van der Heide et al., 2024) have made the distinction between primary and secondary factors that need to be specified as requirements for point clouds. *Primary components* relate and have such an influence on the quality that the type and usage of the point cloud can be altered. In addition, *secondary components* are recognized in the literature. Secondary components either exert less influence on the quality or are unrelated to the quality of a point cloud.

Primary Components

Point clouds can be utilized for diverse purposes, each requiring a unique strategy. Quality considerations vary depending on the specific application. For example, requirements for one application may prioritize certain characteristics over others. The primary components reflect the intended use of the point cloud in terms of quality. Meeting the specified standards is essential to ensure the effectiveness of the intended purpose. The primary components are identified as (1) *consistency* or *coverage*, (2) *relative accuracy*, and (3) *absolute accuracy*.

The term *consistency* refers to the variation of the distribution of points throughout the point cloud. The consistency ensures not only that there are enough points but also that the points are distributed in such a way that objects are complete. For example, an object is considered complete when captured from all angles. The aspect of having enough points, or the distribution of points, falls under the category *coverage*. Coverage does not address the completeness of objects but rather focuses on the distribution of points. Within this study, the **focus is exclusively on the coverage**. The relationship between consistency (the overall concept), coverage (the distribution of points), and density (the metric of coverage) is visualized in Figure 2.7.

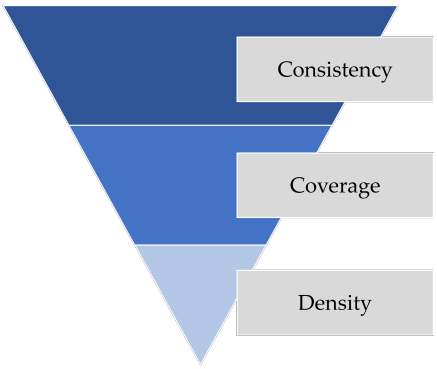

Figure 2.7. *Relation between consistency, coverage, and density*

The distribution of points is commonly defined as the combination of the *spacing* and *density* (Stanley and Laefer, 2021). Spacing refers to the distance between adjacent points within the point clouds and reflects how densely or sparsely points are within the dataset. Density is the concentration of the number of points within a predefined area or volume of the point cloud. Density and spacing are directly related; higher density leads to reduced point cloud spacing, while lower density results in increased spacing. The relation is visualized in Figure 2.8, where a low-density (left) and high-density (right) point cloud is shown.

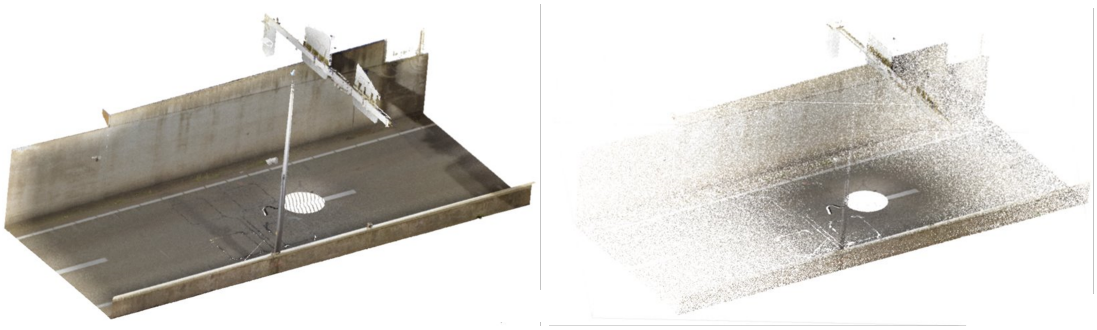

(a) *High point cloud density*
Approximately 50 million points

(b) *Low point cloud density*
Sampled to approximately 0.5 million points

Figure 2.8. *Primary component coverage*

The distinction can be made between local and global density (Wu et al., 2011). The *local density* refers to how dense data points are distributed within a specific region, and *global density* is the overall distribution across the dataset. Typically, lower point densities are observed at greater (travel) distances, resulting in significant gaps at the edges of the measurement setup. This leads to uncertainty in local point density, which incorrectly adjusts global consistency. The density requirement is commonly based on the areal perspective as $points/m^2$.

Relative accuracy refers to the measure of local differences within a point cloud. The most popular way to evaluate the relative accuracy is by measuring how well data points align from different acquisitions[7]. The concept is illustrated in Figure 2.9, where two conceptual point clouds are shown in an overlapping area. The colors (blue and red) illustrate point clouds originating from different measurement setups. Both clouds align perfectly when the relative accuracy is zero (left). When the relative accuracy between two point clouds at the same location is greater than zero, a shift can be seen between the two point clouds (right).

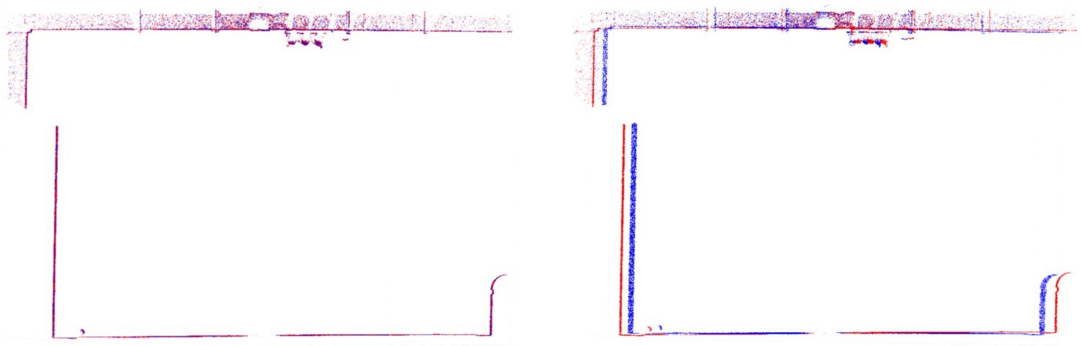

(a) *High relative accuracy*

(b) *Low relative accuracy*

Figure 2.9. *Primary component relative accuracy*

The images depict a cross-section featuring two point clouds from different scanners, one represented in blue and the other in red.

[7]Other methods may be used to evaluate the relative accuracy, such as the use of targets as demonstrated in (Kim et al., 2022) and (Kregar et al., 2013). The method to evaluate the relative accuracy within overlapping regions is incorporated within Rijkswaterstaat.

Absolute accuracy for point clouds refers to the measure of how closely features of the point cloud correspond to the true geographic positions or elevations. Typical values for the maximum absolute accuracy range from 0.05 meters to 0.15 meters. The quality requirement is strongly influenced by the type of acquisition platform and scanner and the various error sources. The combination of errors introduces a variation between the determined coordinates and the real world.

Figure 2.10 visualizes a point cloud of highway projected onto an aerial background with a high (left) and low (right) absolute accuracy.

(a) *High absolute accuracy* (b) *Low absolute accuracy*

Figure 2.10. *Primary component absolute accuracy*

Left image shows the highway projected onto an aerial background at the correct location. Right image shows the highway with low absolute accuracy, where the correct location is indicated by the red dashed lines.

In discussions regarding point clouds, accuracy is typically divided into two components: the accuracy of the horizontal dimension across the XY-plane (referred to as *planimetric accuracy*) and the accuracy of the height component along the Z-axis (known as *vertical accuracy*).

Secondary Components

Secondary components, while important, do not wield enough influence to fundamentally alter the type and usage of the point cloud. When formulating requirements for the point cloud, the following factors must, at the very least, be considered. If such factors are not explicitly outlined in the user requirements, subcontractors may not deem it necessary to provide them and may, therefore, omit them from the deliverables.

- *Calibration*: Includes information such as when the scanner must last be calibrated and the specified calibration method.
- *Environmental impact*: Involves documenting environmental conditions during data acquisition, including factors like weather conditions, presence of water, snow, or vegetation. Requirements may be the presence of leaves allowed on trees and the maximum vegetation height.
- *Coordinate system*: Specification for the desired coordinate system and transformations. Coordinate system preferences vary between countries. Additionally, requirements regarding the placement of decimal separators should be clearly defined.
- *Noise and outliers*: Maximum amount of outliers allowed in the data where an *outlier* is a point that significantly differs from other surrounding observations.
- *Gaps*: Maximum amount of gaps allowed in the data. Minimizing gaps is essential for obtaining a complete and accurate representation of the surveyed area. Failure to address gaps can result in incomplete or misleading analyses and interpretations. Exemptions might be considered in certain circumstances, such as areas covered by water bodies.
- *Red Green Blue (RGB) coloring*: Specification of the color encoding scheme and encoder parameters (bit depth).
- *Classifications*: Entails the class definitions (classes that need to be identified, including the method of labeling), accuracy requirement (how much needs to be correctly classified), and methodology (the algorithm used for classification).
- *Data removal*: Details the criteria and method for removing outlying data points from the dataset.

2.3 Quality Standards for Point Clouds

The following sections delve into the quality standards for point clouds. A distinction is made between European policy standards, quality requirements of countries within Europe, Dutch quality requirements, and finally, quality standards from Rijkswaterstaat. This progression of quality standards is visualized in Figure 2.11.

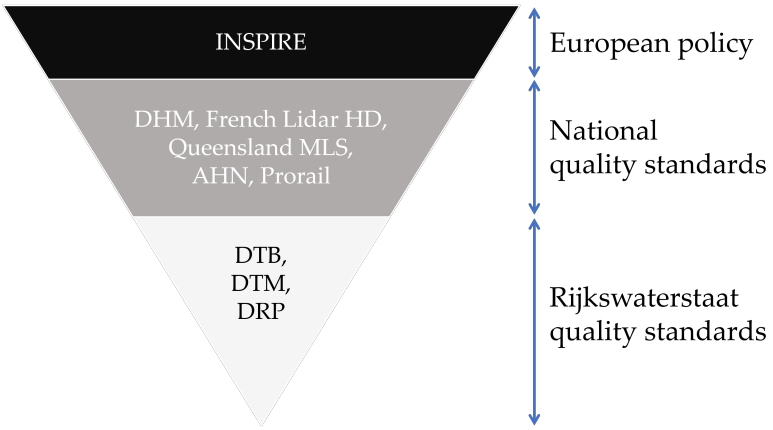

Figure 2.11. *Progression of Quality Standards*

2.3.1 European Policy Standard

The examination of directives at the European level is important due to the function of the European Union as a central authority capable of streamlining regulations and standards across its member states. The European directives, therefore, can directly influence underlying data collection layers, such as in the Netherlands. The INfrastructure for SPatial Information (INSPIRE) directive, published in 2007, stands out as a key framework directing the governance of geospatial data across member states.

The data collected at a European scale relating to point clouds often consists of global DTMs. Examining the technical guidelines for data specification on elevation (INSPIRE, 2024) reveals descriptions of quality criteria and their associated measurements that should be assessed. The categorization is made between:

- *Completeness*: Evaluates the commission (excess) and omission (absence) of data from the dataset as described by the scope.
- *Logical consistency*: Divided into conceptual consistency (how well data aligns with the conceptual rules and definitions established; an example is checking whether features are representing their intended use), domain consistency (validity of attribute values), format consistency (whether the data follows specified format rules), and topological consistency (spatial relationships between features; an example is verifying the continuance of features such as river flows without inconsistencies in its path).
- *Positional accuracy*: Assesses the absolute or external accuracy (defined as the closeness of reported coordinate values to values accepted as or being true) and the gridded data-position accuracy (defined as the gridded data-position accepted as being true).

The emphasis on completeness within the quality criteria is interesting. The aspect being within the primary focus contrasts with the earlier understanding, where it was considered a secondary component (equivalent to data removal). Rather than falling under quality requirements as expected, component consistency falls under data capture. The document discusses recommendations for grid spacing in relation to vertical accuracy, consistency rules, and the relationship between contour equidistance and the scale of mapping.

In the provided quality criteria, the term relative accuracy is noticeably absent. However, looking at the subdivisions within logical consistency, the term can be interpreted as the relative accuracy but on a larger scale. Additionally, the terminology "external accuracy" is noteworthy as the term is not common to use for absolute accuracy.

Minimum data quality requirements for the theme elevation are not specified. INSPIRE only specifies that elevation data provided through INSPIRE should have the best spatial, temporal, and thematic accuracy available.

2.3.2 Quality Requirements of Open National Point Clouds in Europe

Several countries within Europe have established national point cloud datasets that are publicly available. Subsequent sections explore the quality requirements of datasets from selected countries. The products that are investigated are:

- Danish Height Model (DHM)
- French Lidar HD
- Queensland Mobile Laser Scanning Technical Guideline

Danish Height Model (DHM)

The Danish Height Model (DHM) consists of several data sets developed from laser scanning of Denmark using airplanes. Starting in 2018, the DHM products are updated once every five years, dividing the country into 5 blocks. According to (Danish Agency for Data Supply and Efficiency, 2022), the latest DHM is considered the best national height model of the world, comprising over 415 billion point data, which are used to map height differences for terrains and areas in a 0.4-meter grid for the entire country.

According to the specifications outlined in (Danish Agency for Data Supply and Efficiency, 2020), the geometric quality of the point cloud is defined by precision and accuracy.

- *Precision*: Also referred to as a measure of internal geometric consistency, it describes the degree to which data from one flight line aligns with data from other flight lines and the consistency of measurements for the same object. The precision is subdivided into a horizontal and vertical component and between the intra- (within the same flight line) and inter- (different flight lines) flight lines. Vertical precision is evaluated by comparing points on surfaces of roads from within overlapping flight lines, whereas horizontal precision is assessed by comparing points on the roofs of gable buildings. Table 2.1 presents the precision requirements.

Precision (RMS)	Intra-flight line (cm)	Inter-flight line (cm)
Vertical	3	5
Horizontal	3	7

Table 2.1. *Precision requirements of DHM according to (Danish Agency for Data Supply and Efficiency, 2020)*

- *Accuracy*: Explains the extent to which the entire point cloud aligns with known real-world coordinates. Relies on *Ground Control Points (GCP)* for vertical and horizontal accuracy. Vertical accuracy is achieved using GCPs such as manhole covers and road markings. Horizontal accuracy is assessed by using the roofridges of rectangular houses with gable roofs. The DHM point cloud is ensured to align with the available GCPs with a vertical accuracy not exceeding 6 cm RMS (1σ) and horizontal accuracy not exceeding 15 cm RMS (1σ).

Other requirements are specified, such as the reference system. Classification is performed on a best-effort basis without guarantees concerning the accuracy of the assigned classes. Coloring, if available, is not subjected to any requirements.

The Root Mean Square Error (RMSE) is employed as a metric for assessing accuracy. Concept is also included in the INSPIRE documentation. However, while the DHM refers to it as RMS, it is more likely to refer to RMSE based on contextual usage.

Note the interchangeable terminology within the document. For instance, it is opted to use the term ”geometric quality” instead of simply ”quality”. Additionally, the use of ”precision” instead of ”relative accuracy” is noteworthy.

French Lidar HD

France has a national product called the LidaR HD (for High Density) which maps the French territory. The acquisitions and productions are spread over 5 years according to the priority needs expressed by the national and local sponsors of the project and their uses. The point cloud products are derived from aerial LiDAR acquisitions with a density of at least 10 points per m^2 and 5 points per m^2 above 3200-meter altitudes.

According to (IGN, 2023), the quality requirements for the point cloud products are:

- *Accuracy*: maximum RMSE of 50 cm in horizontal positioning and 10 cm in vertical.
- *Relative accuracy*: maximum RMSE of 25 cm in horizontal positioning and 5 cm in vertical.

Furthermore, the checks that need to be performed on raw point clouds are the completeness, the effective density, the geometric such as the presence of artifacts and noise, and finally the conformity of the cloud’s planimetric and height accuracy.

Queensland Mobile Laser Scanning Technical Guideline

Queensland has written a technical guideline that aims to provide consistent terminology and understanding to the MLS capture for the Department of Transport and Main Roads Queensland and industry. While not an official standard, the technical guideline in (Department of Transport and Main Roads State of Queensland, 2023) is developed with the aim to standardize common terms and methods currently being adopted in the industry. As many national point cloud products are currently surveyed primarily through airborne methods (like the DHM and French Lidar HD), the technical guideline from Queensland may provide new insights specifically regarding MLS.

In terms of quality, the following is mentioned: The delivered point cloud must meet a sufficient quality standard to enable accurate identification of features at the desired level of accuracy.

Other specifications related to quality are:

- *Density*: The department requires the density of the delivered point cloud to be adequate so that points, lines, and surfaces meet the accuracy requirements specified. The point density must be provided for specified horizontal and vertical surfaces (e.g., directly under, above, left of, and right of the scanner and on road level, scanner level, and 5 meters above)
- *Survey uncertainty*: Divided into horizontal and vertical. Uses checkpoints throughout the project area where their shift expresses the uncertainty.
- *Relative uncertainty*: Divided into horizontal and vertical. Uses check sites throughout the project area.

The density specification is intriguing because it deviates from the earlier density specifications for airborne-based point clouds. Queensland introduces the concept of determining density for different points relative to the scanner, adding a quasi-3D dimension to a previously 2D specification. For instance, the requirement to determine density at various distances and directions from the scanner, both horizontally and vertically, offers a more comprehensive understanding of point cloud density distribution.

2.3.3 Quality Requirements of Dutch Publicly Available Point Clouds

The Netherlands offers several national point cloud datasets that provide insights regarding the country's infrastructure, urban environment, and topography. The LiDAR point clouds, which are made accessible to the public in the Netherlands, are:

- Actueel Hoogtebestand Nederland (AHN)
- Prorail

Actueel Hoogtebestand Nederland (AHN)

The AHN (Dutch for 'Actual Height Model of the Netherlands'), represents a multi-year initiative and partnership between water boards, provinces, and Rijkswaterstaat, aiming at the development of a digital elevation model covering the entirety of the Netherlands. Since 1997, the ongoing program has seen four releases with new elevation data introduced every three to six years (AHN, 2023b). The acquisition of the fifth

release is currently in progress. The data is acquired using a sensor mounted onto an aircraft. The acquisition of each AHN version occurs in phases based on the partition of the Netherlands. Each of these parcels is outsourced separately and may be carried out by different parties.

For each version of the AHN, a set of tender requirements for the delivered point clouds and datasets is established, which applies to all parcels (except for the coastlines). In this thesis, the most recent requirements are investigated which are from the tender of 2023-2025 for the ongoing acquisition of AHN5 (AHN, 2023a).

In terms of the quality of the LiDAR data, the tender splits the quality requirements into 3 categories:

- *Height accuracy*: The height accuracy should have no more than 5 cm systematic deviation. The standard deviation should be less than 3 cm, which adheres to the 1 sigma (1 σ) criteria.
- *Planimetric accuracy*: The stochastic deviation should be less than 5 cm, adhering to the 1 sigma criteria, and the systemic deviation should be less than 8 cm.
- *Point density*: The point density should be at least 10 pt/m^2 in 99% of the 1x1 meter raster cells. Exceptions encompass surfaces such as water bodies and points experiencing occlusion (shadowing).

Prorail

ProRail, the entity overseeing the Dutch railway system, has made a nationwide point cloud available covering its jurisdictional area. By employing trains equipped with LiDAR measurement devices, Prorail can map out its network. Prorail typically integrates the acquired data into the broader infrastructure of Prorail, accessible through the SpoorInBeeld portal (Prorail, 2022).

Their tender requirements for terrain surveying outline the technical specifications that the delivered points clouds must adhere to (Prorail, 2017). These requirements mandate a sufficiently high spatial density and positional quality of the point cloud, guaranteeing that, the geometric position of location-based objects in the (Rijksdiehoeksmeting (RD), Normaal Amsterdams Peil (NAP)) system is equal to or better than the following positioning requirements.

- *Absolute positioning*: At most 12 cm at ground scale and adhering to 1 σ criteria. This means that the precision is related to standard normal distributions and implies that 68.26% of the possible values of the stochastic quantity deviate at most once from the standard deviation from the center of the distribution. Systematic positional deviations are not allowed.
- *Relative precision*: At most 6 cm between two points with a maximum distance of 100 meters.
- *Systematic deviations*: Not permitted.

Furthermore, the point cloud must be free from outliers, which are points that have no relationship with the objects presented in the point cloud. Each point must possess an RGB color value.

2.3.4 Quality Standards regarding Point Clouds from Rijkswaterstaat

Point clouds are employed in projects on a much smaller scale for varying purposes. Point clouds are not the main product in these projects; they only serve as source data. It is still essential to specify the accuracy of the input point cloud as the analysis relies on it. Several products that are derived from point clouds are:

- Digitaal Topografisch Bestand (DTB)
- Digitaal Terrein Model (DTM)
- Doorrijprofielen (DRP)

Digitaal Topografisch Bestand (DTB)

The Digitaal Topografisch Bestand (DTB) maintained by Rijkswaterstaat serves as a representation of the Dutch terrain. The DTB contains highly detailed geo-information on elevation, landforms, and surface characteristics across the country. Although the dataset is based on many point clouds, Rijkswaterstaat has not specified that a particular data acquisition method must be used to acquire the DTB. However, it is specified that certain accuracy levels must be maintained during acquisition. Acquired data must adhere to the product specifications as described in (Rijkswaterstaat, 2022a).

For connections, it is required that points appearing in both elements must have identical coordinates. For the acquired points, the accuracy requirements as shown in Table 2.2 apply, which are categorized into 4 classes. The classes are based on the level of recognizability of an object and are thus subjective to its user.

1. Contains well-recognizable objects e.g., road markings.
2. Contains reasonably recognizable objects e.g., road edges.
3. Contains moderately recognizable objects e.g., slope lines.
4. Contains objects that are outside the Obstacle Free Zone (OFZ) e.g., vegetation.

	Absolute (cm)		**Relative (cm)**	
Class	σXY	σZ	σXY	σZ
Hard - 1	5	10	2	4
Medium - 2	10	12	5	6
Soft - 3	15.5	15	19	9
Soft, outside OFZ - 4	60	30	40	20

Table 2.2. *Accuracy requirements of DTB according to (Rijkswaterstaat, 2022a) Accuracy divided into planimetric σXY and vertical component σZ*

Digitaal Terrein Model (DTM)

For the design of a project, engineers might require a digital 3D representation, known as a Digital Terrain Model (DTM). Point clouds may be employed for such purposes. In principle, creating such a DTM is the responsibility of the contractor; however, in certain cases, it may be desirable to stipulate requirements regarding the use in the request specification of a construction contract.

Rijkswaterstaat has product specifications regarding DTMs, as can be found in (Rijkswaterstaat, 2021). The accuracy requirements are divided into precision and reliability. The *precision* requirements are divided into hard and soft topography and can be found in Table 2.3.

- Examples of soft topography are waterline, slope lines, and semi-paved.
- Examples of hard topography are road edges, road markings, and buildings.

	Precision (cm)	
Topography	σXY	σZ
Hard	≤ 7.5	≤ 2.5
Soft	≤ 25.0	≤ 6.5

Table 2.3. *Accuracy requirements of DTM according to (Rijkswaterstaat, 2021) Relative accuracy divided into planimetric σXY and vertical component σZ*

Reliability refers to the verifiability of measurements and the sensitivity of the final product to undetected errors. The measurement should be designed in such a way that systematic errors are detected.

Doorrijprofielen (DRP)

Doorrijprofielen or clearance profiles are being measured for various purposes, such as reconstruction work on structures, incident management, validating clearance heights after overlay work, and preventing or handling damage claims. Possible end users of the product are RWS and the traffic center.

Clearance measurements are divided into width and height. The minimum clearance height is the distance perpendicular to the road surface between the object and the underlying road section. The clearance width is the minimum horizontal distance between objects just excluded from the road surface, such as the guardrail.

Clearance measurements must adhere to the requirements as specified in (Rijkswaterstaat, 2022b). The document divides the quality requirement into precision and reliability. Absolute accuracy is not of the highest priority for such specific purposes. The precision requirements are:

- Clearance heights - Precision 1σ[8] - ≤ 1.0 cm
- Clearance widths - Precision 1σ - ≤ 5.0 cm

[8]The precision is within the DRP specifications referred to as the spread of a stochastic variable relative to the expected mean. A measure of the precision of a single variable is the standard deviation (σ).

Infrastructure Point Clouds

As point clouds become increasingly integrated with RWS, the organization has released a set of product requirements outlining requirements for acquiring, processing, and delivering point cloud data (Rijkswaterstaat, 2023). The document outlining the product specifications was first published in December 2023 and is now starting to be implemented in projects.

The document divides the requirements into general, accuracy, format, and delivery. The following general requirements must be adhered to:

- *Calibration*: The measurement system must have been calibrated within the past year, following the prescribed calibration intervals provided by the supplier.
- *Measurement Conditions*: Data must be free from disruptive disturbances caused by weather and natural conditions (e.g., snow, rain).
- *Coordinate System*: All coordinates must be provided in RD and NAP and expressed in meters with 3 decimals.
- *Outliers*: Depending on the level specified by RWS, the outliers must be removed with an automatic route, free from outliers, or project-specified.
- *Point Density*: For at least 95% of the entire project area, point density must meet the specified requirement.
- *Gaps*: Gaps in the final product are not allowed. Exemptions might be gaps related to water bodies or resulting from unavoidable occlusion (shadowing).
- *RGB Coloring*: Required if mentioned in the project specifications.
- *Classification*: Must be carried out with careful consideration of the purpose of the measurement, ensuring that at least 95% of classes are correctly assigned.
- Remove Data Outside Project Boundaries: Clip point clouds outside boundaries.

In terms of accuracy requirements, the division between terrestrial laser systems and laser altimeters (airborne) is made. When employing terrestrial laser scanners, configured static or mobile, both the absolute accuracy — defined by system noise and positioning error — and the relative accuracy are assessed across the X, Y, and Z directions. Therefore, to make the accuracy requirements specific, RWS must provide the subcontractor with the maximum system noise, positional error, and relative accuracy. If laser altimetry is utilized, the absolute and relative accuracy pertain specifically to height measurements. Additionally, it is essential to specify both the absolute and relative planimetry accuracy.

Regarding format specifications, the point clouds must be provided in the LAZ format. The required attributes for each point are X, Y, Z, intensity, return number, number of returns, scanner channel, classification, point source ID, GPS time[9].

It is important to note that the DTB, DTM and point cloud specifications refer in terms of accuracy requirements and not quality requirements.

[9]The explanation of the attributes are explained in Chapter 3 Data.

Use of Quality Terms in Point Cloud Specifications

Various terms related to point cloud quality have been identified and categorized in the specifications. Table 2.4 provides a summary of these quality terms. The terminology varies within each standard, but generally, ”relative accuracy” is referred to as ”precision,” and ”absolute accuracy” as ”accuracy.” From the context provided by each standard, it appears these terms are used interchangeably.

Earlier, the term ”consistency” was introduced as a primary component. However, according to the quality standards reviewed, consistency falls under the category of relative accuracy rather than being related to point cloud density. The terms specified in the standards are more closely associated with coverage.

Coverage	**Relative accuracy**	**Absolute accuracy**
Completeness	*Logical consistency*	*Positional accuracy*
Point cloud density	*Internal consistency*	*External accuracy*
	Relative precision	*Survey uncertainty*
	Relative uncertainty	*Absolute positioning*

Table 2.4. *Observed terms in quality standards regarding point clouds*

2.4 State-Of-The-Art Validation Methods

This section investigates state-of-the-art research surrounding the validation of LiDAR point clouds. The research is based on the primary components as described in Subsection 2.2.3, which are coverage, relative accuracy, and absolute accuracy.

2.4.1 Existing methods for Assessing the Coverage

Currently, assessing point cloud density in 2D is standard practice, with established metrics for assessment. However, there is a growing trend towards investigating density in 3D, reflecting a more recent emphasis on understanding spatial distribution and volume density, as highlighted by developments such as voxel-based analysis.

2D Point Cloud Density

(Stanley and Laefer, 2021) and (Kodors, 2017) describe that traditional aerial LiDAR multi-pass scan missions have density metrics most commonly related to aggregate counts. Such counts include the *Nominal Pulse Density (NPD)*, the number of LiDAR points per unit area expressed as pulses per m^2 and the *Nominal Pulse Spacing (NPS)*, which is the distance between LiDAR points in meters calculated by the square root of the inverse of the pulse density.

(Dai et al., 2013) proposes a method to evaluate a point cloud with respect to the completeness. The surfaces of the ground truth model are partitioned into small square regions (in the study 1 × 1 cm). The presence and density of points are determined for each region, resulting in a percentage of coverage, point density, and density distribution.

Rather than investigating a 2D cell, (Rebolj et al., 2017) determines the density of the point cloud and the BIM model directly by calculating the number of points on an element's surface, whereby a distance tolerance from the surface is given.

The open sourced project CloudCompare can be employed to calculate the density of a point cloud according to (CloudCompare, 2022). CloudCompare offers two methods:

- *Precise Method*: The precise method estimates the density by counting for each point the number of neighbors N inside a sphere of radius R. The formula for surface density is:
$$\text{Surface Density} = \frac{N}{\pi R^2}$$
- *Approximate Method*: The approximate method estimates the density by determining the distance to the nearest neighbor, which is generally faster. The distance is considered as being equivalent to the above spherical neighborhood radius R (and $N = 1$).

An example of the 2D surface density for a point cloud is visualized in Figure 2.12.

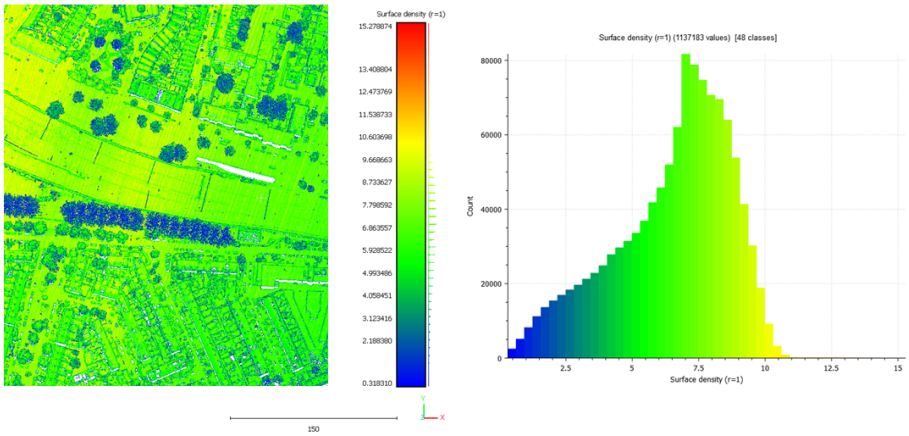

Figure 2.12. *Output of surface density CloudCompare*

3D Point Cloud Density

Since CloudCompare is a versatile point cloud processing software, it can handle both 2D and 3D data, allowing one to calculate point cloud density in either context. Instead of calculating the surface density, the volume density can be determined.

(Y. Wang et al., 2016) does not project the point cloud into planar 2D methods but rather employs a volume method that processes filled and empty voxels as shown in Figure 2.13. *Voxels* are standard cubes that record the serial numbers of the contained LiDAR points. From the serial numbers, the point density within each voxel can be determined.

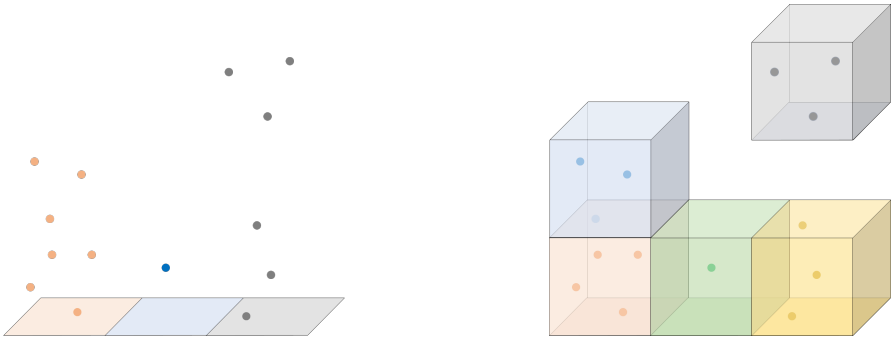

(a) *2D representation (cell)* (b) *3D representation (voxel)*

Figure 2.13. *Representation of point clouds in 2D and 3D*

(Zhang et al., 2021) acknowledges that the focus of existing descriptors is presented as a histogram. Histograms are very simple and functional for representing 1D or 2D data, making them a practical and rapid visualization tool. However, histograms can hardly deal with three (or more) dimensions. The author presents a Kernel Density Descriptor (KDD) for 3D point clouds to overcome the limitation. First, the local reference system around a feature point is established, creating a cubic region around it. Then, the kernel density of each cube in the 3D space is estimated.

2.4.2 Existing methods for Assessing the Relative Accuracy

The methods for assessing the relative accuracy vary depending on the type of laser scanning (static, mobile, or airborne) as different overlapping areas are captured from different positions or passes. Each type has unique challenges and methodologies for ensuring data quality.

Determining the Relative Accuracy for TLS

Assessing the relative accuracy of point clouds derived from static laser scanning involves comparing corresponding points within overlapping regions of adjacent scans acquired from different static positions.

CloudCompare provides a tool for calculating distances between two sets of point clouds (CloudCompare, 2015). By default, the 'nearest neighbor distance' method is employed, wherein for each point in the compared cloud, CloudCompare identifies the closest point in the reference cloud and computes the Euclidean distance. However, if the density of the reference point cloud is insufficient, this nearest neighbor distance may sometimes lack precision. In such cases, it becomes necessary to obtain a more accurate representation of the surface.

Once CloudCompare identifies the nearest point in the reference cloud, it proceeds to model the underlying surface locally by fitting a mathematical model based on this 'nearest' point and several of its neighboring points. Subsequently, instead of measuring the distance to the nearest point in the reference cloud, each point in the compared cloud is measured against the model. The approach offers greater statistical precision and reduces dependency on cloud sampling. The result of the cloud-to-cloud distance is shown in Figure 2.14. In the Figure, blue represents a low absolute distance, indicating that most road surface has high relative accuracy. Red, seen to the left, highlights objects within the soft topography, which exhibit a much higher absolute distance between point clouds from two measurement set-ups.

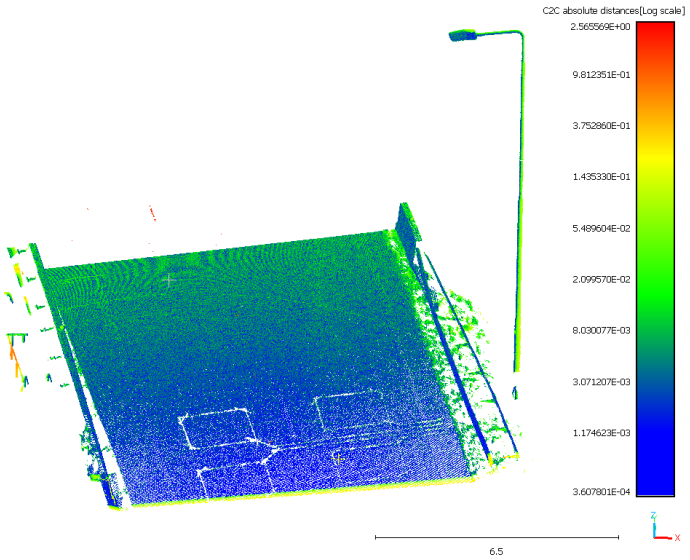

Figure 2.14. *Output of cloud-to-cloud distance CloudCompare*

Determining the Relative Accuracy for MLS

During data acquisition, mobile mapping system vehicles travel along predefined paths, capturing point cloud data from different perspectives. Assessing the relative accuracy of such a point cloud is done by relating points between adjacent scans that are related to passes of the vehicle. This is often done by considering points within a certain neighborhood or radius around each point in one scan and searching for the closest neighbors in the other scan. Various spatial indexing structures such as octrees can be used to efficiently search for neighboring points (Zhu et al., 2023).

Using such a method is demonstrated in (Kalvoda et al., 2020), where the authors conducted two separate data collection passes using MMS vehicles over two distinct areas or environments, resulting in two different MLS data sets. The approach allows for the comparison of data acquired from different perspectives. Figure 2.15 from (Altyntsev, 2022) shows an example of point clouds obtained from different passes.

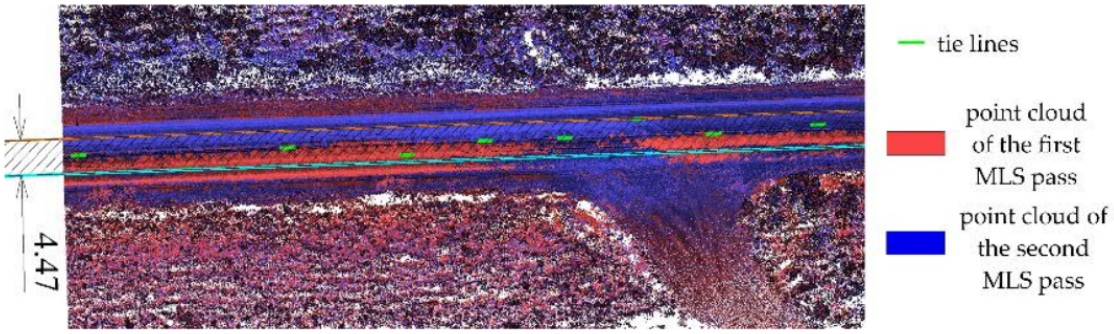

Figure 2.15. *Example of MLS point clouds from different passes, as can be found in (Altyntsev, 2022)*

Determining the Relative Accuracy for ALS

According to (ASPRS, 2015), the relative accuracy of airborne derived point clouds, without regard of surveyed ground control, includes two aspects:

- *Swath-to-swath* assessment: Assessment of data collected between swaths/ adjacent flight lines (*inter-flight line*). It involves comparing tie points from overlapping sections in adjacent swaths. Performed in (Elaksher et al., 2023) and (Latypov, 2002), which both quantitatively assess the relative accuracy of airborne LiDAR data.
- *Within-swath* assessment: Assessment of data collected within the same swath or flight line (*intra-flight line*). It indicates how stable the LiDAR system is, such as the internal stability of the instrument. It involves inspecting areas of relatively flat, hard surfaces which should only have a single return value. The difference between the minimum and maximum value within each pixel is calculated, and a threshold is applied. Demonstrated in (Dewberry, 2022), where Z-range rasters are created that colorize the precision of the laser point density within each swath.

2.4.3 Existing methods for Assessing the Absolute Accuracy

Assessing the absolute accuracy can be done by comparing reference features within the point cloud to features with known locations. Possible reference benchmarks, which serve as crucial features for comparison and quality assessment, are discussed. Followed by the methods to extract target or road markings. Finally, the absolute accuracy is addressed.

Reference Benchmarks

Reference benchmarks serve as features for comparison and are used to assess the absolute accuracy of point cloud data. One can verify the quality by comparing the acquired data to established sources. Inspired by the work of (Hofmann and Brenner, 2016), the division can be made between:

- Direct co-registration benchmarks
- In-direct co-registration benchmarks

Direct co-registration benchmarks are strategically placed objects distributed in the environment, each with accurately determined coordinates. At selected locations, a marker or **target** is placed.

In-direct co-registration benchmarks consist of features or objects extracted from the data. A range of publicly available datasets data contains geometric information about features such as buildings, roads, sidewalks, and objects. Using existing benchmarks has advantages, such that no installation or maintenance is needed. For example, (Hofmann and Brenner, 2016) uses existing structures in urban environments that are visible from public drive-able roads, such as ledges, doorways, and facades.

The accuracy of open data sets may vary, highlighting the importance of careful selection of the objects used for the validation. According to the DTB and DTM specifications for the Netherlands, the hard topography is to be measured with a high accuracy (in comparison to other publically available datasets). An example of well-defined, easily discernible [10], stable[11], and publically available hard topography data is the **road markings** of Dutch highways. Road markings are also specified as a GCP within the Danish point clouds specifications (Danish Agency for Data Supply and Efficiency, 2020).

[10] Examples of not easily discernible objects in infrastructure environments include thin wires or small utility boxes.

[11] Objects should remain stable under different conditions. Examples of not fitting features are traffic lights or signs as they might shift or sway in strong wind conditions.

Extraction of Targets

Targets come in a variety of forms, and the type and shape may change depending on the choice of the contractor or subcontractor. The size of the targets affects the density of the full scan; smaller targets require higher-density scans to capture. Figure 2.16 shows some examples of targets.

(a) *Spherical benchmark*

(b) *Flat checkerboard*

Figure 2.16. *Possible targets used in point cloud projects (Alhasan et al., 2015)*

The targets must be recognized and extracted from the point cloud data. This involves identifying distinct features or patterns that represent only the targets, such as geometric shapes, unique reflectance properties, or color contrasts. Automated algorithms or manual inspection can be employed to identify targets. This study focuses on **spherical targets**. Some features that can be used to extract spherical targets are curvature (expect a high curvature), intensity (expect a high contrast in intensity), and density (at the location of the target, expect a dense cluster of points).

After extracting the points corresponding solely to the spherical target, the next step is to estimate its center coordinate. This task can be accomplished using either Least Squares or the RANSAC (Random Sample Consensus) algorithm. In the Least Squares approach, the center coordinate of the sphere is computed by minimizing the sum of the squared distances between the observed points and the fitted sphere. Alternatively, the RANSAC algorithm is employed to robustly estimate the center coordinates in the presence of outliers or noise. RANSAC randomly samples subsets of points and fits spheres to each subset. The center coordinate with the highest inlier count, i.e., the most consistent with the observed data, is selected as the final estimation.

Extraction of Road Markings

(Pan et al., 2019) describes that research related to road marking operations from MLS data sets mostly extracts the road surface based on the profile image of curb features. Afterwards, different intensity threshold algorithms are exploited for the 3D point cloud or 2D geo-referenced feature image.

(Meinderts et al., 2022) proposes a method for isolating the road markings for the purpose of clearance measurement validation for highway infrastructure using mobile LiDAR point clouds. Starting, a simple intensity filter is applied on a segmented road, and subsequently, a DBSCAN algorithm is employed. A cluster-based feature filter is used with PCA features such as orientation, length, width, roughness, linearity, and planarity for filtering the road markings. Different thresholds are applied to filter out dashed and block-markings. Additionally, for continuous road marking lines, a Hough Transform is used to find straight lines. For the edges of the asphalt, the Canny operation can be utilized.

The study by (Martínez Sánchez et al., 2020) concentrates on road point extraction, effectively filtering out non-road elements such as vegetation and road markings. This means that instead of directly identifying road markings, their shape could be examined through the residual patterns they leave on the road. The study proposes a method that segments ground and non-ground points by grouping them into clusters based on 3D coordinates, intensity, and normal vectors. It includes the assumption that road points have a low intensity, lie on a plane, are surrounded by mostly road points, and are within a set of road points with meaningful size. The pipeline consists of four sequential stages: an intensity filter, a curvature filter, a density filter, and an area filter.

Assessing the Absolute Accuracy

The deviation between reference data and any point cloud is determined by computing, for every point in the reference data, the orthogonal distance to the closest surface in the point cloud (Hofmann and Brenner, 2016).

One commonly used metric for point-to-point comparisons is described by (INSPIRE, 2024) and is the *Root Mean Square Error (RMSE)*. The RMSE quantifies the overall discrepancy between observed coordinates (x_i, y_i, z_i) and predicted coordinates (x_j, y_j, z_j) across all n points. As described earlier, accuracy is often described in terms of planimetric accuracy over the XY-plane (σ_{xy}) and height accuracy for the z-direction (σ_z). The formulas for the RMSE are as presented in Equation 2.1. A low RMSE indicates better accuracy.

$$\sigma_{xy} = \sqrt{\frac{1}{n}\sum_{i=1}^{n}(x_i - x_j)^2 + (y_i - x_j)^2} \qquad \sigma_z = \sqrt{\frac{1}{n}\sum_{i=1}^{n}(z_i - z_j)^2} \tag{2.1}$$

2.5 Fundamental Principles

This section presents fundamental principles that are used in methods to assess the quality of point clouds. This includes the alpha shape, plane fitting using PCA and sphere fitting using both Least Squares and RANSAC.

2.5.1 Alpha Shape

The *alpha shape*, first introduced by (Edelsbrunner et al., 1983), is a tool for reconstructing shapes from point clouds. The alpha shape represents a concave hull around the sampled points, effectively outlining the outer boundary of the point cloud. Unlike other algorithms, such as the convex hull, an alpha shape can represent both convex and concave regions, making it useful for point clouds with intricate boundaries.

Choosing the Right Alpha

The alpha (α) parameter controls the level of detail in the resulting shape. When α is very low, the alpha shape simplifies to something like the convex hull, capturing the outer boundary without fine details as shown in Figure 2.17a. Conversely, a very high α value results in a highly detailed shape that closely follows the contours of the point cloud, capturing all the minor irregularities as shown in Figure 2.17c. Therefore, selecting the appropriate α value is crucial for balancing the shape's detail and generalization.

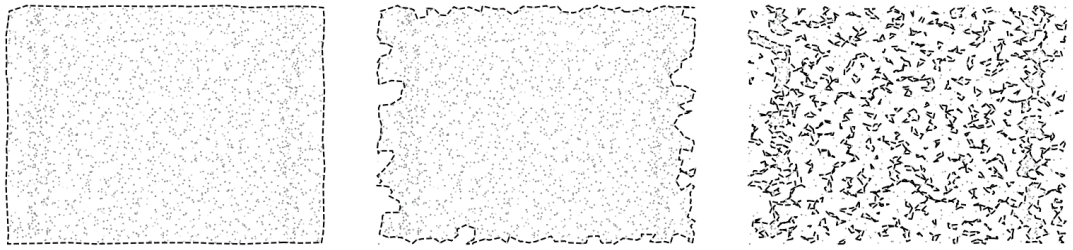

(a) $\alpha = 0.1$ (b) $\alpha = 2$ (c) $\alpha = 5$

Figure 2.17. *Border of point cloud using different alpha values*

2.5.2 Plane Fitting

To examine the difference between two point clouds, a plane can be the reference from which point distances are measured. The equation to describe a plane in 3D space with parameters (A, B, C, D) is given by linear Equation 2.2. A, B, and C are the coefficients of the coordinates x, y, and z respectively and define the normal vector to the plan. The normal vector is perpendicular to the plane and determines the orientation in space. D is the constant term that determines the plane's position relative to the origin.

$$Ax + By + Cz + D = 0 \tag{2.2}$$

Estimation of Plane Parameters using PCA

Algorithms, such as *Principal Component Analysis (PCA)*, can be employed to estimate the plane parameters. PCA is employed because the orthogonal distance is minimized, and compared to other algorithms, such as Least Squares, the method is more computationally efficient. However, it's important to note that PCA can be sensitive to outliers and lacks robustness in certain scenarios (Soudarissanane, 2016).

The derived vectors, referred to as *principal components*, align with the greatest variability observed within the point cloud. Imagine the components as the axes along which the data spreads out the most. In addition to the principal components, vectors representing the plane can be computed. These plane vectors span in 3 directions: two within the plane's orientation and one perpendicular, known as the *normal vector*.

Since the PCA algorithm is sensitive to variances, the point cloud must first be centralized. This involves subtracting the mean coordinates $\bar{X} = [\bar{x}, \bar{y}, \bar{z}]$, from the coordinates $X = [x, y, z]$. Mathematically, this centralization process, denoted as X_C, is represented by Equation 2.3.

$$\bar{X} = \frac{1}{n}\sum_{i=1}^{n} X \qquad X_C = X - \bar{X} \tag{2.3}$$

After centralizing the data, the relationship between the point cloud coordinates and the variability is identified by computing the covariance matrix C_X using Equation 2.4.

$$C_X = \frac{1}{n-1} X_C X_C^T \tag{2.4}$$

Eigenvalue decomposition is performed on the covariance matrix to obtain *eigenvalues* $\lambda_1, \lambda_2, \lambda_3$ and corresponding *eigenvectors* v_1, v_2, v_3. Eigenvalues show how much the data spreads out along specific directions, while eigenvectors show us those directions themselves. The eigenvectors are ordered in descending eigenvalue size (i.e., the first column of the eigenvector has the direction of the largest variance). The eigenvector corresponding to the smallest eigenvalue is selected as the normal vector N to the plane. This choice ensures that the plane is perpendicular to the direction of the least variance in the data[12].

The plane equation's parameters are determined using the normal vector as shown in Equation 2.5.

$$N = [A, B, C] \qquad D = -\bar{X} * N \tag{2.5}$$

[12]This process enables to fit planes to both vertical and horizontal surfaces, such as tunnel walls (vertical) and the road surfaces (horizontal).

For demonstration purposes, a point cloud is generated over an area of 2 meters by 0.5 meters, consisting of 2000 points. The points are randomly distributed over the x and y axes. The height of the points is normally distributed within a range of 10 millimeters. A fitted plane is shown in Figure 2.18.

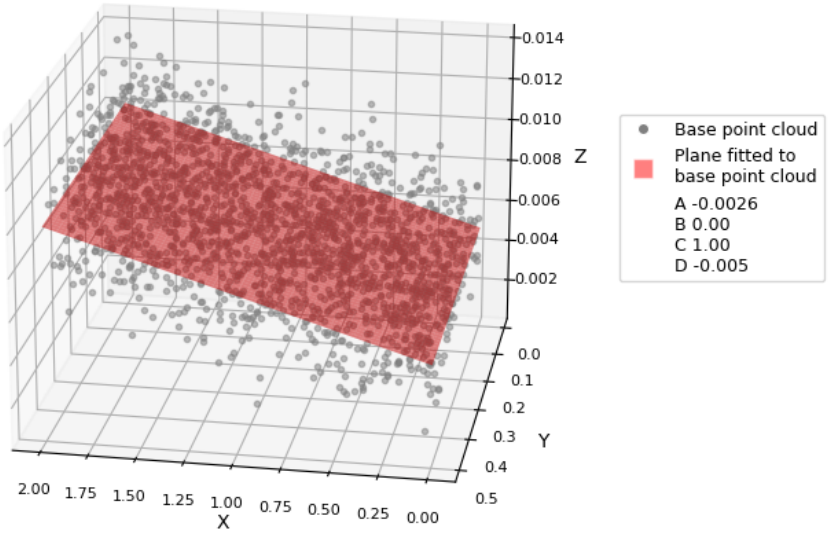

Figure 2.18. *Fitted plane using PCA*

Point-to-plane Distances

To determine how well the fitted plane represents the points, the distance from the points to the plane are determined. The distance, known as the *residuals*, is computed as the orthogonal distance from the point cloud to the fitted plane, as described in (Soudarissanane, 2016). Equation 2.6 utilizes the plane parameters to calculate the perpendicular distance from each point to the plane.

$$\hat{d} = \frac{|Ax + By + Cz + D|}{\sqrt{A^2 + B^2 + C^2}} \tag{2.6}$$

The result is the *absolute distance* from the points to the plane as shown in Figure 2.19. Since the points are distributed normally in height over a range of 10 millimeters, the plane is fitted at the midpoint of this range, where the density of points is highest. The largest absolute distance is then 5 millimeters. This is shown in the Figure by the range of distances in the color bar and the histogram, which visualizes the distribution of the distances.

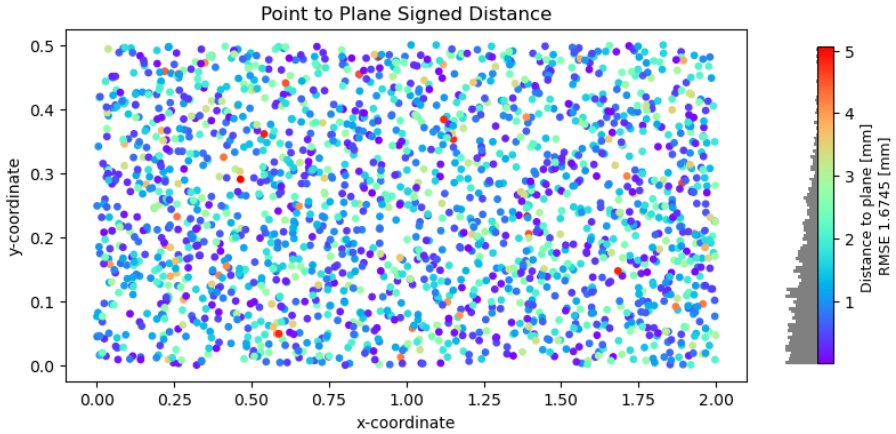

Figure 2.19. *Point-to-plane absolute distance*

Alternatively, considering the *signed distance* incorporates the direction of each point relative to the plane as shown in Figure 2.20. This can be calculated using a modified version of Equation 2.6, where the absolute operation is omitted from the numerator. Now, the distribution of distances to the plane clearly reflects the normal distribution established, spanning 5 millimeters in the negative and 5 millimeters in the positive direction. Positive distances signify points situated on one side of the plane, while negative distances indicate points on the opposite side.

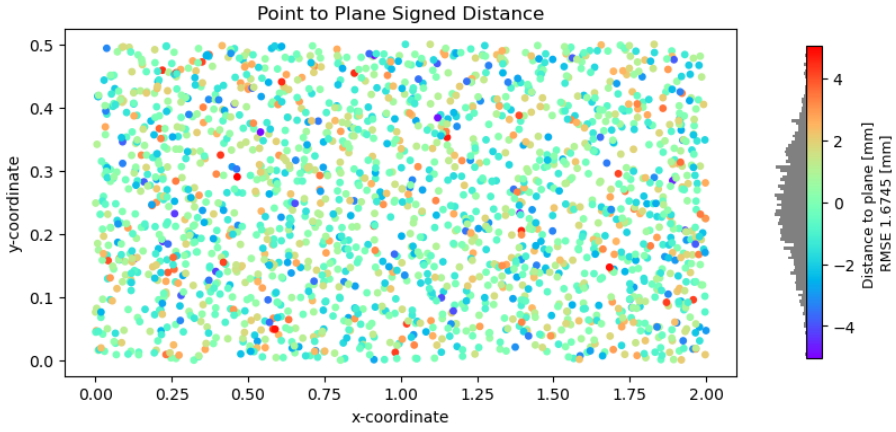

Figure 2.20. *Point-to-plane signed distance*

Root Mean Square Error

From the distances between points and the fitted plane, the Root Mean Square Error (RMSE) can be calculated to quantify the overall goodness-of-fit of the plane to the observed points. The RMSE, as described in (Soudarissanane, 2016), can be mathematically represented as Equation 2.7.

$$\hat{e} = X_c N \qquad \text{RMSE} = \sqrt{\frac{\hat{e}^T \hat{e}}{n - m}} \tag{2.7}$$

2.5.3 Sphere Fitting

To compare and analyze differences between two point clouds, a sphere can serve as a reference, enabling the measurement of point distances from its surface. The mathematical expression defining a sphere in 3D space, with parameters (x_0, y_0, z_0, r), is provided by Equation 2.8. x_0, y_0, and z_0 are the coordinates of the sphere's center and r is the radius, the distance from the sphere's center to its surface.

$$(x - x_0)^2 + (y - y_0)^2 + (z - z_0)^2 = r^2 \tag{2.8}$$

Estimation of Sphere Parameters using LS

With Least Squares (LS), the objective is to estimate the parameters that minimize the sum of squares of the distances from the points to the sphere's surface (Forbes, 1989). Rewriting Equation 2.8 to a set of linear equations gives the matrix multiplication in Equation 2.9.

$$\underbrace{\begin{bmatrix} x_1^2 + y_1^2 + z_1^2 \\ x_2^2 + y_2^2 + z_2^2 \\ \vdots \\ x_n^2 + y_n^2 + z_n^2 \end{bmatrix}}_{b} = \underbrace{\begin{bmatrix} x_1 & y_1 & z_1 & 1 \\ x_2 & y_2 & z_2 & 1 \\ \vdots & \vdots & \vdots & \vdots \\ x_n & y_n & z_n & 1 \end{bmatrix}}_{A} \underbrace{\begin{bmatrix} 2 * x_0 \\ 2 * y_0 \\ 2 * z_0 \\ x_0^2 + y_0^2 + z_0^2 - r_2 \end{bmatrix}}_{x} \tag{2.9}$$

The LS solution of the matrix multiplication is given by Equation 2.10.

$$\hat{x} = (A^T A)^{-1} A^T b \tag{2.10}$$

After obtaining the least squares solution $\hat{\hat{x}}$ with coefficients a, b, c and d as given in Equation 2.11, further computations are needed to determine the radius and center of the sphere. The radius r and center coordinates (x_0, y_0, z_0) are determined using Equation 2.12.

$$a = 2 * x_0, \quad b = 2 * y_0, \quad c = 2 * z_0, \quad d = x_0^2 + y_0^2 + z_0^2 - r^2 \tag{2.11}$$

$$r = \sqrt{\frac{a^2}{4} + \frac{b^2}{4} + \frac{c^2}{4} + d}, \qquad (x_0, y_0, z_0) = \left(\frac{a}{2}, \frac{b}{2}, \frac{c}{2}\right) \tag{2.12}$$

Estimation of Sphere Parameters using RANSAC

RANdom SAmple Consensus (RANSAC) proves particularly effective in scenarios where input data is noisy or contains outliers, as RANSAC can robustly estimate sphere parameters while effectively disregarding outliers. pyRANSAC-3D is an open-source implementation of the RANSAC method. This package samples a random subset of four points and calculates the center and radius. It then evaluates the distance from each point in the point cloud to the estimated sphere and identifies inliers whose distances fall within a certain threshold t from the sphere's surface. Suppose the number of inliers

found in the current iteration exceeds those found in previous iterations. In that case, the current set of inliers, center, and radius is updated as the best estimate so far [13].

Point-to-sphere Distances

To determine how well the fitted sphere represents the points, the distance from the points to the sphere surface will be determined, denoted by d. This involves calculating the distance from each point to the center of the sphere and then subtracting the radius as shown in Equation 2.13.

$$\hat{d} = \sqrt{(x - x_0)^2 + (y - y_0)^2 + (z - z_0)^2} - r \tag{2.13}$$

A synthetic point cloud representing a sphere is generated. The radius is initiated as 10 centimeters and visualized in Figure 2.21a. To simulate real-world measurement errors, Gaussian noise with a standard deviation of 0.01 meters is added to each of the Cartesian coordinates. Each coordinate x, y, z has been perturbed by the added noise, producing a sphere with a slightly irregular surface. Figure 2.21b shows the distance for each point to the surface of the sphere.

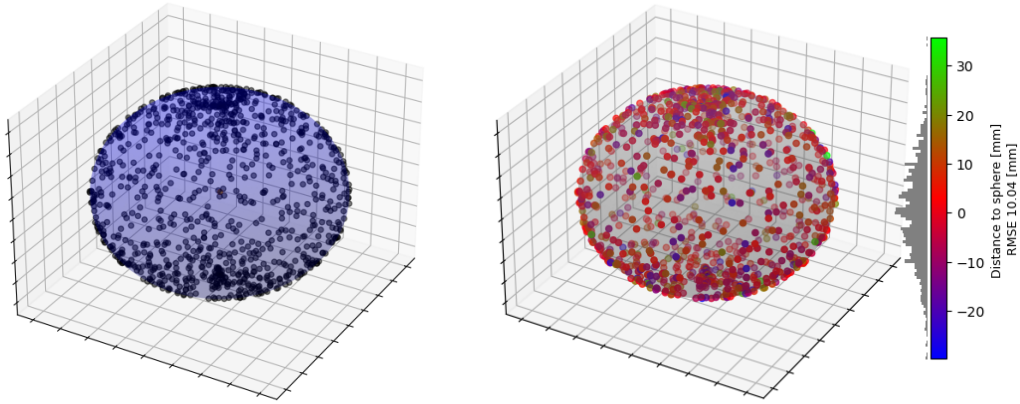

(a) *Fitted sphere* (b) *Point-to-sphere distances*

Figure 2.21. *Result sphere fitting*

Root Mean Square Error

The RMSE is calculated to quantify the deviation of the points from the sphere surface, providing a summary statistic for the quality of the fit. This is achieved using Equation 2.14.

$$\text{RMSE} = \sqrt{\frac{1}{n}\sum_{i=1}^{n}(\hat{d})^2} \tag{2.14}$$

[13] Source code of pyRANSAC-3D for spheres can be found here: https://github.com/leomariga/pyRANSAC-3D/blob/master/pyransac3d/sphere.py

3 Data Description

This chapter presents the different datasets used in this study. Section 3.1 introduces the project Tunnelrenovaties Zuid-Holland. The study encompasses a statically derived point cloud described in Section 3.2, an airborne point cloud described in Section 3.4, and a mobile point cloud in Section 3.3. Section 3.5 provides an overview of the main differences between the datasets.

3.1 Introduction Project Tunnelrenovaties Zuid-Holland (PTZ)

Mostly built in the 1950s and 1960s, a large portion of the Netherlands' vital infrastructure has undergone extensive use and requires repairs to ensure continued safety. In response, the Replacement and Renovation program overseen by Rijkswaterstaat focuses on renovating or replacing 100 infrastructure projects. This includes the renovation of 7 tunnels in Zuid-Holland, referred to as Project Tunnelrenovaties Zuid-Holland (PTZ)(Rijkswaterstaat, 2024). In this study, data regarding the **Drechttunnel** is used.

Built in the 1970s, the Drechttunnel is part of the A16 highway and is located between Zwijndrecht and Dordrecht as shown in Figure 3.1 (red circle). The tunnel provides a connection for motor vehicles underneath the river the Oude Maas. The tunnel has a total of 4 tunnel tubes, each containing 2 lanes and a total length of just over half a kilometer (Rijkswaterstaat, n.d.-b).

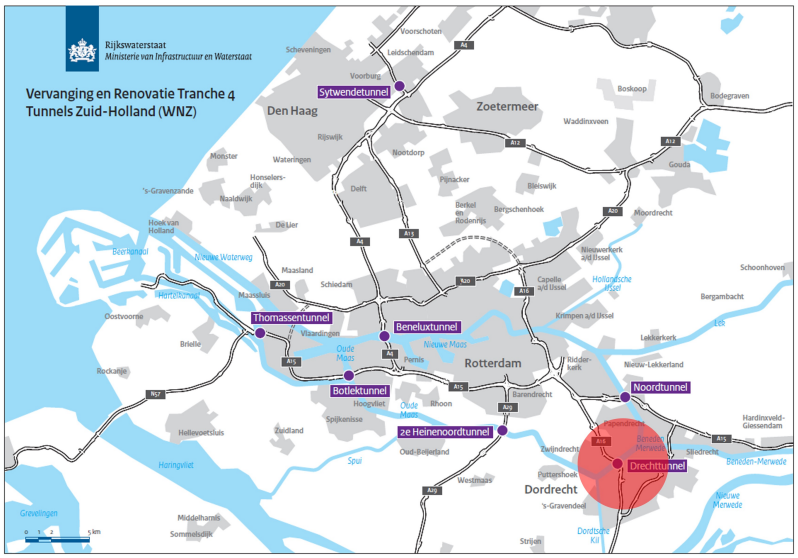

Figure 3.1. *Overview tunnels in PTZ project RWS (Rijkswaterstaat, 2024)*

3.1.1 Project Objective

RWS started the planning phase of the PTZ in September 2019. According to the specifications in (Rijkswaterstaat, 2020), the main objective of the PTZ project is to ensure the safety and availability of the tunnels through renovation. Additionally, the project aims to contribute to strengthening the robustness and sustainability of the network and improving the efficiency of management, maintenance, and operation. Part of this includes organizing asset data and ensuring a smooth transfer of project data to the administrator.

The planning phase focuses on preparing for the execution phase to ensure that the renovations can be carried out safely and with minimal disruption. During the preparation phase, one of the first tasks includes mapping the existing situation. Due to sometimes lacking (digital) accurate drawings and design data, 3D scans can effectively map the position of tunnel technical installations and the civil situation. Later, during the design, realization, management, and maintenance, 3D BIM models constructed from these scans can be utilized.

3.1.2 Project Quality Specifications

Requirements regarding the creation of 3D scans, ground radar research, production of 3D models, and processing of civil data into the 3D model for the planning phase of the PTZ project are specified in (Rijkswaterstaat, 2020). The document includes specifications regarding the activities that need to be carried out such as the 3D scanning. The objects that need to be scanned are the tunnel tubes, exterior areas, emergency- and service roads, service buildings, cable ducts, and entrance installations.

The objects are surveyed using a combination of static, mobile, and airborne scanning configurations. The tunnel itself is only surveyed using static configurations as due to the lighting conditions, mobile scanning was not permitted as the desired accuracy will not be obtained. The following requirements are specified regarding the quality of the scans:

- Relative measurement accuracy of the static scans in the tunnels and service buildings must be $\sigma < 0.5$ cm.
- Point density of the static scans must be at least 10 points per 1 cm^2.
- Absolute measurement accuracy of the exterior areas, exits and entrances, and roads surveys from the sky must adhere to $\sigma < 2.5$ cm.
- Scan data must be delivered in RDNAP coordinates (ESPG:28992).
- Scan data must be filtered, removing vehicles/ bicycles, traffic, and pedestrians.
- All laser scans must be conducted in color.
- Expected Ground Sampling Distance (GSD) is: 1cm or lower.

The quality requirements from RWS regarding point clouds as outlined in Subsection 2.3.4 did not exist at the time of acquisition and thus were not used within this project.

3.2 Point Cloud 1: Static

The Drechttunnel and a portion of the road leading to its entrance were surveyed using TLS. At intervals of approximately 20 meters, a measurement set-up is created, comprising of a tripod fitted with a LiDAR laser scanner, as depicted in Figure 3.2a. The instrument used is the Trimble TX8-II which can generate one million points per second with an accuracy of ±2 mm (Trimle, n.d.). The color values are derived from 360° panoramic camera (Nikon D5003 SLR SLR camera in combination with Nodal Ninja adapter). Service corridors and buildings are measured with the Trimble TX7 laser scanner.

Following the specifications outlined in (Rijkswaterstaat, 2020), the roadway, rural areas, and tunnels must be provided with targets to establish a link with fixed reference- or baseline points. Initially, prisms are mounted to bolts embedded within the walls, as illustrated in Figure 3.2b. These prisms are then surveyed using tachymetry to determine their precise locations. Outside of the tunnel, the measurements were taken with GNSS and were levelled to NAP. Subsequently, before scanning operations, the prisms are replaced with spherical targets mounted on the same bolts. The heart of the prism is equal to the heart of the sphere (diameter of 12,1 cm). To ensure a strong alignment between the scan measurements, additional targets have been used.

(a) *LiDAR measurement device*

(b) *Prism mounted onto wall*

Figure 3.2. *Laser scanning procedure within PTZ project*

3.2.1 Composite Processed Point Cloud

The delivered point cloud data is categorized into the east and west sections of the tunnel (indicated with 'O' or 'W'). Within each section, the data is divided into smaller point cloud tiles, each measuring 20 by 20 meters as shown in Figure 3.4 (left; grey tiles). Additionally, the distinction between 'tti' and 'civiel' is made, where the 'tti' files only contain the technical installations and 'civiel' all other objects.

The point clouds are stored as LAZ files and contain the attributes **RGB color, Intensity, and Classification**[14]. The *RGB color* stores the red, green, and blue value for each point which together colorize the point cloud as shown in Figure 3.3a. The values of this

[14] Additionally, the point cloud contains the attributes Return Number and Number of Returns. However, they do not contain any information.

attribute range from 0 to 255 for an 8-bit-encoder scheme. The *intensity* represents the pulse return magnitude. Different objects (such as road markings) lead to a different reflectivity and thus intensity than the surroundings. Its values range between 1 and 4096 due to the 12-bit encoder scheme. This is visualized in Figure 3.3b where black represents a low intensity and white high. Finally, the *classification* represents the class of each point as determined by the subcontractor. Visualized in 3.3c, the 'tti' files contain class (1 - red) representing the technical installations. The 'civiel' files contain the classes (2 - blue) representing the road surface, (3 - green) for the tunnel walls, and (4 - yellow) for the tunnel ceiling.

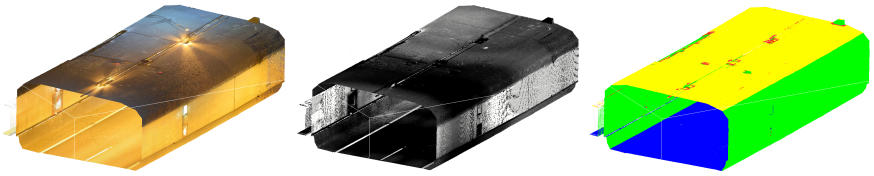

(a) *RGB* (b) *Intensity* (c) *Classification*

Figure 3.3. *Point cloud attributes present in static derived composite point cloud*

3.2.2 Original scanned point cloud

As introduced in Section 1.3 Scope, for this study some original data is requested from the subcontractor. Figure 3.4 shows the location of the consecutive measurement set-ups that are provided. The data starts outside of the tunnel only being road (red - 5 set-ups) and then progresses inside (blue - 12 set-ups). This area is defined as the area of interest (AoI) for this study. Additionally, Figure 3.4 presents the locations of the benchmarks within the AoI (right - yellow stars).

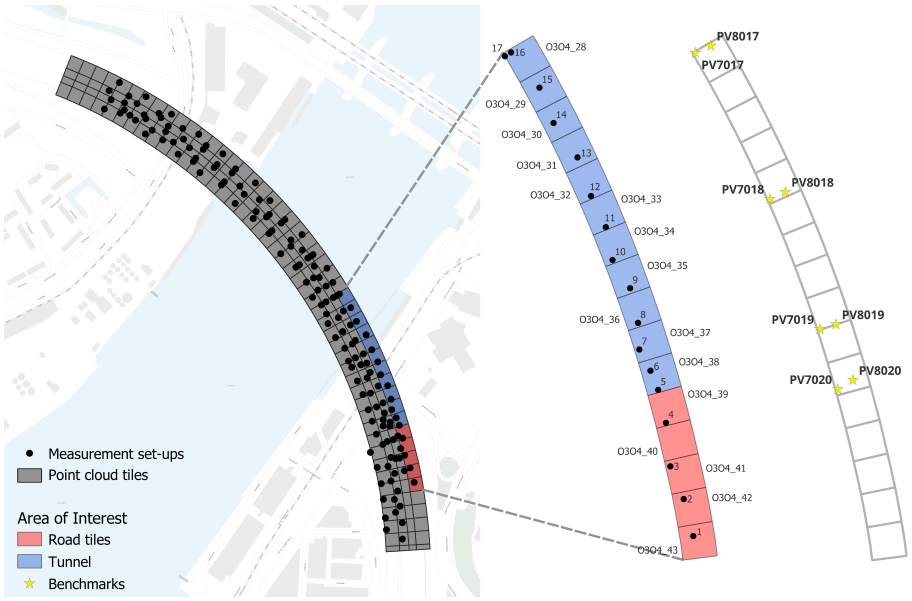

Figure 3.4. *TLS measurement set-ups, sub-division tiles, AoI and benchmarks*

The original point clouds contain the attributes **RGB color** and **Intensity**.

3.3 Point Cloud 2: Mobile

From the tunnel entrance to the traffic control system installation and on the service roads, mobile laser scans were made with the Riegl VMX450 Mobile mapping system. Within the tunnel itself, MLS could not be utilized due to GPS inaccuracies, which resulted in drift. The scanner has a high measurement rate, capable of capturing up to 1.1 million measurements per second. An accuracy of 8 mm and a precision of 5 mm is claimed (one sigma at a 50-meter range under test conditions) in the scanner specifics (Riegl, 2015). The Riegl is equipped with a Ladybug 360-degree camera used to colorize the laser scans. A note is made that this coloring is never exact and it is intended to be indicative. Because each lane was driven separately, the different projections create a distorted image. These manifest as shifts and are particularly visible on surfaces such as road markings or tunnel walls.

The mobile scans at the entrance and exit of the tunnel are connected to the static scans, and to align the mobile scans with coordinates further away from the tunnel, reference fields were measured. As a result, this measurement fits very well with the static laser scan measurements in the tunnel tubes.

3.3.1 Composite Processed Point Cloud

A total of 8 point clouds are provided, each representing various areas surrounding the Drechttunnel. The furthest areas surveyed have only one lane captured, while the closest areas have data for all lanes. Figure 3.5 illustrates the AoI for this study where the AoI corresponds to the static point clouds, focusing solely on the road.

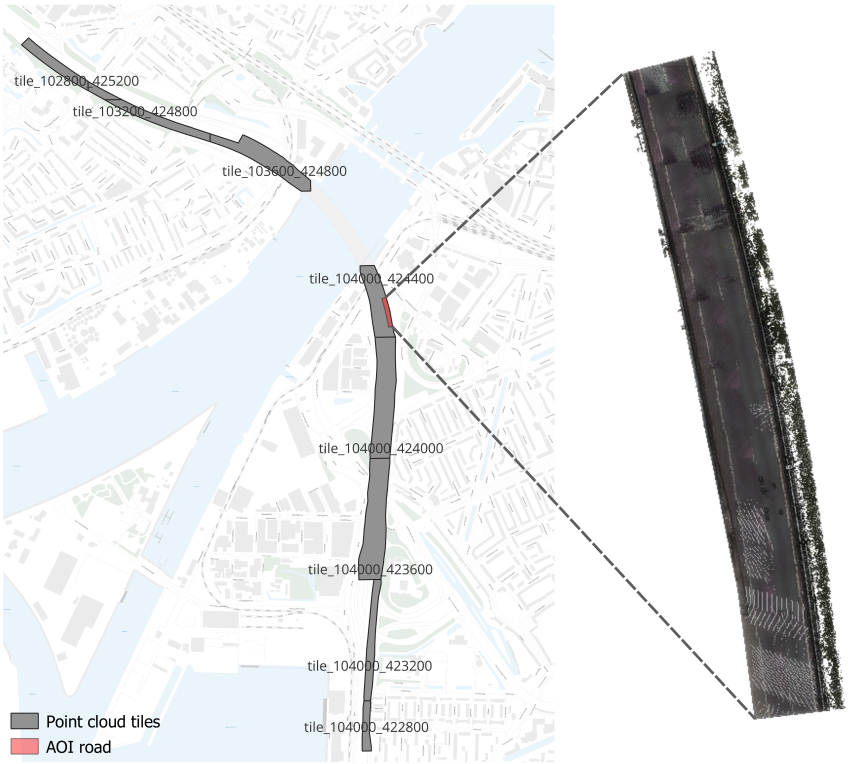

Figure 3.5. *MLS sub-division tiles and AoI*

The point clouds are stored as LAZ files and contain the attributes **RGB color, Number of Returns, and Return Number**[15]. The *Number Of Returns* indicates the total number of returns generated by the laser pulse. On solid surfaces, such as the road, the laser scanner will generally only record a signal signal. For complex structured surfaces, such as that of vegetation, the scanner can encounter multiple layers before reaching the ground and thus result in multiple returns for a single pulse. The *Return Number* contains information about the order of the return pulse for a given laser pulse. The return number starts from 1 for the first return and increases for subsequent returns.

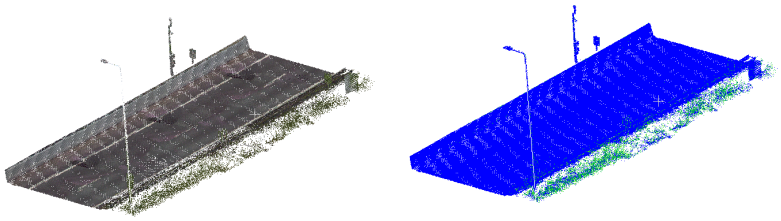

(a) *RGB* (b) *Number of Returns*

Figure 3.6. *Point cloud attributes present in mobile derived composite point cloud*

3.3.2 Original scanned point cloud

For this study, point clouds from the original mobile data have been provided. These point clouds contain the attributes **RGB color, Number of Returns, Return Number, Intensity, Scan Angle**[16] **and GPS Time**. The *Scan Angle* measures the angle between the direction of the laser pulse and a reference plane. In a typical LiDAR scan, the laser scanner rotates or oscillates to capture multiple measurements from different angles. In Figure 3.7a the scan angle ranges from -128 (green) to 128 (red) to represent both directions. *Global Positioning System (GPS) Time* represents the time at which the pulse was emitted from the laser scanner. In Figure 3.7b, blue represents the starting time and red the ending. The time is stored in GPS seconds of the week.

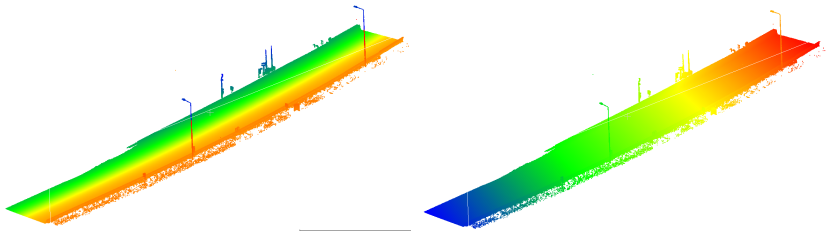

(a) *Scan Angle* (b) *GPS Time*

Figure 3.7. *Point cloud attributes present in mobile derived original point cloud*

[15] Additionally, the point cloud contains the attribute EdgeOfFlightLine which is not applicable to mobile derived point clouds and does not contain any information.

[16] In the point cloud itself, the attribute Scan Angle is named *Scan Angle Rank* which does not seem consistent with the result.

3.4 Point Cloud 3: Airborne

For the aerial survey, the Leica Citymapper was used, supplemented with a Phase-One camera. (Leica, n.d.) asserts that the vertical accuracy is consistently less than 5 cm with a confidence level of 68% (1 σ), while the horizontal accuracy remains below 13 cm within the same confidence interval. These accuracies are purportedly achieved under specific conditions: data collection is conducted at an altitude of 1,000 meters Above Ground Level (AGL) with an aircraft speed of 60 m/s.

3.4.1 Composite Processed Point Cloud

In total approximately 10 million km^2 is surveyed and split into a total of 8 point clouds. Figure 3.8 illustrates the Area of Interest (AoI) for this study. This AoI is exactly the same as that of the static point and mobile point cloud as shown in Figure 3.8.

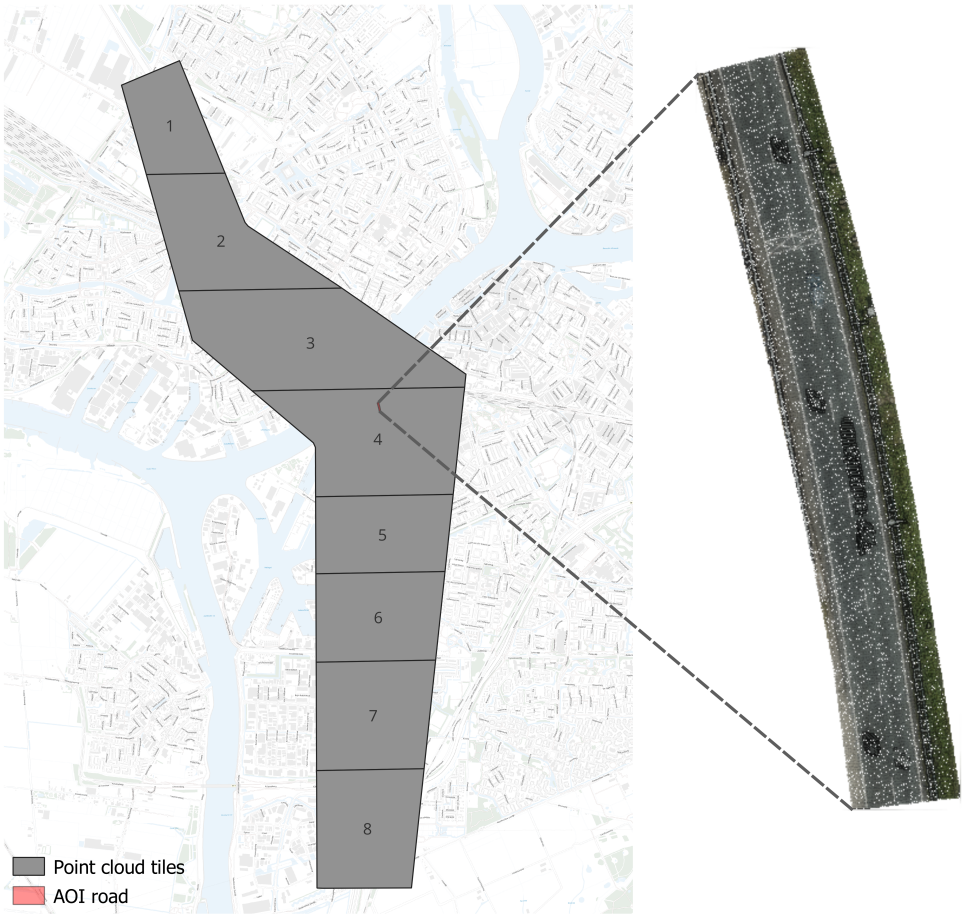

Figure 3.8. *ALS sub-division tiles and AoI*

The point cloud contains the attributes **RGB color, Intensity, Number of Returns, Return Number, Scan Direction Flag, Point Source ID, Overlap Flag, and GPS time**. The *Scan Direction Flag* is an indicator of the direction during the scanning process. It is denoted by binary values of either 0 or 1 in the opposite direction, as shown in Figure 3.9.

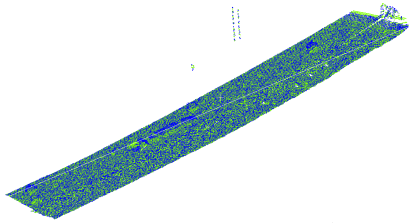

Figure 3.9. *Scan direction flag attribute present in airborne derived original point cloud*

The *Point Source ID* contains values that identify the different flight strips. Figure 3.10a visualizes the flight strips surrounding the Area of Interest (AoI). In this figure, the points on the left are from flight strips 165 and 166 (dark blue and green), while the points on the right are from flight strips 166 and 167 (green and yellow). The *Overlap Flag* indicates overlapping areas, with values of 0 or 8 assigned, as shown in Figure 3.10b. The AoI is located within an overlapping area indicated by 0 (blue).

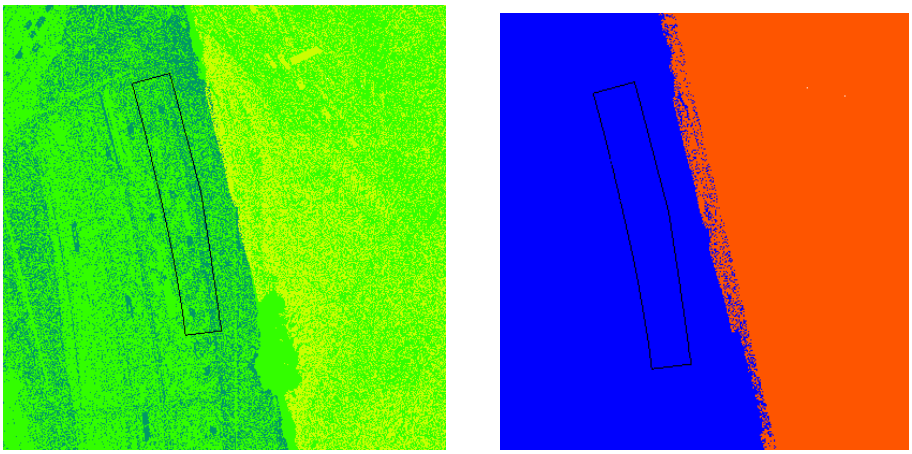

(a) *Point Source ID* (b) *Overlap Flag*

Figure 3.10. *Point cloud attributes present in airborne derived original point cloud*

3.5 Point Cloud Density

Table 3.1 shows an overview of the attributes for each dataset. The static derived point cloud contains approximately 143 million data points, marking a substantial lead over the mobile dataset, which contributes 1.9 million data points, and the airborne dataset, which comprises 160 thousand data points. Put into perspective, the static dataset contains approximately 75 times more data points than the mobile dataset and nearly 900 times more data points than the airborne dataset.

Attribute	**Static** *composite*	**Static** *original*	**Mobile** *composite*	**Mobile** *original*	**Airborne**
RGB					
Intensity					
Classification					
Return Number					
Number of Returns					
Scan Angle					
GPS Time					
Scan Direction Flag					
Point Source ID					
Scan Direction Flag					
Overlap Flag	1.25 billion				
Point count AoI road	143 million		1.9 million		160 thousand

Table 3.1. *Overview of attributes of each point cloud dataset*

4 Methodology

This chapter outlines the methodology of the research. Figure 4.1 provides a schematic overview of the steps required for the quality assessment of point clouds based on the primary components. The method to determine the point cloud density, described in Section 4.1, assesses the primary component of coverage. The method determining the alignment between overlapping points, detailed in Section 4.2, evaluates the relative accuracy. The benchmark alignment explained in Section 4.3 assesses absolute accuracy.

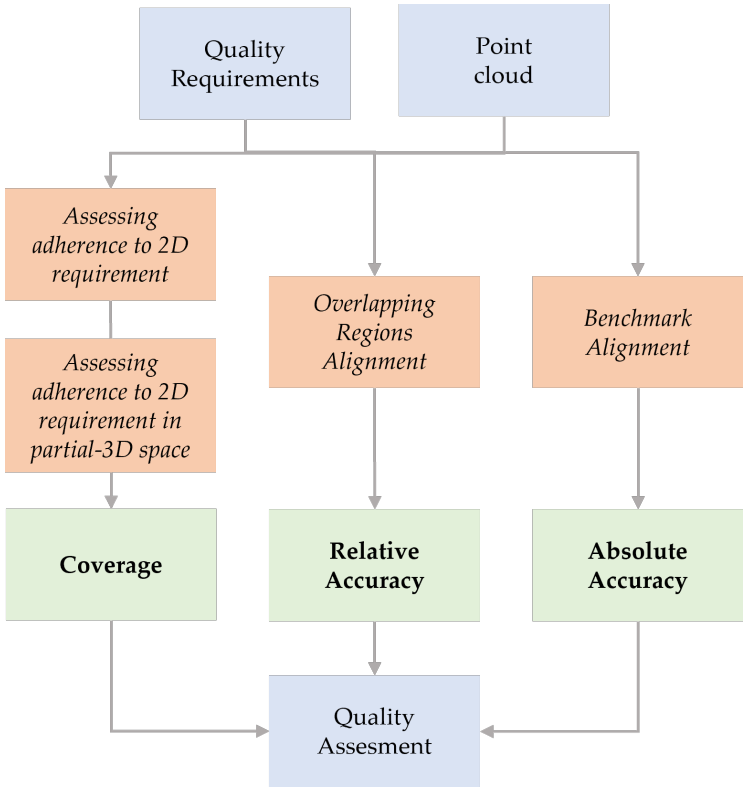

Figure 4.1. *Schematic overview steps for quality assessment of point clouds. Blue are the in- and outputs, green are the primary components, orange are the methods used to assess each quality component.*

4.1 Point Cloud Density

The point cloud density is a metric to evaluate the component *coverage*. First, the point cloud density is investigated in a 2D space since the density requirement is typically specified in such a way. Next, the 2D requirement is investigated in a partial-3D space.

To demonstrate and validate the method, a point cloud with known densities is generated. The point cloud covers an area of 15 by 15 meters, representing a highway scene with a road in the middle and guide rails on either side. The points are randomly distributed across the area in the x, y plane. In the top half of the point cloud, each cell contains 15 points per m^2, while in the bottom half, the density is reduced to half. To simulate the guide rails, cells on the left and right edges contain 20 points per m^2. Additionally, some cells next to the guide rails were completely devoid of points to represent vegetation gaps. Furthermore, three cells were altered: two to represent lampposts, with points concentrated at higher heights, and one with a point at a significantly lower height, demonstrating an outlier.

4.1.1 2D Point Cloud Density

Figure 4.2 shows an overview of steps to determine the 2D point cloud density.

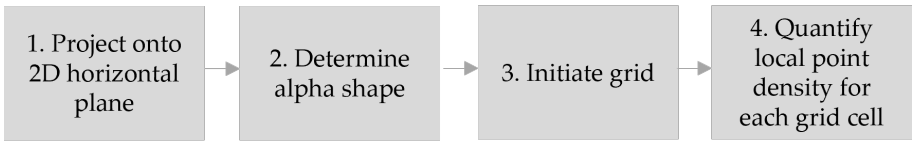

Figure 4.2. *Schematic overview steps determining 2D point cloud density*

1. Project onto 2D horizontal plane: To investigate the point cloud in a 2D space, one can project the 3D points onto a 2D plane. One approach is to project along the Z-axis onto the XY horizontal plane, effectively creating a top-down view of the point cloud[17]. The top view offers a visualization of the spatial arrangement of points, as illustrated in Figure 4.3 (right).

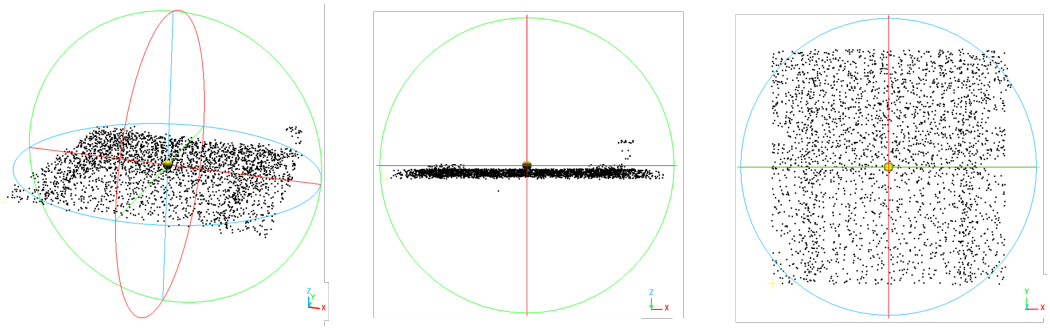

Figure 4.3. *Projecting point cloud (blue z-axis, red x-axis, green y-axis)*
Left: 3D view of demonstration point cloud
Middle: side-view of point cloud; projected along the X-axis onto YZ plane
Right: top-view of point cloud; projected along the Z-axis onto XY horizontal plane

[17]Projecting along the Z-axis is common practice as described in Subsection 2.4.1 State-of-the-art.

2. *Determine alpha shape*: The outside border of the point cloud is determined using the alpha shape, as introduced in Section 2.5.1. The alpha shape, as shown in Figure 4.4a, represents a concave hull around the sampled points, effectively outlining the outer boundary of the point cloud.

3. *Initiate grid*: Within the specifications, the cell size from which the density is determined is consistently defined as 1 m^2. To achieve this, a structured grid is created along the horizontal plane, dividing the point cloud into uniform cells of a specified cell size, 1 m^2 in this case. The grid is created in a local reference system, where the origin is the point corresponding to the lowest x- and y-coordinates. Each cell within the grid is classified as either "full" or "empty". If a cell contains at least 1 point, it is considered "full". The threshold for "full" cell classification should be adjusted based on the input point cloud's density. For point clouds with an expected high density, a higher threshold is more appropriate. Cells classified as "empty" are discarded [18]. Any missing cells within the body of the point cloud indicate *gaps*. Figure 4.4b illustrates the 2D horizontal grid.

Creating the grid, cells along the borders of the point cloud might not be fully filled, leading to potential misrepresentation. To address this issue, one could choose a smaller grid size or iteratively adjust the grid size. However, this study maintains a cell area of 1 m^2 for computational efficiency. In Figure 4.4b, cells containing border points are visualized in red using the alpha shape.

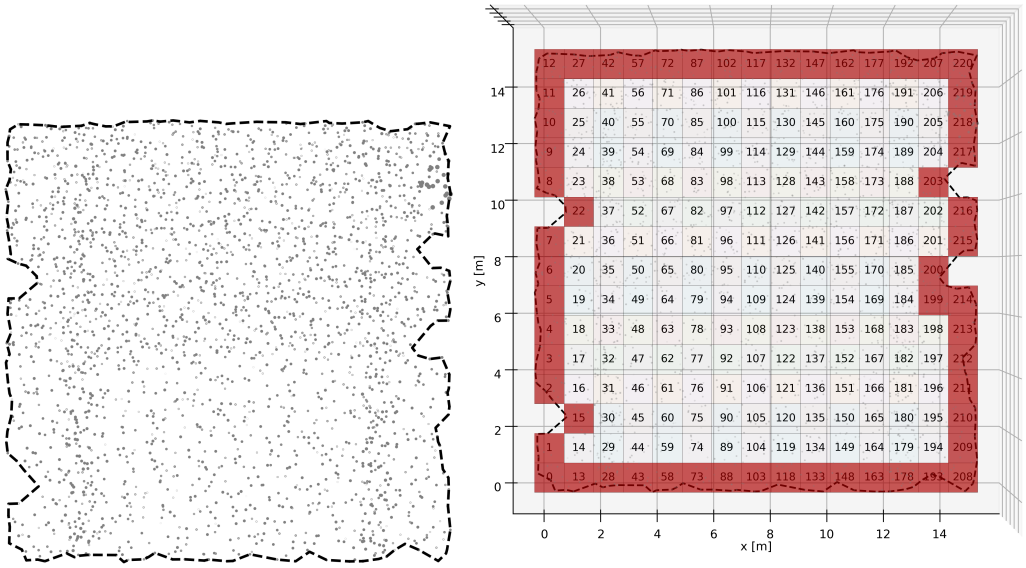

(a) *Alpha shape representing the border.* $\alpha = 2$ *Grey points visualize the point cloud.*

(b) *Top view of 2D grid with cell area of 1* m^2. *Red cells contain the border.*

Figure 4.4. *Initializing 2D horizontal cell grid*

[18] Source code for creating and filtering the 2D grid is from (Truong-Hong and Lindenbergh, 2022).

4. Quantify local point density for each grid cell: For each "full" cell, the number of points within it is quantified to measure the local point density. Figure 4.5 shows the top view of the densities within each cell, providing a simple representation of the spatial distribution. Different colors represent varying densities within the cells, offering an indication of areas with higher or lower point concentrations. The plot can be visualized using either a logarithmic scale or a linear scale, depending on the range of densities. Since the range in this scenario spans from 0 to 20 points per m^2, a linear scale provides enough detail.

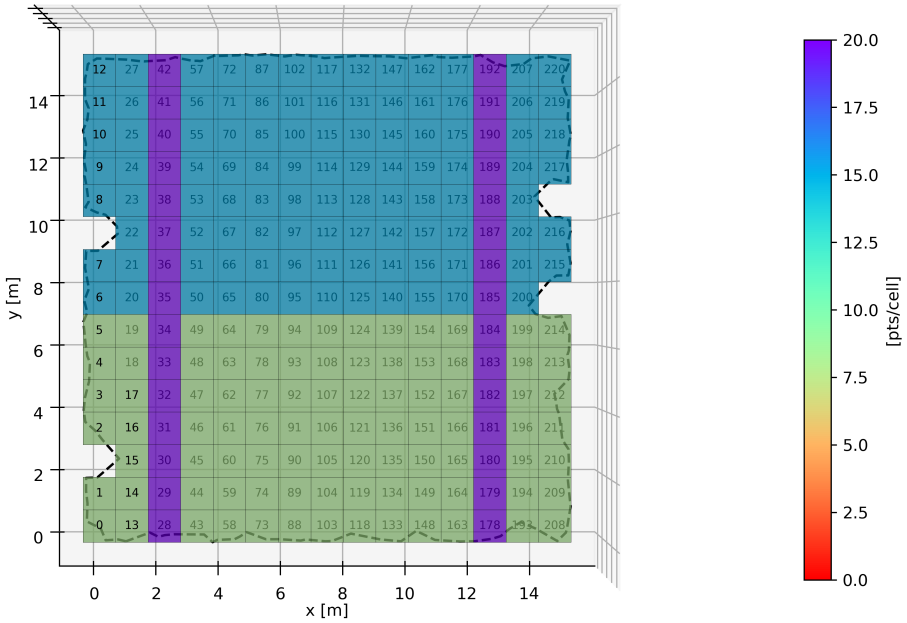

Figure 4.5. *Local point cloud density of 2D Horizontal cell grid*

4.1.2 Assessing adherence to 2D Density Requirement

Validation of the point cloud density involves assessing the adherence to specified requirements. The process entails comparing the density of each cell to the 2D requirement[19]. The assessment focuses exclusively on non-border cells. The results are visually represented using a color-coded system for easy interpretation:

- *Green*: Compliant with requirement (> requirement)
- *Orange*: Compliant with requirement (between 95% and requirement)[20]
- *Red*: Not compliant with requirement (<95% of requirement)

The demonstration point cloud must meet a hypothetical requirement of 10 points per m^2. The outcome is presented using the top view as shown in Figure 4.6.

[19] Conversion between either the requirement or the point cloud density might be necessary to ensure they are on the same scale. Typically m^2 is used.

[20] Even though 95% compliance is accepted, close attention should still be paid to the cells.

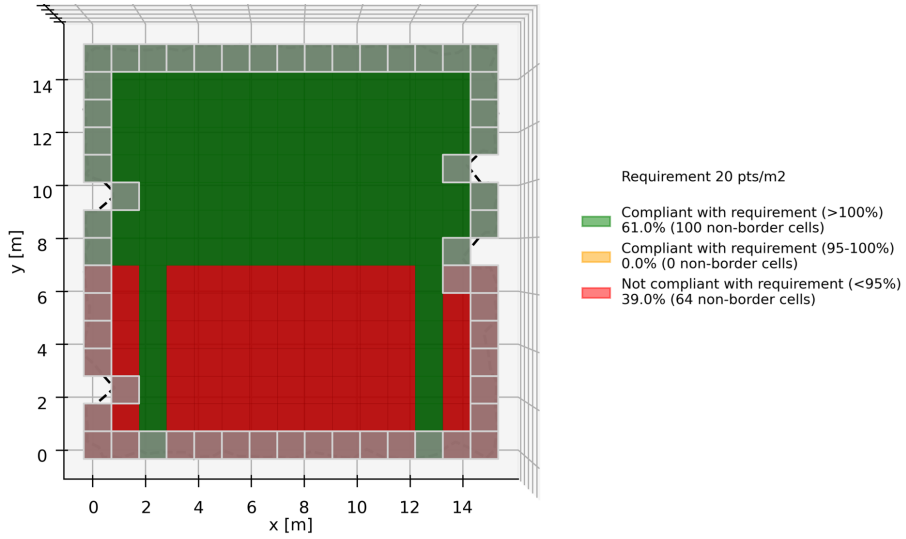

Figure 4.6. *Top view visualizing adherence to density requirement*

The *global point density*, representing the overall distribution across the dataset, is interpreted as the mean of the local densities. The histogram in Figure 4.7 visualizes the local point density distribution and the spread in relation to the global point density. In this view, it can be seen whether most points are close to or exceed the requirement.

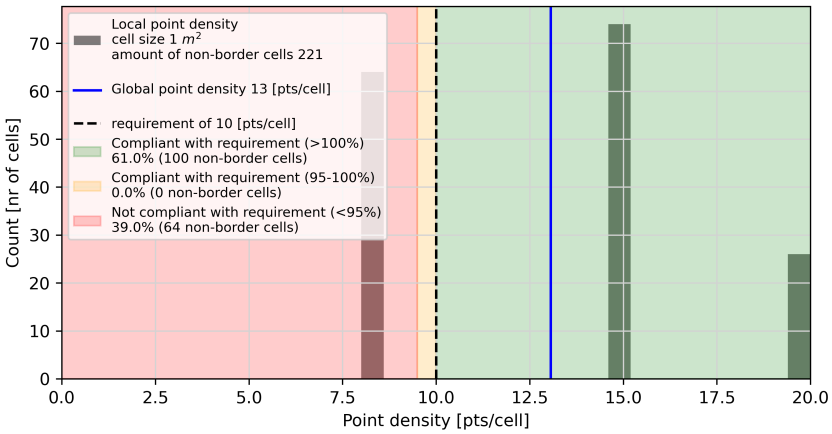

Figure 4.7. *Histogram visualizing adherence to density requirement*

The green-orange-red color scheme highlights cells where the point density falls below the requirement threshold. However, simply coloring cells red does not offer detailed insight into the extent of non-compliance. It is crucial to distinguish between cases where the point density is (only) slightly below the requirement and cases where it significantly deviates, possibly approaching an empty cell. To provide an isolated representation of densities below the requirement, the densities can be visualized, similar to Figure 4.5, but with a new color scheme. In the scheme, different hues of red indicate the range of densities, white represents a value above the requirement (and not of interest here), and black indicates a density of 0 points/m^2 (implying no points). The color scheme allows interpretation of the spatial arrangement of only the point densities under the requirement. For the demonstration point cloud, this analysis does not show much detail and thus is not shown here.

4.1.3 Height Analysis 2D Horizontal Cells

The current investigation of the point cloud focuses solely on the XY horizontal plane, and it is essential to recognize that this approach overlooks the height component. Given the nature of point clouds within a 3D space, exploring from a 3D perspective can unveil new insights and reveal previously unseen patterns. By examining key height metrics (such as the minimum, maximum, and mean) for each cell, the aim is to transition towards a partially-3D space.

The examination of the minimum and maximum heights within each cell reveals *extreme values* or *outliers*. Visualized in Figure 4.8 (top left and right), a high or low height compared to that of the surroundings is seen for the 3 modified cells. One can identify common infrastructure components like vehicles or light poles by analyzing the distinct cells.

On the other hand, examining the mean height for each cell provides information about the general height distribution within the area, as seen in Figure 4.8 (bottom left). The mean height offers a measure of overview, indicating the typical height within a given area. This information helps understanding the general elevation and identifying any areas of interest, such as regions with consistently high or low heights. Infrastructure elements typically exhibit consistent height patterns: for instance, road surfaces usually maintain uniform elevations across the spans but include a slope over their length.

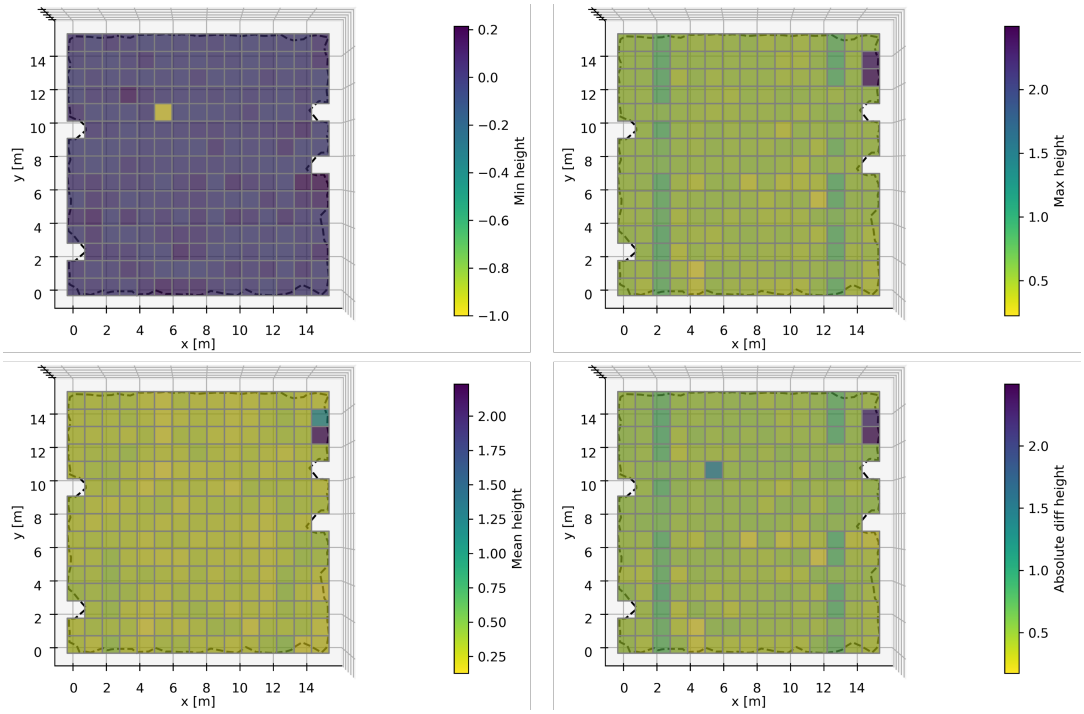

Figure 4.8. *Height analysis of 2D horizontal cells*
Top left: Minimum height of each cell, right: Maximum height of each cell
Bottom left: Mean height of each cell, right: Absolute difference between min and max of each cell

To investigate the heights within each cell , the user must be familiar with the point cloud data and understand object behavior within the dataset. This means that one must examine the point cloud to see what happens at particular locations. The point cloud could be viewed in RGB to provide users with easily interpretable information.

Key metrics such as minimum, maximum, and mean heights per cell offer only a singular perspective, neglecting a look at the broader distribution of height values within each cell. The histogram is employed to visualize the distribution of heights within each cell. Figure 4.9 (left) visualizes the points for one cell of 1 m^2. This schematic visualization provides a direct visual representation of the heights recorded in that specific cell. Figure 4.9 (middle) shows the resulting histogram, which visualizes the height distribution within the cell. The bars indicate the different height values occurring within the cell. Specifically, some heights are represented by only 1 point, while others have up to 3 points.

Unlike the histogram, which provides information about the individual height increments, the cumulative histogram accumulates the height information as it progresses through the height range. The function progresses from the bottom upwards. Thus, in Figure 4.9 (right), the top bar signifies the cumulative density of points within the cell. The cumulative view is particularly useful for understanding the *total point density* within a cell.

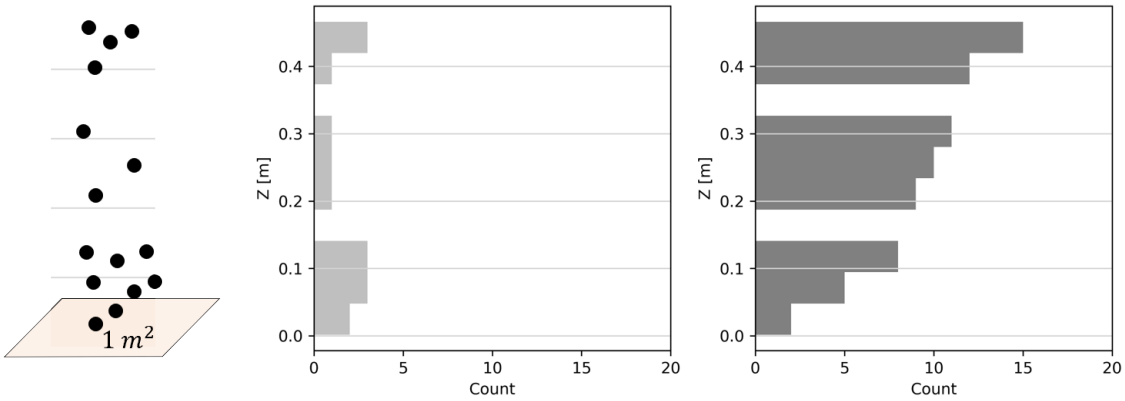

Figure 4.9. *Histogram and cumulative histogram of Z-values for one cell*
Left: Schematic visualization of points within one cell
Middle: Histogram representing the height distribution within cell.
Right: Cumulative histogram, which accumulates all points across height. The uppermost bar denotes the cumulative density of the entire cell, confirmed by the known density of 15 points per m^2.

4.1.4 Assessing adherence to 2D Density Requirement in Partial-3D Space

Section 4.1.2 demonstrated the assessment of the point cloud density in a 2D space. However, assessing the point cloud in a 3D space offers another perspective on visualizing adherence to the density requirement. By using the histogram and/or cumulative histogram for each cell, the heights are combined with the horizontal projections, moving towards a partial 3D-space.

Examining the adherence to the requirement within the histogram provides more detailed insights. Now, for each height, it can be assessed whether it meets the requirement. In Figure 4.10, heights (grey bars) that meet the requirement will exceed the requirement (blue line). In the 2D assessment, the density requirement was evaluated by comparing the total points within each cell, equivalent to evaluating within the top bar of the cumulative histogram.

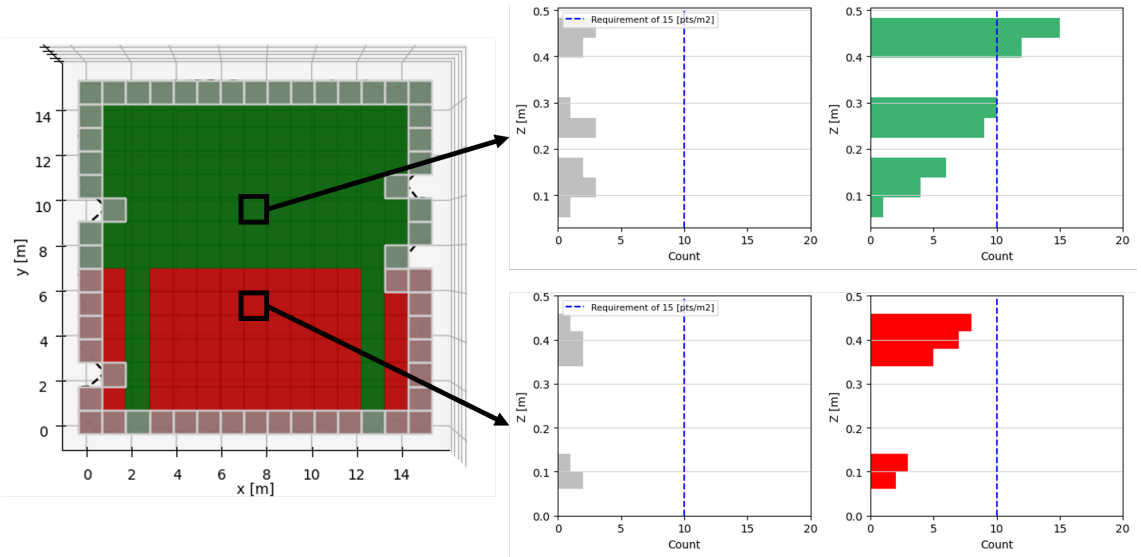

Figure 4.10. *Validation of 2D density requirement in partial-3D space*
Top: Histogram shows that the points are randomly distributed over a height of approximately 0.5 meters and do not meet the requirement. The cumulative histogram visualizes that the total of the cell adheres to the requirement.
Bottom: Histogram reveals that the requirement is unmet across all heights. Cumulative histogram illustrates that the overall cell density falls short of the requirement.

As illustrated in Figure 4.10, it could be that points in totality adhere to the requirement but that within each height range do not. In 3D environments (like tunnels) or for 3D objects (like lampposts), where different elevations are present, this way of validation becomes important.

4.2 Overlapping Regions Alignment

The alignment of points within overlapping regions is one of the methods that can be used to assess the *relative accuracy*. First, surfaces within the overlapping regions are extracted. Next, surfaces within the overlapping regions are compared. Finally, the adherence to the relative accuracy requirement will be assessed.

4.2.1 Location of Overlapping Regions

Subsection 2.4.2 introduced that the location for assessing the relative accuracy varies depending on the type of laser scanning (static, mobile, or airborne). In static configurations, multiple stationary set-ups are needed to adequately cover the desired extent due to the equipment's limitations. Each setup covers its own area with a 360-degree scan, creating a point cloud. For each scanner, a unique attribute should be assigned to keep track of the origin of the points within the composite point cloud. When using mobile or airborne configurations, the transport mode with the mounted laser moves and continuously captures multiple scans from various perspectives over time, leading to redundant measurements along the trajectory. Properly logging scanner trajectories is crucial for determining the location of overlapping regions.

The overlapping regions can be evaluated using different cross-sections as visualized in Figure 4.11.

- *Halfway Cross-Section*: Positioned midway between two adjacent measurement setups. The cross-section holds interest as it offers insight into the behavior of the scanners within a localized area.
- *Full-Length Cross-Section* Encompasses the entire span of the point cloud, including multiple measurement setups, the cross-section provides a comprehensive view. Allows for the assessment of relative accuracy across the entirety of the point cloud.

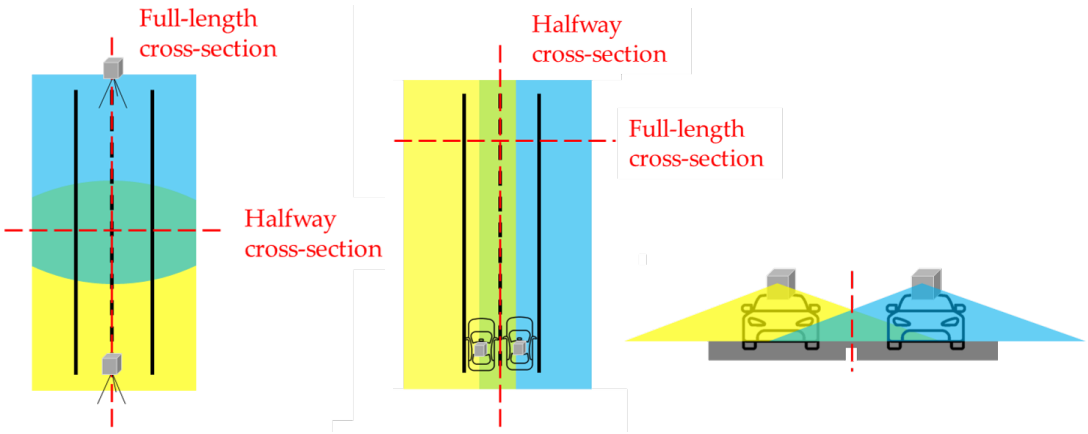

(a) *Static configuration* (b) *Mobile configuration*

Figure 4.11. *Overview location of cross sections between overlapping regions Yellow and blue represent 2 point clouds from different configurations. Green indicates the overlapping region. Red shows the cross-section location.*

4.2.2 Selection of Surfaces within Overlapping Regions

At the location of the cross-section, points are extracted. Rather than capturing a profile, which involves selecting only the points closest to the cross-section line, a broader strip of approximately 0.30[21] meters[22] is taken. By widening the cross-section, more data points are accessed, providing a more comprehensive understanding of the region's behaviors.

The task of directly comparing points from two (or more) point clouds within a cross-section strip is challenging due to the noise and irregularities in the data. The use of point-to-point distances is not effective as the points from different point clouds are captured from varying perspectives or at different times, leading to differences in point densities and distributions. It becomes necessary to represent the points using a geometric shape, which allows for the determination of distances in a manner that is not influenced by the distribution of the points and noise. As a result, a plane is selected to represent the points.

Representing the cross-section with a single plane is not reliable due to the presence of objects of varying heights. To achieve millimeter-level accuracy in the analysis, it is crucial to represent the point cloud within the cross-section as a collection of multiple planes. For example, the road surface would be represented by a nearly horizontal plane, while a lamp post would be represented by a vertical plane. Figure 4.12 shows an extracted cross-section strip of the highway, including the selection of different surfaces.

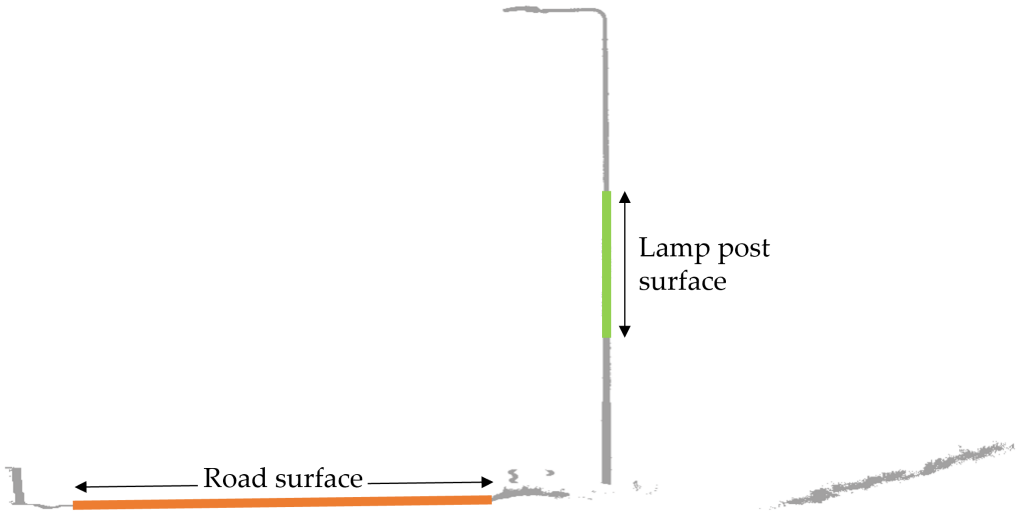

Figure 4.12. *Cross-section strip of highway*

Grey shows the full cross-section of 0.30 meters. Orange highlights a horizontal road surface. Green shows a vertical lamp post surface.

[21] This results in 0.15 meters at either side, i.e., 0.30 meters in total.

[22] Depending on the density of the point cloud, this distance may need to be adjusted. For mobile and airborne point clouds, it might be necessary to use a strip width of 0.50 meters to ensure an adequate number of points for analysis.

Horizontal surfaces, such as roads, provide insights into variations in height (Z) across the terrain. Conversely, vertical surfaces, like lampposts, offer valuable information for assessing XY-plane variations. It is sufficient to select one plane of each type, as it is expected that surfaces within the strip exhibit consistent behavior.

To demonstrate and validate the method for determining the relative accuracy, an (almost) horizontal surface is selected, subtly inclined to simulate a road surface. Across a 2 by 0.3-meter area, two different point clouds, labeled A and B, are generated, simulating different measurement set-ups. The x- and y-coordinates of the points are randomly distributed, reflecting differences in data origins from various scanners. Additionally, all scanners exhibit systematic deviations alongside inherent noise. This is represented by generating the height data as a normal distribution with a standard deviation of 5 millimeters. For the purpose of demonstration and analysis, the two point clouds have differing slopes: point cloud A descends while B ascends along the x-axis range, as depicted in Figure 4.13. Alternative configurations, such as one point cloud being offset from the other, are also possible.

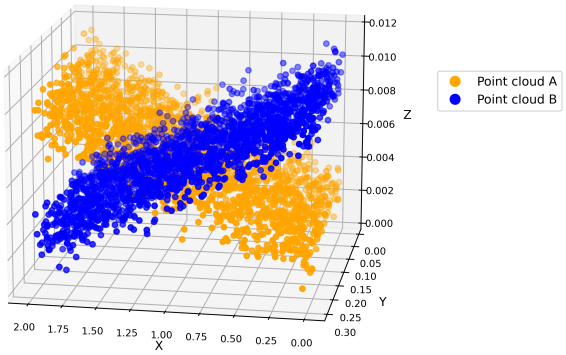

Figure 4.13. *Point clouds created for demonstration method*

4.2.3 Comparison of Surfaces within Overlapping Regions

The workflow for comparing the surfaces within overlapping regions includes the steps shown in Figure 4.14.

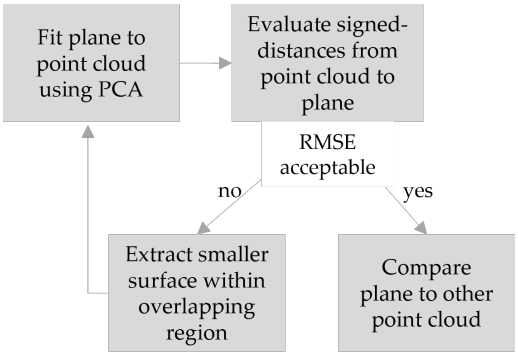

Figure 4.14. *Schematic overview comparing surfaces within overlapping regions*

1. Fit plane to point cloud using PCA: First, the focus is on point cloud A, shown in orange in Figure 4.13. The point cloud can be represented by a plane. As described in Subsection 2.5.2, a linear equation can describe a plane, and the parameters can be estimated using PCA. The fitted plane is shown in Figure 4.15.

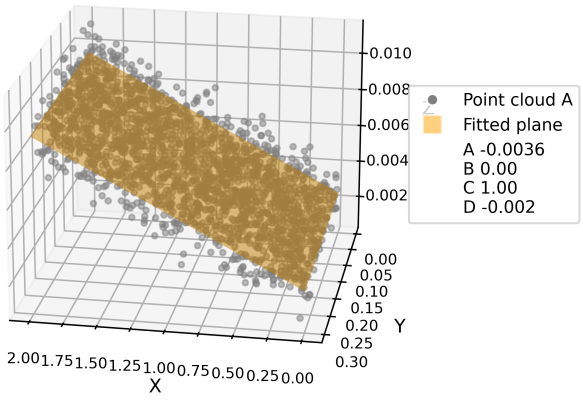

Figure 4.15. *Fitted plane to point cloud **A** using PCA*

2. Evaluate signed-distances from point cloud to plane: The representation of the plane is evaluated by calculating the signed distances from the point cloud to the plane, as introduced in Subsection 2.5.2. Figure 4.16 demonstrates this for point cloud A. As expected, the maximum distance in both directions is 3 millimeters. To determine if these distances are low enough for the plane to accurately represent the point cloud, the RMSE and the histogram of the distances must be considered. This evaluation serves as an overall test of the model's performance in representing the point cloud data. If the RMSE and histogram indicate that the distances are within an acceptable range and exhibit a suitable distribution, it suggests that the plane accurately represents the point cloud. However, if the results suggest otherwise, adjustments need to be made, such as selecting a smaller surface and fitting a new plane to improve the representation of the point cloud.

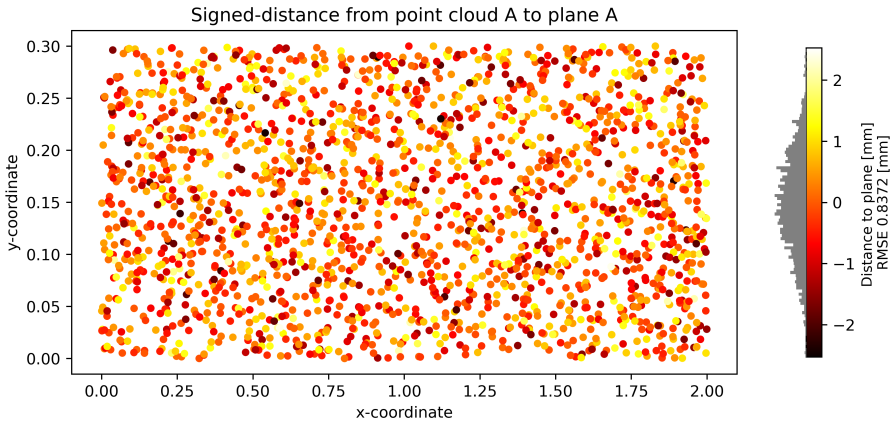

Figure 4.16. *Point-to-plane signed distance from point cloud **A** to plane based on point cloud **A***

3. *Compare plane to other point cloud*: Once the plane accurately represents the point cloud, a comparison can be made to the other point cloud. This involves calculating the point-to-plane distances for point cloud B relative to the plane fitted to point cloud A, shown in blue in Figure 4.13. The results are displayed in Figure 4.17, revealing a distinct pattern: to the left, the distance is 8 mm; in the middle, the distance is 0 mm; and to the right, the distance is -8 mm. This pattern aligns with expectations from Figure 4.13, where the point clouds cross each other in the middle.

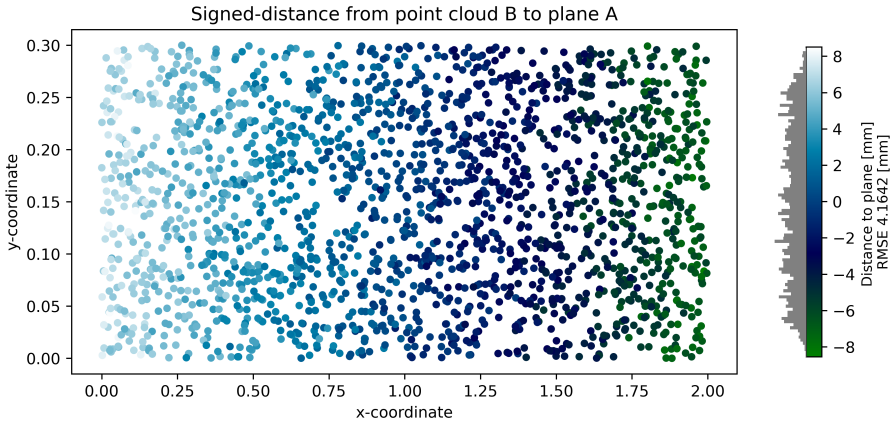

Figure 4.17. *Comparing the point cloud by analyzing the point-to-plane signed distance from point cloud **B** to plane based on point cloud **A***

Repeat Analysis: Repeat steps 1 - 3, but this time, fit the plane based on the comparison point cloud (point cloud B). This process is shown in Figure 4.18. Repeating the process serves as a form of cross-validation, ensuring the robustness of the plane fitting process. By fitting a plane to point cloud B and then comparing it to point cloud A, it can be verified whether the observed patterns are consistent and reliable. Additionally, this approach mitigates the risk of bias that might arise from relying solely on one point cloud for plane fitting. Notably, this process should yield almost identical results.

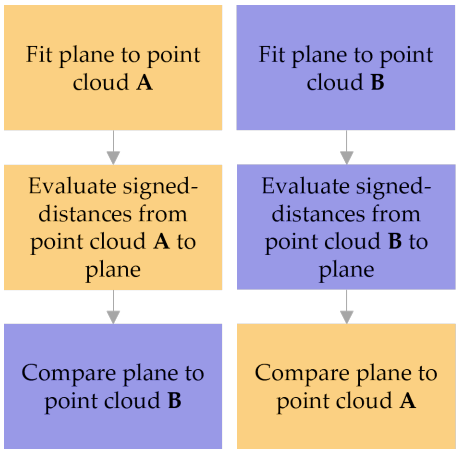

Figure 4.18. *Workflow analysis for comparison point clouds*

For the demonstrated point cloud, the only differences observed are in the figures showing the signed distances. When fitting the plane to point cloud B, the opposite pattern in the signed distances is seen.

4.2.4 Assessing adherence to Relative Accuracy Requirement

Validating the point cloud's relative accuracy requires assessing the adherence to the requirement. Similar to what is described in subsection 4.1.2, a color-coded system will be used to visualize and represent the results.

- *Green*: Compliant with requirement (< requirement)
- *Orange*: Compliant with requirement (between requirement and 105%)
- *Red*: Not compliant with requirement (>105% of requirement)

The relative accuracy of the point cloud can be intuitively assessed using the RMSE. The RMSE provides a measure of the overall deviation of the points from the fitted plane. A lower RMSE suggests that the points are closely clustered around the plane, whereas a higher RMSE indicates greater deviations. If the RMSE is below the relative accuracy requirement threshold, the point cloud can be considered to meet the accuracy requirements. For the demonstration point cloud, the RMSE value is displayed in Figure 4.17 next to the color bar as 4.162 mm. The requirement for this hypothetical situation is set at 5 mm. Given this threshold, the RMSE for the point cloud is evaluated as follows:

$$\begin{aligned} \text{RMSE} &\leq \text{requirement} \\ 4.162\,[\text{mm}] &\leq 5\,[\text{mm}] \end{aligned}$$

Evaluating the relative accuracy using the RMSE suggests that the requirement is met within the overlapping area. However, when testing the requirement against every point in the point cloud, a distinct pattern emerges, as shown in Figure 4.19. The pattern highlights areas of compliance (green and orange) and non-compliance (red). Notably, compliance is observed in the middle of the point cloud, while closer to the edges, deviations exceed the specified threshold.

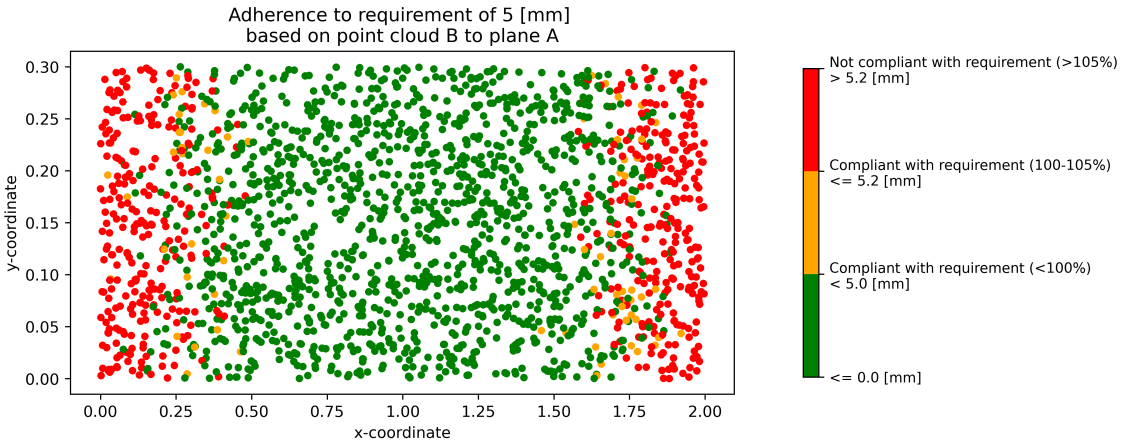

Figure 4.19. *Adherence to relative accuracy requirement from point cloud **B** to plane based on point cloud **A***

Supplementary Figure 4.20 visualizes the histogram showing the distances and adherence to the requirement. The figure provides insights into the distribution of distances across the point cloud and how it aligns with the specified requirement. Additionally, the percentage and count of points within each color group are displayed.

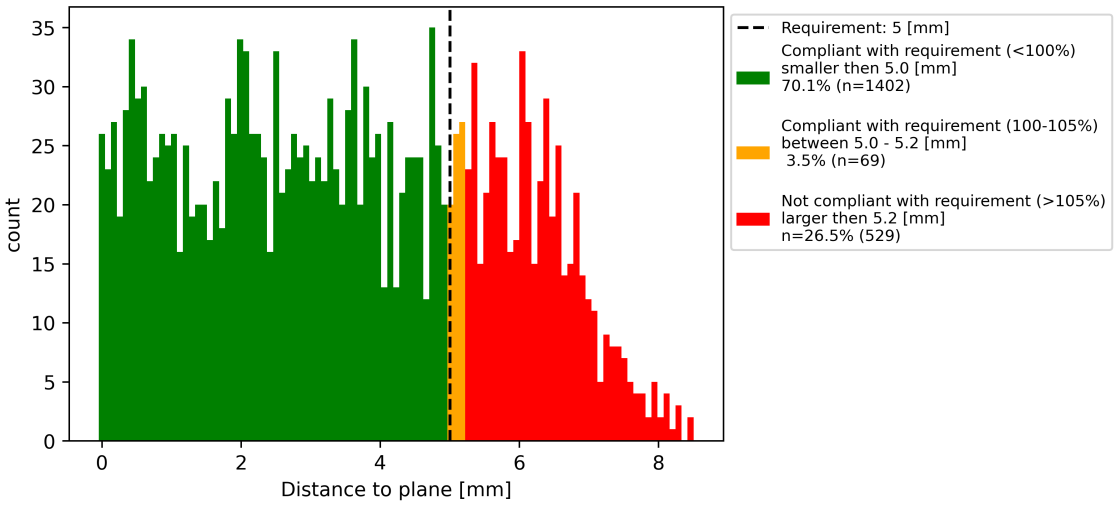

Figure 4.20. *Histogram distances from point cloud **B** to the plane based on point cloud **A** and the adherence to requirement*

Figures 4.19 and 4.20 highlight the importance of considering the distribution of deviations across the entire point cloud, rather than relying solely on aggregate measures like the RMSE. By examining individual points, a more nuanced assessment of compliance with accuracy requirements can be achieved, leading to a more robust evaluation of the point cloud's overall quality.

4.3 Benchmark Alignment

To evaluate the *absolute accuracy*, the alignment between known positions of benchmarks and estimated locations within the point cloud is examined. Discrepancies between the coordinates indicate the level of alignment. First, the points corresponding to the spherical targets are extracted, followed by estimating the center coordinate of the sphere. Finally, the absolute accuracy requirement is validated for each sphere.

Assessing the absolute accuracy of the entire point cloud requires the evaluation of multiple spheres, as each sphere provides only partial information. Only when considering the collective data from multiple spheres, can a comprehensive assessment of the absolute accuracy of the entire point cloud be made.

4.3.1 Extraction of Points corresponding to the Spherical Targets

Within this study, only spherical benchmarks will be investigated. To identify points corresponding to the spherical targets in the point cloud, a multi-step process is employed, integrating various techniques as shown in Figure 4.21.

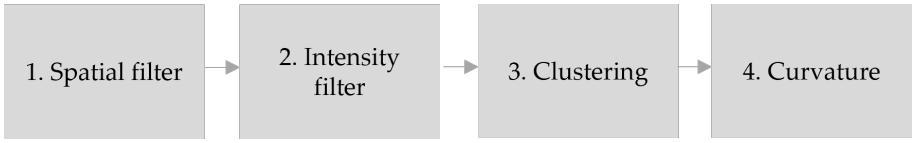

Figure 4.21. *Schematic overview steps extraction points spherical targets*

1. Spatial filter: A search radius of 0.5 meters[23] around each benchmark's coordinates is employed to extract points in its vicinity, as illustrated in Figure 4.23a.

2. Intensity filter: Leveraging the known fact that benchmarks have a higher intensity than that of the surrounding, an intensity filter will be employed. Rather than relying on a fixed intensity threshold, a dynamic approach is adopted that considers the distribution of intensity values. Adaptability is necessary because different encoders may be utilized, resulting in varying intensity ranges. As shown in Figure 4.22, the intensity histogram typically exhibits a normal distribution with a right tail[24]. The prominent peak in the histogram predominantly originates from points reflecting off surfaces like concrete (such as tunnel ceilings) and asphalt (like roads), while the tail contains high-intensity values associated with features like road markings, tunnel walls, and spherical targets.

To determine the *intensity threshold* that effectively isolates high-intensity points and thus filters out background noise, the inflection point within the histogram must be found, a process illustrated in Figure 4.22. This inflection point can be discerned using the CDF, as it is the point where the CDF stabilizes. Subsequently, points falling below the determined intensity threshold are filtered out. The result is demonstrated in Figure 4.23b where the points filtered out are shown in grey, and the points remaining after the application of the filter are colored.

[23] This assumes that the target already lies within half a meter of the known coordinate. If uncertain, the search radius should be enlarged to ensure that the target is within the extracted area.

[24] This behavior is for static- and mobile-derived point clouds. Airborne-derived point clouds exhibit different behavior due to the stronger influence of the surroundings.

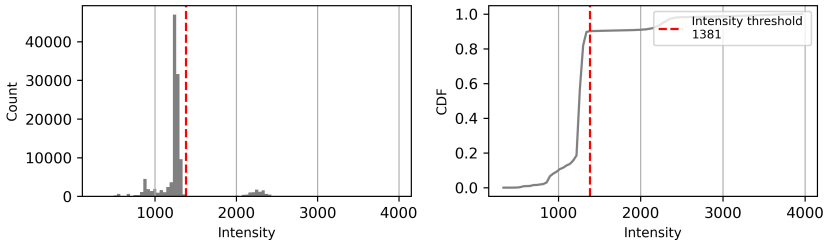

Figure 4.22. *Intensity threshold*

3. *Clustering*: A clustering algorithm is applied to group the data based on spatial proximity. The popular Density-Based Spatial Clustering of Applications with Noise (DBSCAN) algorithm is chosen for its ability to identify clusters of varying shapes and sizes. The parameters of the algorithm, such as the maximum distance defining the neighborhood radius (ϵ) and the minimum number of points required to form a dense region (min_sample), are tailored according to the characteristics of the dataset. The parameters should be configured so the algorithm groups the data into a single cluster in scenarios where only the sphere is present. Figure 4.23c shows the result, where 4 clusters are highlighted with varying colors (green, orange, blue and red).

4. *Curvature filter*: The curvature of each clustered region is computed, with the expectation that the cluster demonstrating the greatest curvature corresponds to the sphere. The curvature is approximated as the ratio of the smallest eigenvalue (determined through PCA) to the sum of all eigenvalues. The resulting cluster contains the points belonging to the sphere as shown in Figure 4.23d (blue).

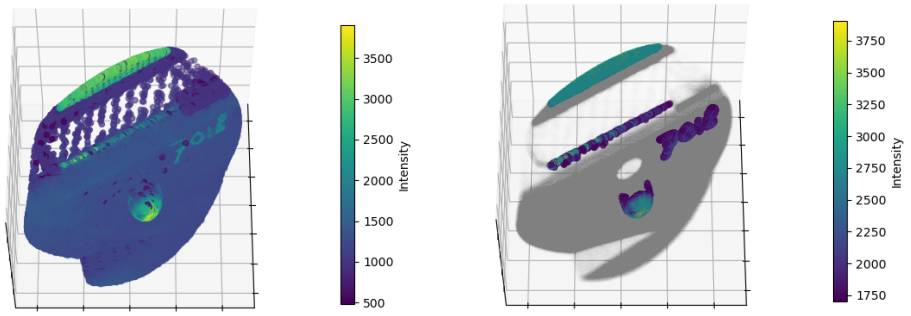

(a) *Result spatial filter* (b) *Result intensity filter*

(c) *Result clustering* (d) *Result curvature filter*

Figure 4.23. *Result extracted target*
Grey points are filtered out, colored points are the result of the filter

4.3.2 Estimating Center Coordinate of Sphere

The points to be compared with the known locations need to be identified. For the spherical benchmarks, this comparison should be made using the center. To estimate the center, either Least Squares (LS) or Random Sample Consensus (RANSAC) can be utilized as described in Subsection 2.5.3. Both LS and RANSAC operate under the assumption that a sphere can adequately represent the data. However, if the actual shape deviates from a perfect sphere, the fitted parameters will inherently contain inaccuracies. When measuring a sphere with a laser scanner, the sphere may undergo slight distortion or incomplete scanning, further complicating the fitting process. The following workflow implements both RANSAC and LS to overcome such implications.

1. *RANSAC for Outlier Removal*: To fit a sphere to the point cloud, the RANSAC algorithm is utilized as described in Subsection 2.5.3. The RANSAC method iteratively selects a random subset of points to hypothesize a sphere model and then determines the number of inliers that fit the model. The RANSAC method removes outliers based on a given distance, this way inliers that conform to the spherical model are selected.

2. *LS Sphere Fitting on inliers*: Least Squares, as described in Subsection 2.5.3, is performed to estimate the sphere parameters based on the inlier points. The estimated radius tends to be too large due to the LS method's susceptibility to outliers. The issue is evident in the distribution of the distances, which follows an (almost) normal distribution centered around the RMSE.

3. *Centralized RMSE Adjustment*: The radius is adjusted by subtracting the RMSE from the initial estimate, effectively centralizing the fit. The adjustment corrects any consistent bias in the initial radius estimate. By reducing the systematic error, the adjusted radius aligns more closely with the actual distribution of points. The final fitted sphere is visualised in Figure 4.24.

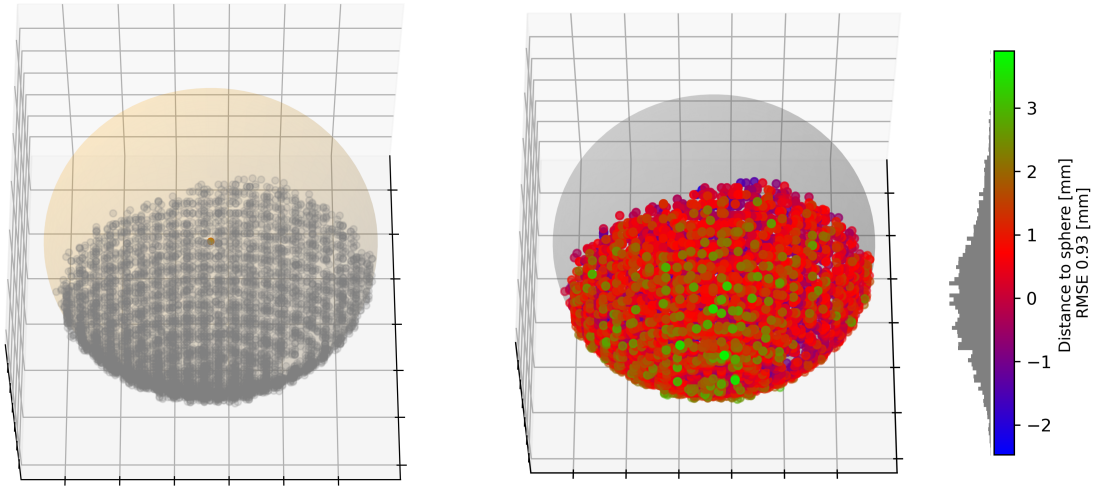

(a) *Fitted sphere* (b) *Distances to fitted sphere*

Figure 4.24. *Final fitted sphere*

4.3.3 Assessing adherence to Absolute Accuracy Requirement

The same color-coded system will be utilized as described in Subsection 4.2.4 for the absolute accuracy requirement. The system visually represents compliance levels with the absolute accuracy requirement using three distinct colors:

- *Green*: Compliant with requirement (<100%)
- *Orange*: Compliant with requirement (100%-105%)
- *Red*: Not compliant with requirement (>105%)

However, in this scenario where only one point is available for comparison, the RMSE is the primary metric for evaluating absolute accuracy. This single-point comparison allows for a direct assessment of the deviation from the reference point, making the RMSE an appropriate measure in this context.

$$\text{RMSE} \leq \text{requirement}$$

Essential to note is the fact that one point alone does not provide sufficient information to ascertain adherence to the absolute accuracy requirement accurately. To comprehensively evaluate absolute accuracy, the assessment must consider multiple benchmarks. Only when considering the collective data from multiple benchmarks can a robust determination of the absolute accuracy of the entire point cloud be made.

5 Results

The following sections apply the methods described in Chapter 4 to the point clouds within the PTZ project. Section 5.1 presents the results of validating the component coverage. Section 5.2 provides the results concerning relative accuracy. Section 5.3 presents the results regarding absolute accuracy.

5.1 Results Validation of Coverage

The following sections present the results regarding the validation of the component coverage. For this, the point cloud density method is investigated for the composite point clouds. Subsection 5.1.1 covers the results for the static point cloud, Subsection 5.1.2 presents the mobile point cloud, and Subsection 5.1.3 presents the airborne point cloud.

5.1.1 Point Cloud Density of Static Point Cloud

The static point cloud density is first processed for the individual point cloud tiles (within the AOI). Tiles ending in numbers 28 through 38 indicate the tunnel area, and tiles 39 to 43 represent the road section.

2D Point Cloud Density

Figure 5.1 visualizes the point density for each 1 m^2 cell, presenting results for all the tiles relative to each other. As the linear scale fails to reveal insights into the lower-density cells due to the large variation of point densities (ranging from 10 to 5,000,000 points/m^2), a logarithmic scale is used.

Within a radius of approximately 5 meters from the stationary scanner (indicated by the white points in the figure), high densities can be seen (indicated by the purple color). Closest to the scanner, point densities can reach up to 5 million points per m^2. The point density decreases with increasing distances from the location of the scanner. This behavior is attributed to the geometry of the laser scanner as discussed in Section 2.1.

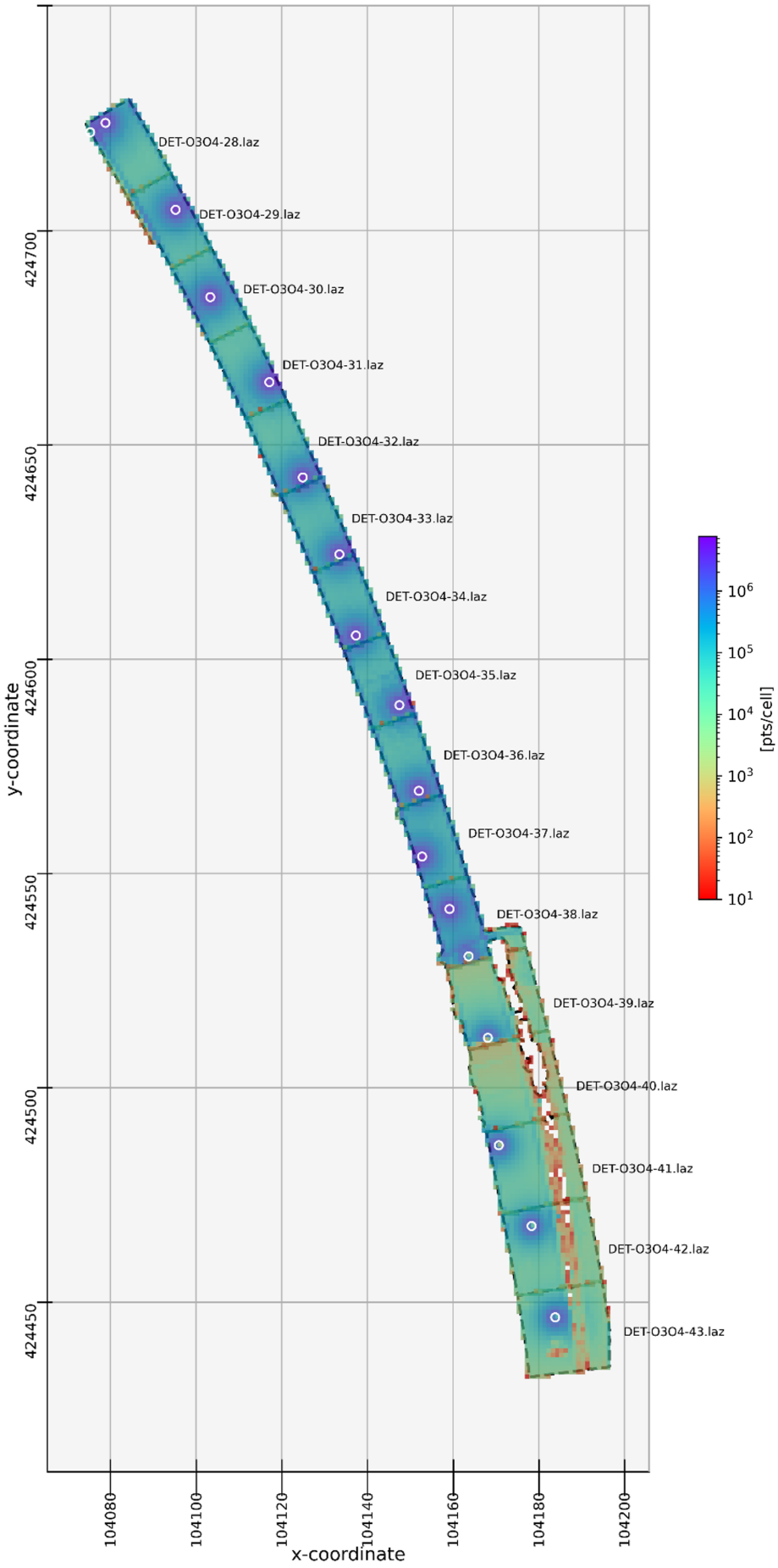

Figure 5.1. *Result local point cloud density static point cloud. Densities displayed on logarithmic scale. Red indicates densities of ten points/m^2, green densities of ten thousand points/m^2, purple a million points/m^2*

Assessing adherence to 2D Density Requirement

In Subsection 3.1.2, the density requirement for the static scans is specified to be at least 10 points per cm^2. However, due to computational costs, the investigation is conducted at the meter level rather than the centimeter level. Consequently, the requirement must be recalculated, translating to 100,000 points per m^2. The resulting compliance to the density requirement is shown in Figure 5.3. Between the road and tunnel tiles, two distinct spatial patterns become evident.

Point cloud density of tunnel tiles: In the tiles including the tunnel, a pattern is seen where cells within a 10-meter radius of the scanners meet the requirement, orange cells appear at the borders of the radius, and cells between the scanners show insufficient densities and are consequently colored red. On average, the tunnel tiles are 66.5% colored green, 1.5% colored orange, and 31.9% red, as presented in Table 5.1.

Figure 5.3 does not illustrate the extent to which the point densities fall short of the specified requirement. To assess the extent of non-compliance among the red classified cells, Figure 5.2 illustrates the densities of only the cells falling below the requirement. The densities are represented with a linear scale where black indicates empty cells (point density close to 0 points per m^2) and grey are cells with densities above the requirement ($\geq$ 100,000 points per m^2). Within the tunnel, the cells that are not compliant have densities averaging around 60,000 points per m^2. However, in the northernmost section (tile 28), densities drop to as low as 25,000 points per m^2.

Point cloud density of road tiles: Where for the tunnel, over half is colored green; in contrast, the majority of road tiles are colored red in Figure 5.3. Even the most satisfactory tile has only 21% of its cells colored green. The least satisfactory tile achieves just 1.6% compliance. The same pattern emerges where only in close proximity of around 5 meters to the scanner the requirement is met. On average, the road tiles are 14.8% colored green, 0.5% colored orange, and 87.7% red, as shown in Table 5.1.

Figure 5.2 highlights the contrast between the point densities of road and tunnel tiles. On average, the road cells contain around 10,000 points per m^2. Notably, to the right of the road, cells with densities close to 0 points per m^2 are observed, which, upon closer examination, reveal to be vegetation. Ideally, the vegetation has to be removed as it lies beyond the project boundary, leading to a potentially misleading representation.

Tile	**Compliant with requirement (>100%)**	**Compliant with requirement (95-100%)**	**Not compliant with requirement (<95%)**
Average for tunnel tiles	66.5%	1.5%	31.9%
Average for road tiles	14.8%	0.5%	84.7%

Table 5.1. *Result of compliance to requirement presented in terms of average percentage for tunnel and road tiles*

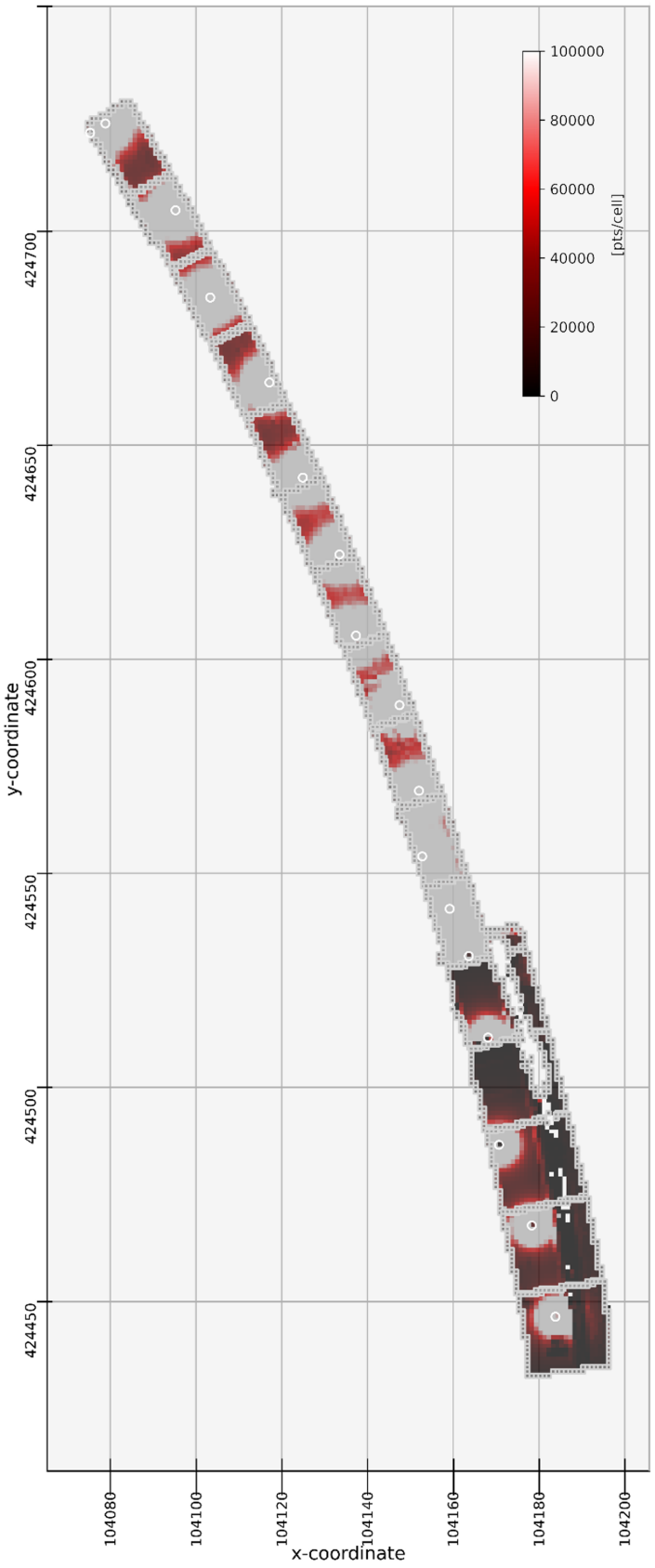

Figure 5.2. *Local point cloud density of cells not compliant with requirement of static dataset Densities displayed on linear scale. Grey for exceeding requirement of 100,000 points/m^2, red in between, black if empty cell*

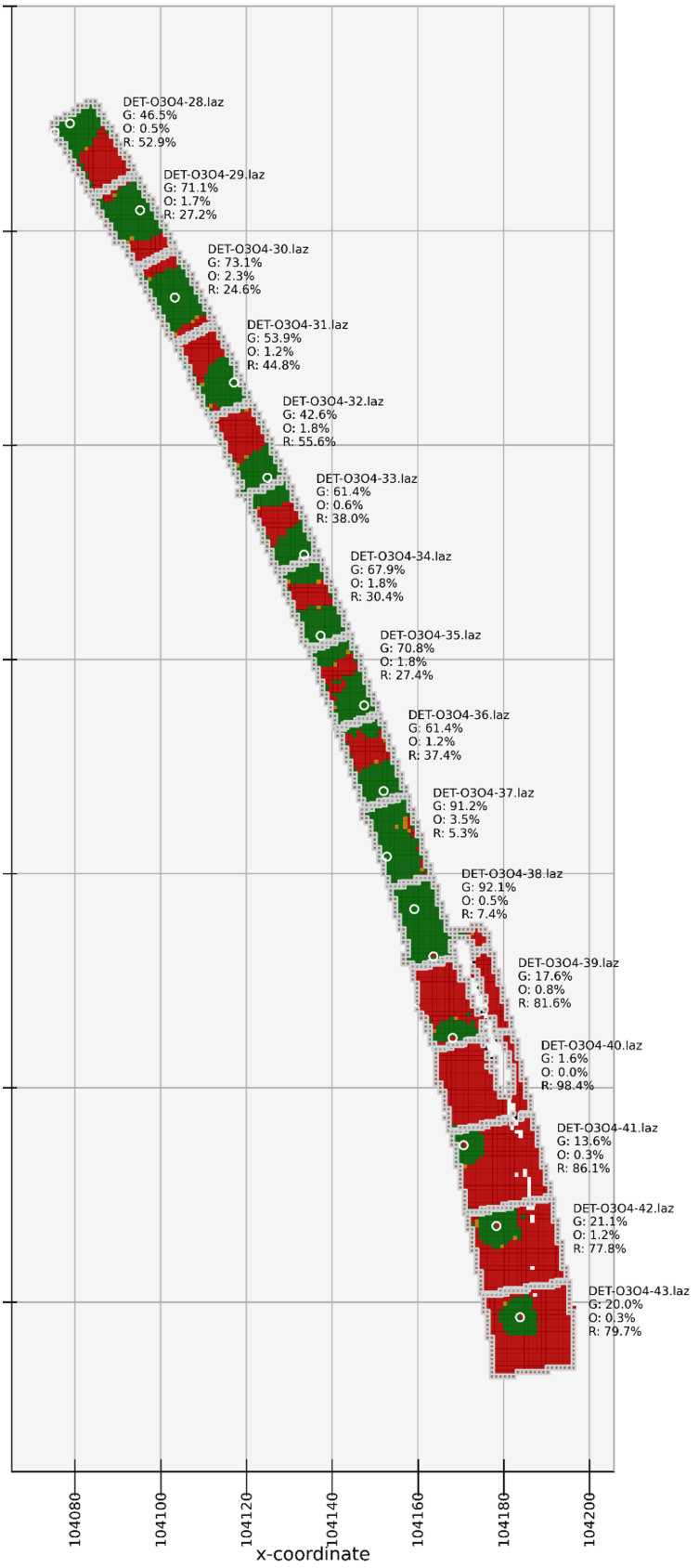

Figure 5.3. *Result adherence to density requirement of 100,000 points/m^2 of static point cloud. Red indicates not compliant with requirement (<95%), orange indicates compliant with requirement (95%-100%), and green compliant with requirement (>100%)*

Overall Point cloud density: The requirement stipulates that 95% of the total point cloud must meet the specified criteria rather than the individual tiles. The total compliance is assessed based on the average density across the entire point cloud, thus encompassing both road and tunnel sections. As shown in Table 5.2, 51.6% of the entire point cloud meets the requirement (green and orange combined), while 48.4% is non-compliant.

Tile	**Compliant with requirement (>100%)**	**Compliant with requirement (95-100%)**	**Not compliant with requirement (<95%)**
Average	50.4%	1.2%	48.4%

Table 5.2. *Result of compliance to requirement for overall point cloud density*

Point cloud requirement: From the presented results, it is evident that the point cloud does not comply with the current point cloud density requirement. Given that the scanners are already spaced at 20-meter intervals, the practicality of the current requirement is questionable. With 150 setups deployed across the project, adding more scanners would significantly impact both time and cost, raising the question of necessity.

Based on Figure 5.2, within the tunnel, a more feasible and realistic density requirement would be 50,000 points per m^2. At the square centimeter level, this translates to one point at each corner of the cm^2 and one in the center. For the road tiles, a requirement of 20,000 points per m^2 is more appropriate. However, even such requirements may be excessive. If the road surface consists solely of asphalt, such a high level of detail may not be necessary. The significant variations in densities across different environments (road and tunnel) demonstrate that a single requirement for all environments is unsuitable. Consequently, relying on an average value that spans multiple environments is inappropriate.

Point cloud completeness: Additionally, relying on the average density over an entire area, even within a single environment, must be critically evaluated. For instance, now if the average density meets or exceeds 99%, the point cloud is deemed acceptable. However, the approach overlooks scenarios where cells are completely empty and the average still indicates overall validity. This poses a significant issue if these empty areas correspond to crucial objects or if the total area is large enough that 1% represents a substantial portion.

A more reliable approach involves assessing the compliance of predetermined areas, such as individual tiles, with a target of 99% adherence rate for each tile. The method ensures that critical regions are adequately covered and that the dataset's integrity is maintained throughout the project.

Validation of 2D Density Requirement in Partial-3D Space

The requirement is investigated in a partial-3D space to assess whether the requirement is met for each height. The evaluation in a partial 3D-space entails examining the histogram for each cell. The analysis is performed for a road and tunnel tile. Figure 5.4 visualizes the result for the tunnel tile 'DET-O3O4-29' of the static point cloud. In the figure, four cells, including the histograms and cumulative histograms, are highlighted and examined more closely. The histograms and cumulative histograms are on the same scale as the requirement, with height ranges for every meter.

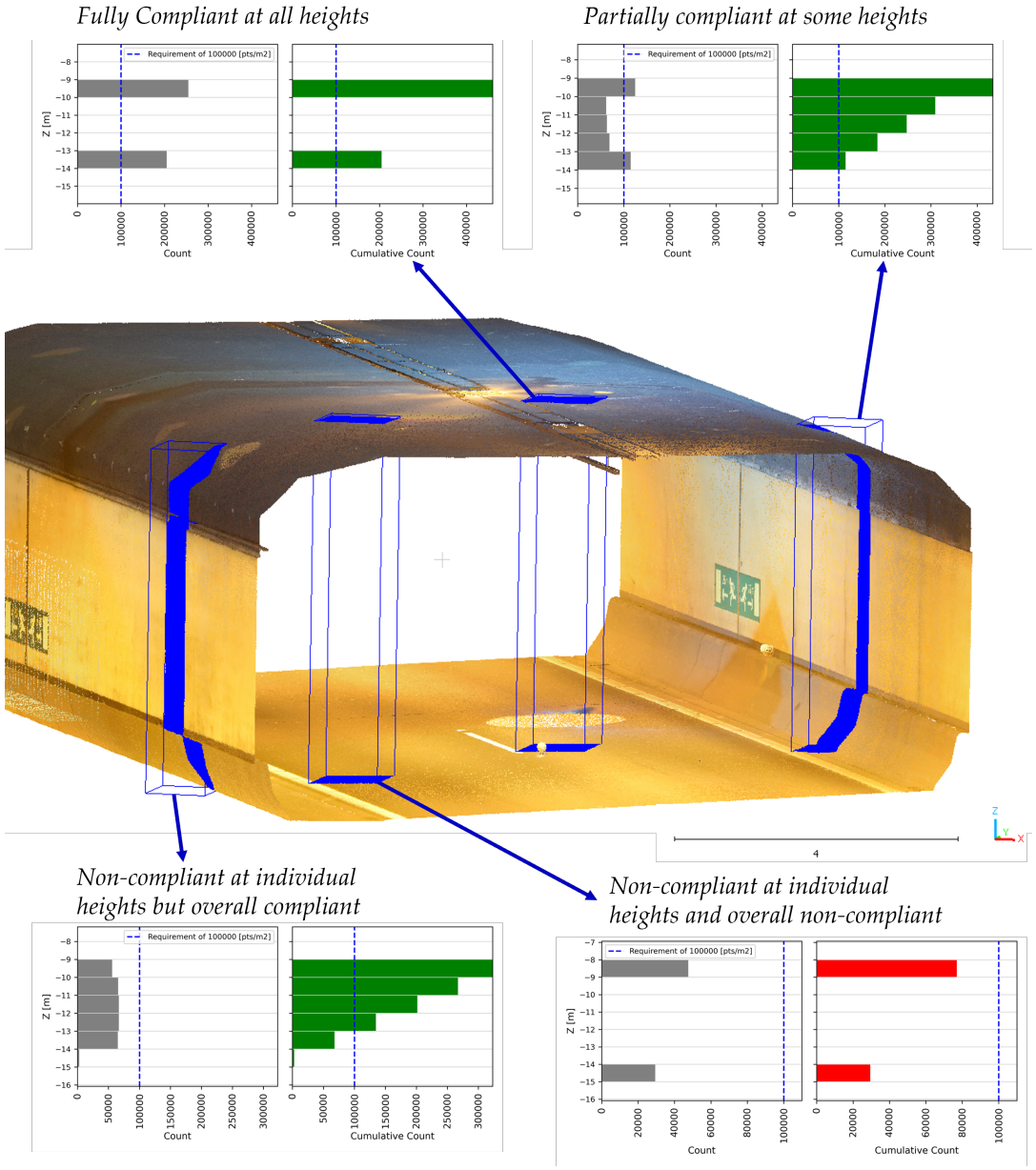

Figure 5.4. *Result validation of 2D density requirement partial-3d space focus on tunnel for static point cloud*

Fully Compliant at all heights: Figure 5.4 (top left) illustrates a cell situated in the middle of the tunnel. In the histogram, this can be observed with heights recorded at -14 meters, followed by a gap of 3 meters, and then points recorded at -10 meters. These values correspond to the tunnel's bottom (road) and top (ceiling), respectively. The histogram demonstrates that at each height range, the requirement (represented by the blue dashed line) is satisfied (indicated by the bars exceeding the requirement line). The cumulative histogram of the cell confirms that the entire cell meets the requirement, which is expected since the individual height ranges are already compliant.

Partially compliant at some heights: Figure 5.4 (top right) shows a cell situated along the wall of the tunnel. This is visible in the histogram, which shows points distributed over a 5-meter height range. The histogram indicates that only the bottom and top bars adhere to the requirement, while the middle three bars fall short. This discrepancy occurs because these cells receive less scanner coverage due to location and angle. Consequently, the cumulative histogram shows compliance (indicated in green) as some height ranges meet the requirement, suggesting that the overall cell adheres.

Non-compliant at individual heights but overall compliant: Figure 5.4 (bottom left) shows a cell situated along the wall of the tunnel. The histogram reveals that the requirement is not met across the individual 1-meter segments. However, the cumulative histogram, which accumulates all the points within the cell, indicates that the total number of points exceeds the requirement, resulting in overall compliance.

Non-compliant at individual heights and overall non-compliant: Figure 5.4 (bottom right) shows a cell situated in the middle of the tunnel. The histogram indicates that the requirement is not met at both the bottom and the top. Additionally, summing up the points in the cumulative histogram reveals that the total number of points is insufficient to meet the requirement, resulting in the cell being colored red.

The four cells are chosen strategically to highlight all possible scenarios when analyzing a 2D requirement within a 3D space. In a 2D analysis, the cumulative histogram of the entire cell is considered to determine compliance. If the overall cell adheres to the requirement, the cell is deemed compliant. However, the analysis of the four cells reveals that while the overall cell may comply with the requirement, individual 1-meter segments within the cell may not.

The discrepancy can be exemplified by scenarios where the majority of points (e.g., 99%) are densely concentrated within a narrow height range, such as near the tunnel ceiling, while only a minimal fraction of points are distributed across other areas, such as the tunnel floor. Despite meeting the requirement in terms of overall density, such a distribution may fall short of fulfilling the intended objectives, particularly in the context BIM, where uniform detail across the entire space is essential.

These findings underscore the importance of tailoring requirements specific to 3D environments. For 3D environments, such as tunnels, a 2D requirement for the entire point cloud does not suffice. Instead, adopting a more nuanced approach by establishing 3D density requirements specific to each object type, such as tunnels, ensures comprehensive coverage across all height dimensions, thereby minimizing gaps within the height dimension.

Additionally, the analysis for road tile 'DET-O3O4-41' is presented in Figure 5.5. The left figure shows a road cell that meets the requirement, while the right figure shows one that does not. Since the height increments are only 1 meter, the histogram and cumulative histogram are identical, making analysis across different heights less relevant.

As a result, assessing 2D density requirements in a partial 3D space for road tiles provides limited insight. When a cell consists solely of road surfaces, points tend to cluster within a narrow height range. Consequently, a 3D analysis focusing on height variations does not reveal significant patterns. However, the presence of objects like lamp posts introduces height variability, making 3D analysis relevant once again.

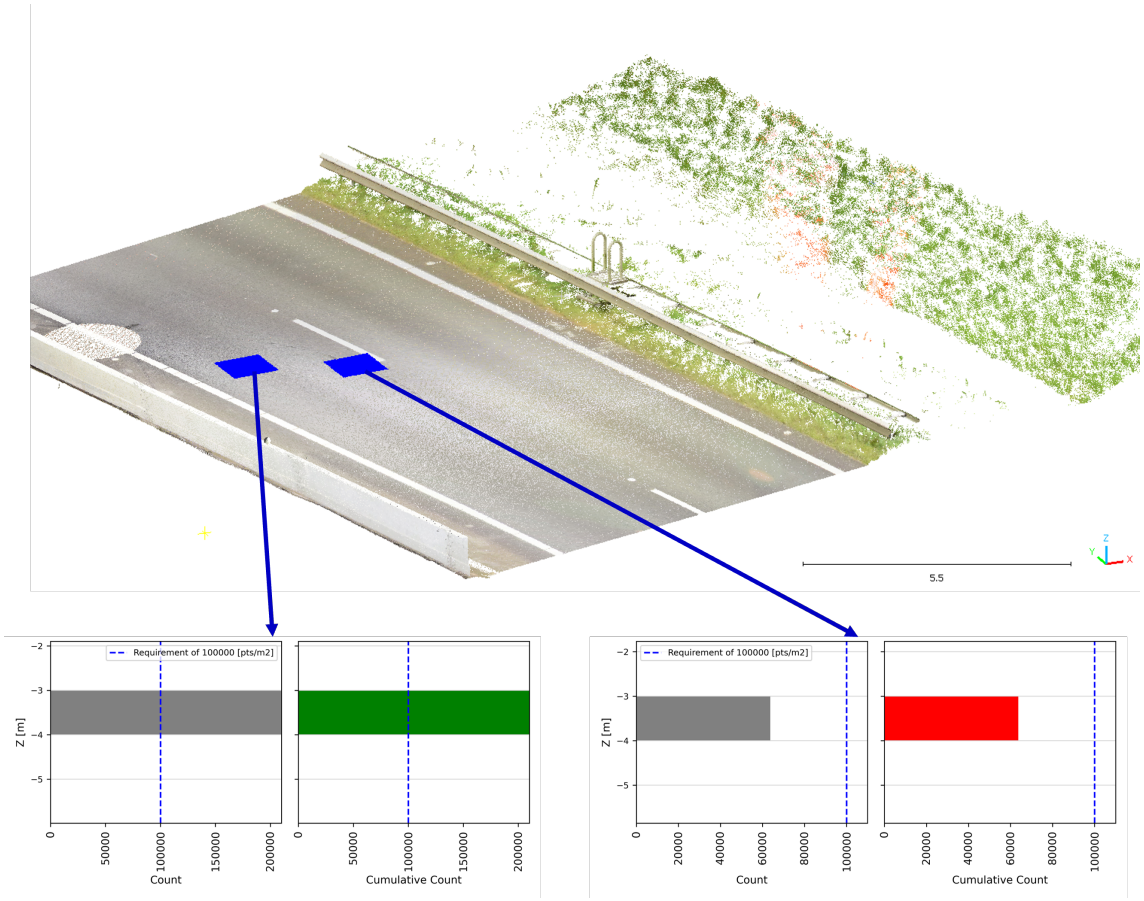

Figure 5.5. *Result validation of 2D density requirement partial-3d space focus on road for static point cloud*

5.1.2 Point Cloud Density of Mobile Point Cloud

The following section presents the results of the point cloud density for the mobile point cloud. The AoI of the mobile point cloud only contains road surfaces over 2 lanes.

2D Point Cloud Density

Figure 5.6 shows the point density for each 1 m^2 cell of the mobile point cloud. A linear scale is used because the range of point densities is not too high, 200 until approximately 3100 points per m^2, such that detail is lost.

In the middle of the point cloud, there is an area with densities of approximately 2000 points per m^2 (blue color). The area includes the two lanes where the scanner has driven and created an overlap of points. The high densities in the strip correspond to both of the paths that the vehicle has driven; one to the left and one to the right within the strip. The high density occurs because the scanner was in close proximity to the road and directly facing it. In contrast, areas adjacent to the road, at oblique angles to the scanner's line of sight, receive less coverage and exhibit lower point densities, around 1000 points per cell (orange color).

Interesting is that at the left border of the figure, high point densities of around 3000 points per m2 are visible. The area corresponds to a guard rail approximately 1 meter in height. It is noteworthy that this is one of the few structures in the vicinity that exhibits variation in height; the remainder of the terrain consists mostly of asphalt and thus remains relatively flat.

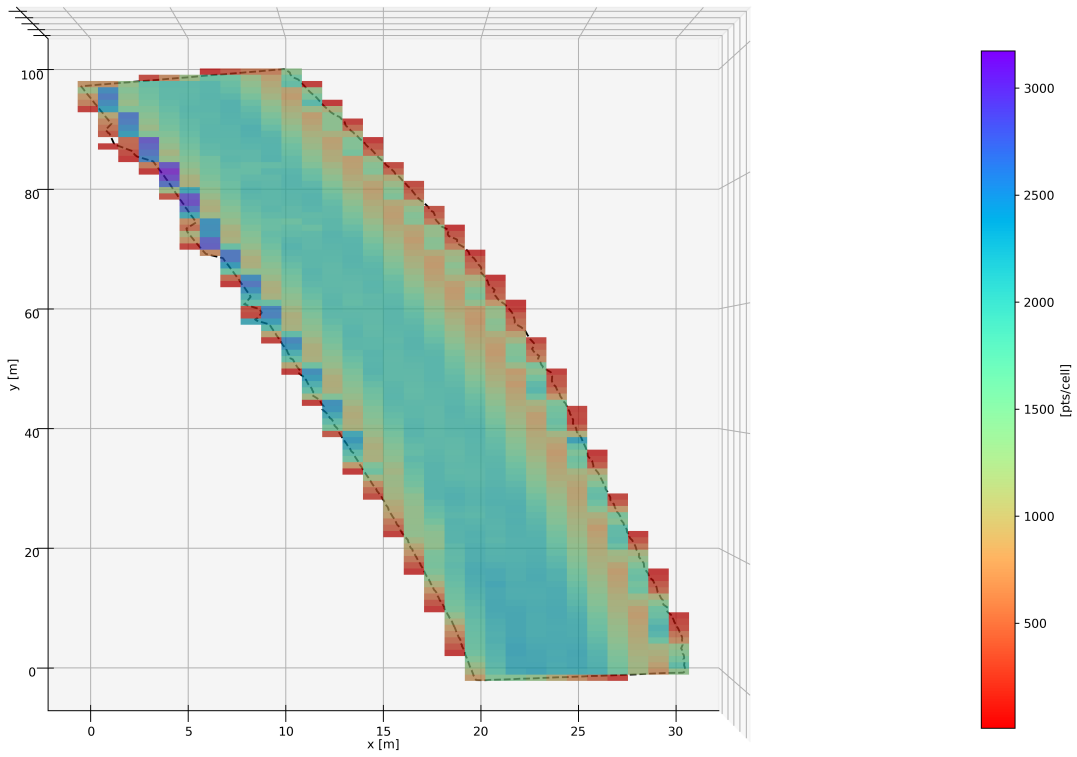

Figure 5.6. *Result local point cloud densities mobile point cloud*

Referring to the specifications of the mobile scanning equipment Riegl VMX-450 (Riegl, 2015), the maximum densities are 300 points/m^2 for long-range applications, 1200 points/m^2 for medium-range applications, and 6000 points/m^2 for high-resolution mobile laser scanning in urban areas[25]. The maximum densities are achieved at a platform speed of 10 km/h. As the speed increases, the densities decrease. The observed densities of the PTZ mobile point cloud are most suitable for high-resolution applications, assuming the vehicle scanned over two lanes at a platform speed of at least 30 km/h.

Validation of 2D Density Requirement

In the PTZ project, no specific density requirement is stipulated for the mobile point cloud data. The point density observed in the mobile point cloud is globally around 1650 points per m^2 as illustrated in Figure 5.9. The minimum point density is around 800 points per m^2.

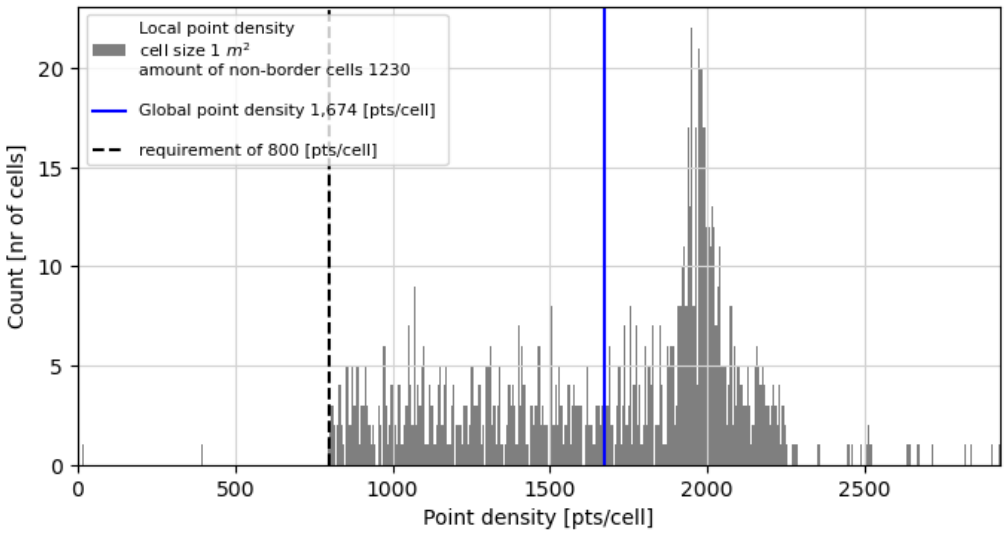

Figure 5.7. *Histogram adherence to density requirement mobile point cloud*

To determine if this density is sufficient for various applications of MLS systems, relevant research was consulted. For example, in (El-Halawany et al., 2012), a point cloud density of 400 points per m^2 was used to detect road curbs. (Gargoum and El-Basyouny, 2022) presents that clearance assessments can be done with point densities with as low as 30 points per m^2. In (Yang et al., 2020), point clouds of 760 and 915 points per m^2 were used for accurate road marking detection. For applications where the MLS point cloud is to be used for an accurate representation of the environment, similar to a BIM model, a higher density is required.

[25] For long-range applications, the Pulse Repetition Rate (PRR) is set to 300 kHz (300,000 pulses per second), which achieves longer ranges due to the longer time interval between pulses. For medium-range applications, the PRR is set to 600 kHz (600,000 pulses per second). For high-resolution mobile scanning, the PRR is increased to 1.1 MHz (1,100,000 pulses per second), resulting in a denser point cloud.

Validation of 2D Density Requirement in Partial-3D Space

In the validation in a partial-3D space, the emphasis lies on understanding how well the point density aligns with specified requirements over the height. While the mobile point cloud consists mostly of road surfaces and predominantly exhibits uniformity in height, variations may occur due to certain features such as guardrails or lamp posts.

The point density analysis in 3D reveals a consistent pattern across the road tiles, with points clustering within a limited height range. This uniform distribution is expected given the predominantly flat nature of road surfaces. However, anomalies such as heightened point densities at specific locations, like the area corresponding to a guardrail at the left border of the figure, warrant attention. The observation of high point densities around the guardrail highlights the significance of accounting for structural variations within the road environment.

5.1.3 Point Cloud Density of Airborne Point Cloud

The following section presents the results of the point cloud density for the airborne point cloud.

2D Point Cloud Density

A cell grid of 1 m^2 is utilized, which is the standard for airborne point clouds. Given the large area covered and the low expected densities, this grid resolution provides sufficient detail. As can be seen, all cells are classified as "full" containing at least 10 points. Figure 5.8 displays the results representing the top view of the airborne dataset showing the densities. A linear scale is selected due to the relatively moderate range of densities (from 80 untill 200 pts/m^2 and 25 pts/m^2 at the borders).

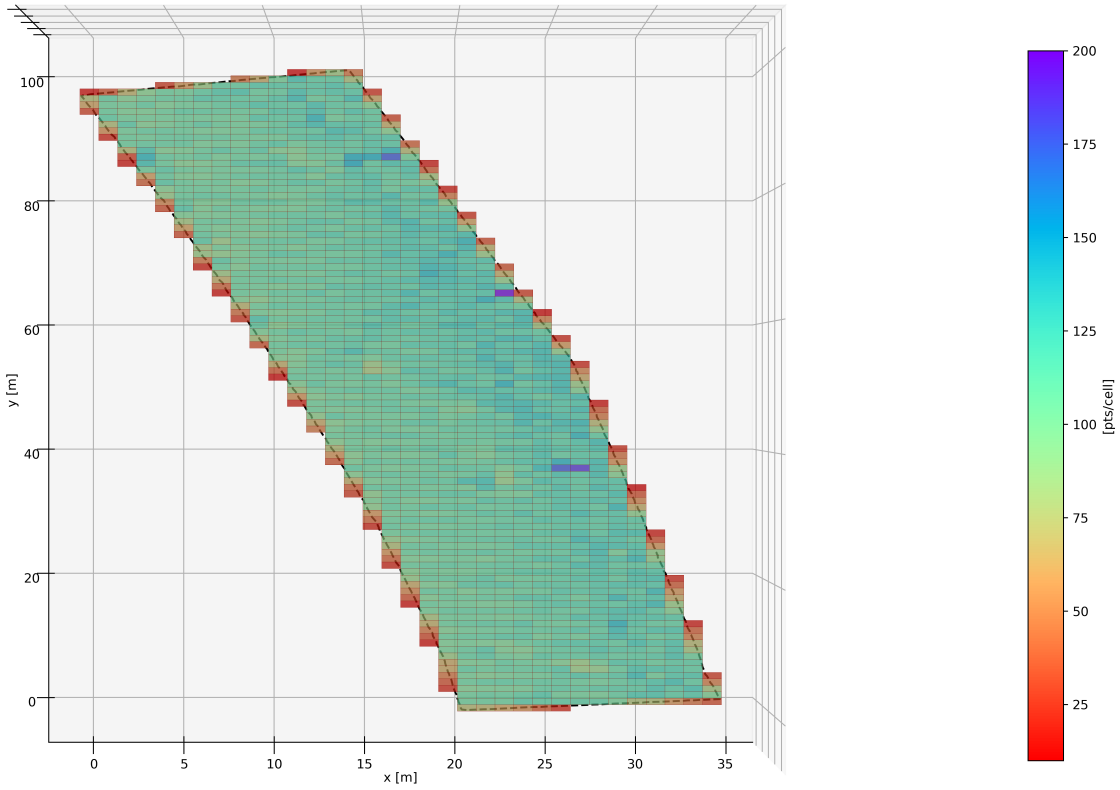

Figure 5.8. *Result local point cloud densities airborne point cloud*

Excluding the borders, the densities appear relatively uniform. The only pattern discernible is that around the right border, where the guard rail is, higher densities are seen. In the event of flight strip overlap, which is common in airborne surveys, the expectation is that (approximately) double the points in the areas of the overlap are observed. In the specific point cloud being discussed, this expectation holds true at the location of the Drechttunnel, where the flight strips are positioned such that overlap indeed occurs. Typically, in ALS scenarios, flight strips can have widths of up to 600 meters, which would usually prevent such overlap.

Consider the specifications of the airborne laser scanning equipment (Leica Citymapper (Leica, n.d.)), which mention that it typically achieves a point density of 8 points per square meter at 1,000 meters Above Ground Level (AGL) and 4 points per square meter at 2,000 meters AGL. The increased density observed in this project implies that the airborne device likely operated at a significantly lower altitude, indicating a definite overlap between two flight strips.

Validation of 2D Density Requirement

No specific requirement is mandated for the airborne point clouds. So, for this study, a sensible requirement will be selected based on the specifications outlined in Section 2.3. It was indicated that both the AHN and French lidar datasets have requirements of 10 pts/m^2. Upon applying this requirement, all cells conform to the standard. The adherence is demonstrated in Figure 5.9 which illustrates the distribution of local point densities for non-border cells in relation to the specified requirement. Notably, the global point density, averaging 115 pts/m^2, significantly surpasses the requirement. As a result, all cells are classified as a green cell.

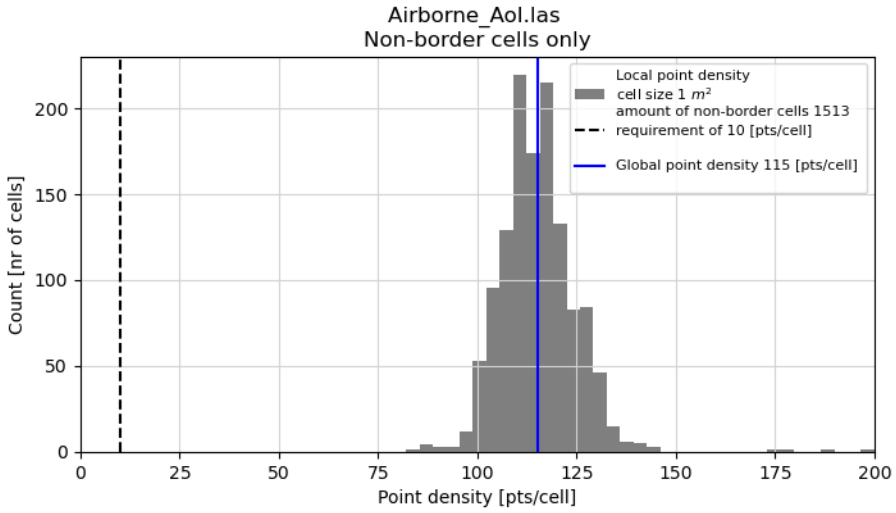

Figure 5.9. *Histogram adherence to density requirement mobile point cloud*

The distribution of densities depicted in Figure 5.9 exhibits a nearly normal distribution. This pattern arises from various factors, including the airborne LiDAR sensor's operational parameters, such as flight altitude, speed, and scanning angle. These parameters directly influence the sensor's capability to capture points across the terrain, resulting in (slight) variations in point cloud density. Additionally, despite the apparent homogeneity of the road area under study, natural variations in terrain characteristics play a significant role in the observed distribution. Elevation changes, surface roughness, and other environmental factors can affect how LiDAR technology interacts with the landscape, influencing the density and distribution of recorded points.

Validation of 2D Density Requirement in Partial-3D Space

Figure 5.10 presents the histogram and cumulative histogram for two cells to demonstrate the validation of the density requirement in a partial 3D space for the airborne point cloud.

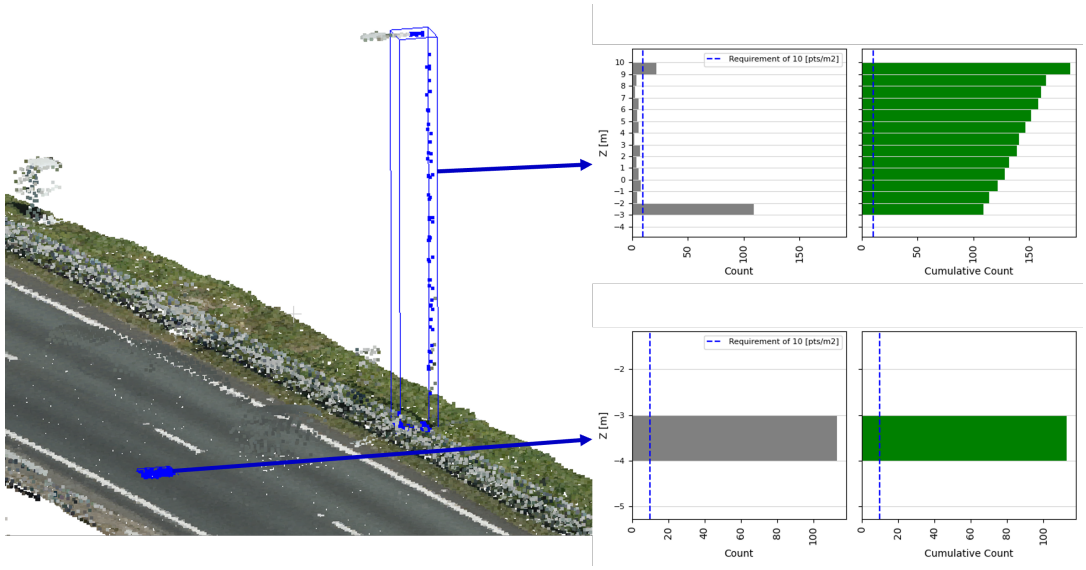

Figure 5.10. *Result validation of 2D density requirement partial-3d space focus on road for airborne point cloud8*

Figure 5.10 (top) illustrates the height distribution of a lamppost adjacent to the road, showing the point distribution across 1-meter increments. The bottom height section contains a high density of points, with 100 points recorded between -3 and -2 meters. The vertical cells of the lamppost, however, have fewer points at each meter, failing to meet the requirement. While the cumulative histogram indicates overall cell adherence, this compliance is predominantly due to the points on the ground; individual surfaces do not uniformly meet the requirement.

Figure 5.10 (bottom) depicts a road cell. In this case, the histogram and cumulative histogram are identical since the points are confined within the same height range of 1-meter increments. For cells containing only road surfaces, variations are expected only at the millimeter scale, not the meter.

When validating airborne point clouds in a partial-3D space, it is important to consider how much information the histogram for each cell can actually convey. Given that airborne point clouds of the infrastructure are typically gathered from a top-down perspective, significant height variations are generally minimal. As a result, the histogram for each cell does not provide substantial insights, as the lack of height fluctuations means that most points will fall within a narrow vertical range.

This raises the question of whether partial-3D validation is necessary for airborne point clouds. Since these point clouds are collected from above and display limited vertical variation, the validation in 2D as performed seems more reliable.

5.2 Results Validation of Relative Accuracy

The relative accuracy assessment uses the method to determine the alignment in overlapping regions. The assessment is performed on the static- and mobile-derived composite point cloud of the PTZ project. The method can be applied to all point clouds since all points are within an overlapping region. However, due to time constraints, the airborne-derived point cloud is not investigated.

5.2.1 Relative Accuracy of Static Point Cloud

The original scanned point cloud data set must be used for this method as the points assigned to each scanner are crucial for identifying the overlapping regions. Ideally, a unique attribute should be assigned to each point in the composite point cloud to indicate its origin. However, this is not the case in the static point cloud data.

Location of Overlapping Regions

The location of the measurement set-ups is imperative for determining where the overlapping regions are in the point clouds. Figure 5.11 visualizes the locations of the measurement setups and the consequent locations of the cross-sections. The halfway cross-section is located exactly halfway in between the scans (point clouds) from scanners 5 and 6, whilst the full-length cross-section goes through multiple overlapping regions.

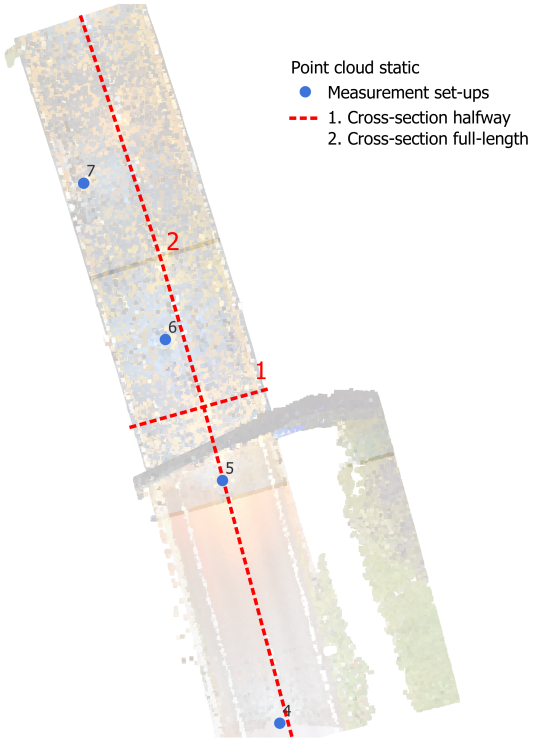

Figure 5.11. *Location of cross-section for static point cloud*

Selection of Surfaces within Overlapping Regions

For demonstration purposes, the halfway cross-section between the scans of 5 and 6 is analyzed. Over the length of the cross-section, a 30-centimeter strip is extracted from each original point cloud scan using the program CloudCompare. For the analysis, it is necessary that enough points are extracted. For the static point cloud, a strip of 30-centimeter ensured that a sufficiently dense set of points is obtained, with over 1 million points combined from both scanners. Figure 5.12 illustrates the extracted cross-section strip.

The figure depicts that the cross-section comprises a tunnel with clearly defined walls, a top surface, and a bottom surface. Given the complex 3D geometry of the tunnel, representing such shape with a single plane does not provide reliable results. Instead, multiple planes must be created to accurately capture the geometry of the tunnel. For the analysis, a specific area corresponding to the road surface (highlighted in blue in Figure 5.12) is chosen. The area is expected to be represented by a nearly horizontal plane with minimal height variations.

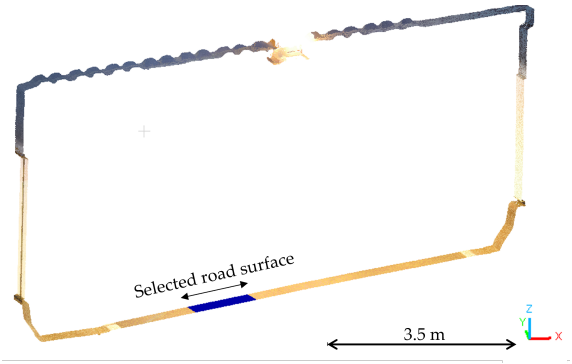

Figure 5.12. *Location of halfway cross-section between scan 5 and 6 static point cloud*

The selected area for investigation measures 0.30 meters by 1.2 meters. A side view of the area is depicted in Figure 5.13, showcasing points from scan 5 (colored pink) and scan 6 (colored blue). Scan 5 contributed approximately 17,000 points, while scan 6 contributed approximately 20,000 points for this smaller area. It's noteworthy that the area exhibits a slight slope, which is expected for a road surface designed for water flow.

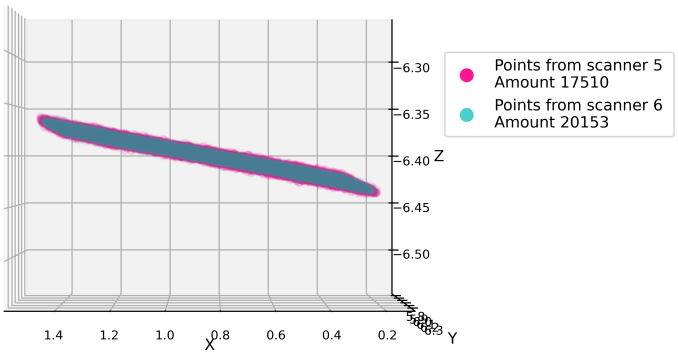

Figure 5.13. *Selected road surface area of halfway cross-section between scan 5 and scan 6 of static point cloud*

Comparing of Surfaces within Overlapping Regions

The objective is to compare the data obtained from scans 5 and 6 by analyzing differences from both perspectives — using scan 5 as the base and subsequently using scan 6 as the base point cloud. First, the point clouds within the cross-section are represented by a plane. Consequently, the plane is evaluated.

Figure 5.14a illustrates the plane fitted to the point cloud from **scan 5**. It is crucial to assess the fit of the plane to the point cloud, which is achieved by examining the distances to the plane depicted in Figure 5.14b. The majority of distances align closely with the surface of the plane, with 75% of the data being within 1.08 mm of the plane and 95% within 3.14 mm[26].

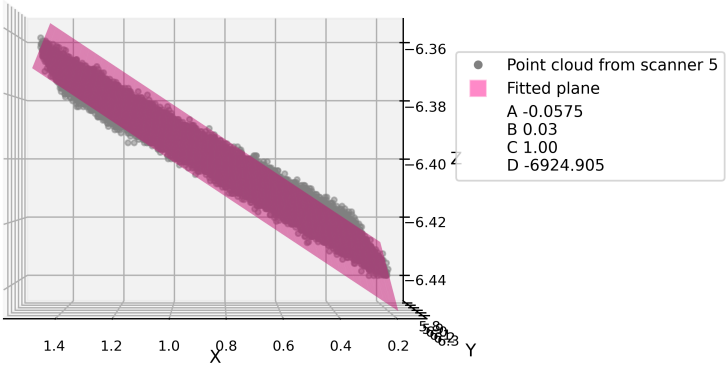

(a) *Fitted plane to **scan 5** using PCA*

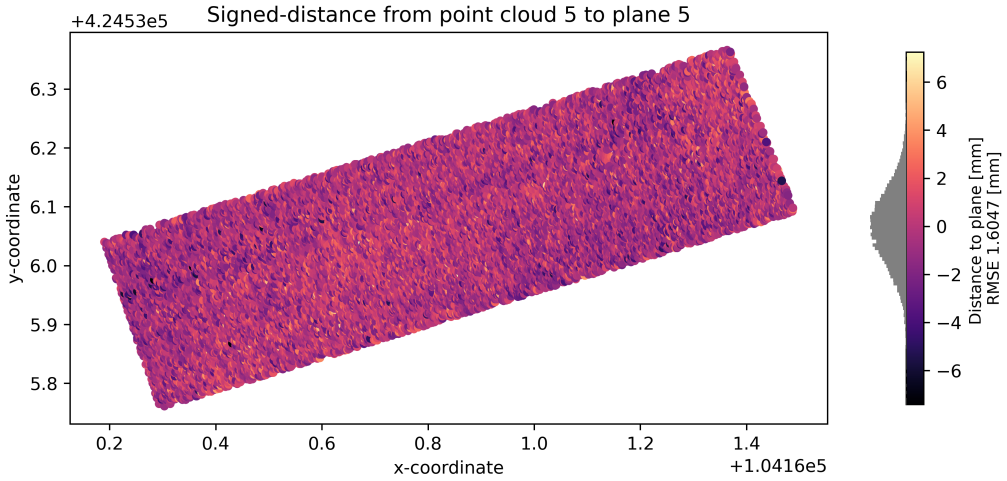

(b) *Point-to-plane signed distance from **scan 5** to plane from **scan 5***

Figure 5.14. *Evaluation plane fitted to **scan 5***

[26]Derived from the distribution of the distances, shown in grey next to the colorbar. The signed distances from the points to the plane follow a normal distribution. To calculate the 75th and 95th percentile bounds, z-scores are used: 1.96 for the 95th percentile and approximately 0.675 for the 75th percentile.

The signed distances can be represented by a single value, the RMSE, which amounts to 1.61 mm[27]. The value of the RMSE aligns with the specifications of the scanner, which is the Trimble TX8-II. In (Trimle, n.d.), the systematic distance deviation is specified as less than 2 millimeters, and the inherent distance noise of the scanner is less than 1 millimeter for distances under 80 meters. Given these values, the RMSE appears reasonable and cannot be reduced further. Attempting to reduce it would compromise the objective of not modeling the noise.

Similarly, in Figure 5.15a a plane is fitted to represent the point cloud from **scan 6**. Figure 5.15b presents the distances from the point cloud to the plane. Similar to the earlier results, the distances are centralized around zero. However, some extreme distances from the surface, up to 10 mm, are observed. The majority of distances closely align with the surface of the plane, with 75% of the data falling within 1.26 mm of the plane and 95% within 3.67 mm. The RMSE for this representation is 1.88 mm. These values indicate that while the distances from the plane are slightly larger and show higher variability compared to the first representation, the model still captures the distribution of distances reasonably well.

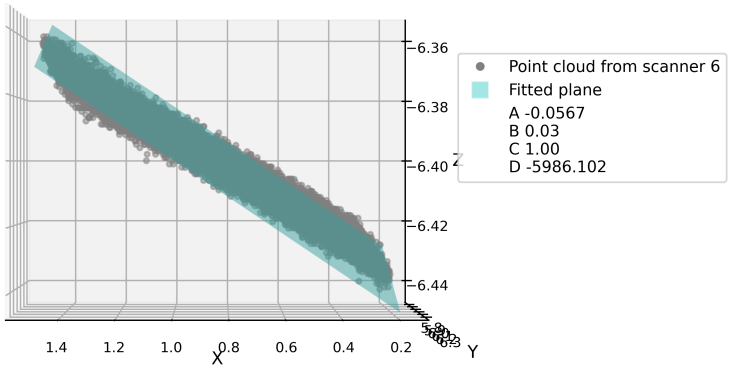

(a) *Fitted plane to **scan 6** using PCA*

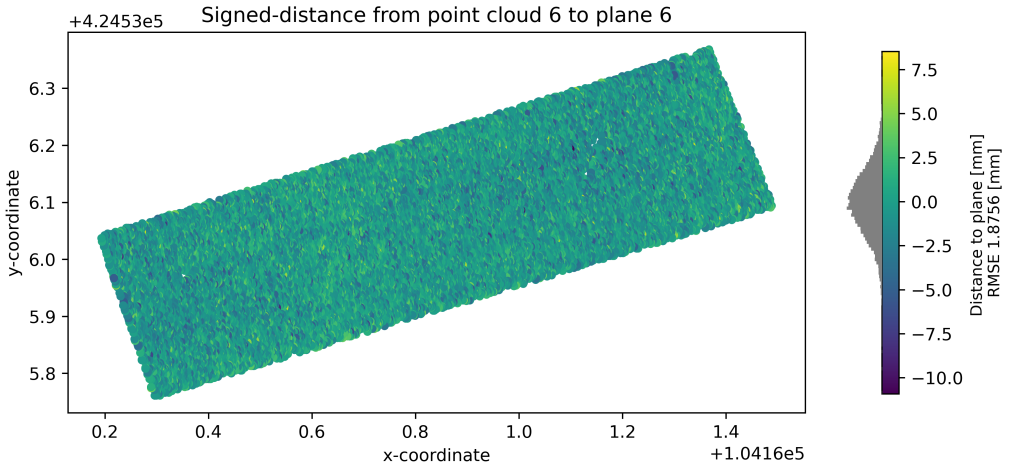

(b) *Point-to-plane signed distance from **scan 6** to plane from scan **6***

Figure 5.15. *Evaluation plane fitted to **scan 6***

[27]The RMSE for the distances can be found in the figure, located next to the colorbar.

With an acceptable representation now in place, the data within the cross-section can be compared. Where the plane represents scan 5, the other point cloud from scan 6 will be compared. This means that the point-to-plane distance is determined as shown in Figure 5.16a. Similarly, the plane represented by scan 6 will be compared to the point cloud from scan 5 as shown in Figure 5.16b.

The distances from the point clouds to the plane remain normally distributed and bound around 0, indicating there are not many large outliers. This suggests that there is no systematic deviation coming from the scanners, as such deviation would typically result in more deviations from zero in the distribution of distances.

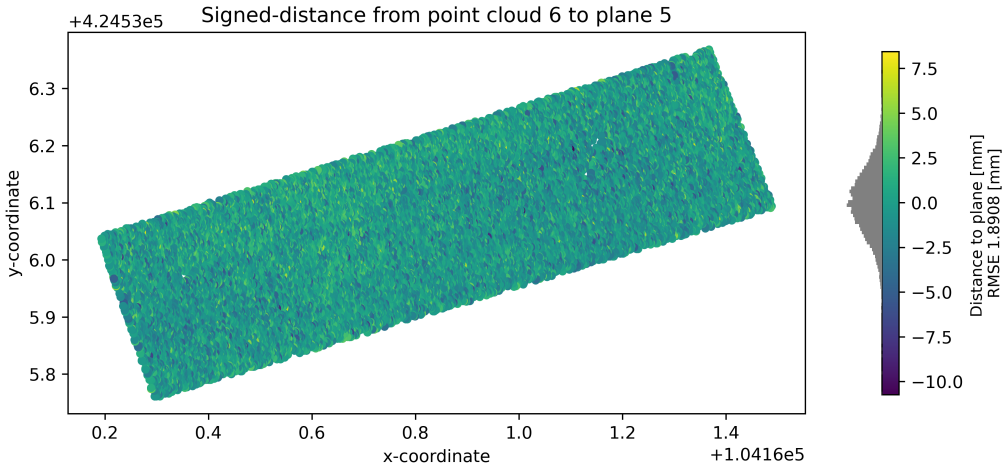

(a) *Point-to-plane signed distance from* ***scan 6*** *to plane from* ***scan 5***

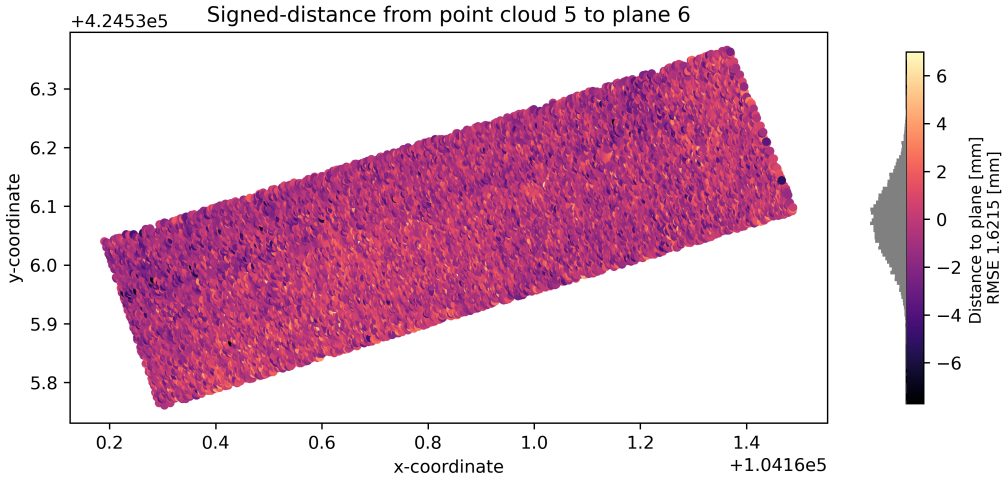

(b) *Point-to-plane signed distance from* ***scan 5*** *to plane from* ***scan 6***

Figure 5.16. *Comparison of distances in overlapping regions static scan*

Assessing adherence to Relative Accuracy Requirement

In Subsection 3.1.2, it was specified that the relative measurement accuracy of the static scans in the tunnels and service buildings must adhere to $< \sigma$ 0.5 cm. As outlined in the method, rather than assessing the RMSE, each point is individually evaluated against the requirement to discern any emerging patterns. Figure 5.17 illustrates the assessment of adherence to relative accuracy requirements. The top figures shows the adherence based on the plane fitted to scan 5 data, while the bottom figures are based on scan 6.

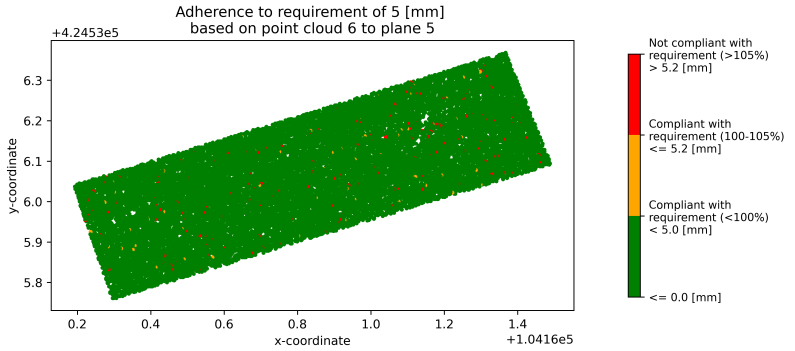

(a) *Adherence to relative accuracy requirement from* ***scan 6*** *to plane based on* ***scan 5***

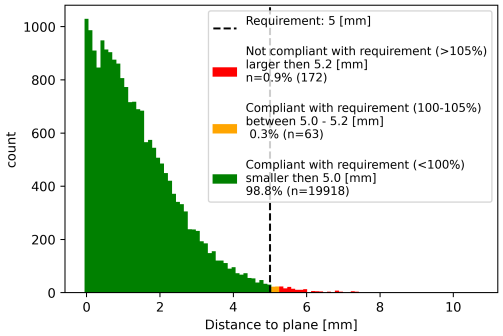

(b) *Histogram of distances* ***scan 6*** *in relation to requirement*

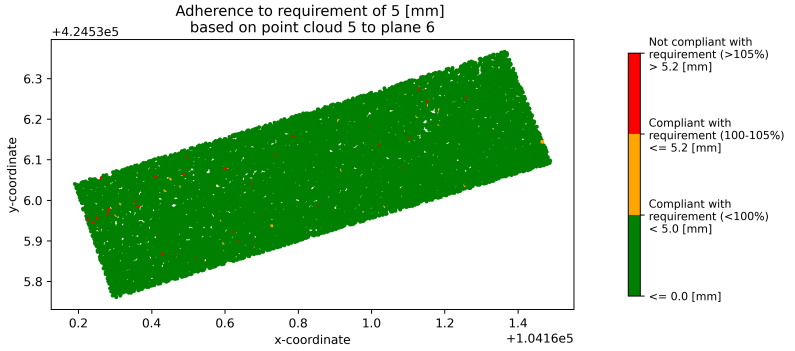

(c) *Adherence to relative accuracy requirement from* ***scan 5*** *to plane based on* ***scan 6***

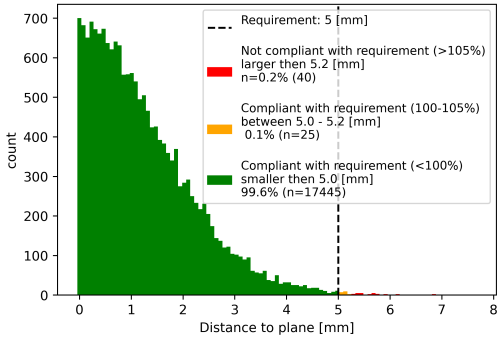

(d) *Histogram of distances* ***scan 5*** *in relation to requirement*

Figure 5.17. *Resulting figures assessing adherence to relative accuracy requirement for static point cloud*

Consistent with expectations, the results from both perspectives align closely. This is attributed to the accurate representation of the point cloud by the fitted planes. The figures predominantly show green, indicating that the vast majority of the area meets the requirement. This is further supported by the histograms of the distances, which indicate that 95% of the distances are within 3.6 millimeters. Specifically, in the top figure, 99.1% of the area is in compliance (green and orange combined), while the bottom figure shows 99.7%.

5.2.2 Relative Accuracy of Mobile Point Cloud

The original scanned point cloud data is used for the mobile point cloud data.

Location of Overlapping Regions

For the mobile scans, the focus is on the road located just before the tunnel entrance. There are 2 scans available for this area; 105604 and 095755. To determine the overlap between the mobile scans, the paths taken by the vehicle for each scan have to be identified. This information is not directly available in the point cloud data, so the original data containing the scans from a single pass are examined.

Analyzing the scan angle rank, as shown in Figure 5.18a for scan 105604, helps identify the path of the vehicle. When the scan angle is 0, the scanner is directly facing the road, indicating the vehicle's position. The figure illustrates the trajectory for scan 105604 (the black line), which is centered in one lane as expected. A similar pattern is observed for the second scan, where the vehicle is also centered in a lane. Figure 5.18b visualizes the trajectories and the locations of cross-sections. The halfway cross-section is positioned exactly between the lanes, while the full-length cross-section spans across all lanes.

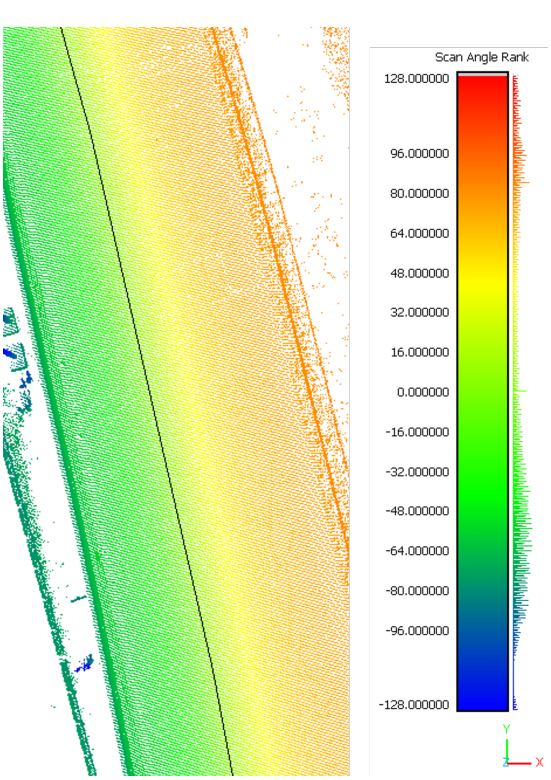

(a) *Scan Angle rank of pass 105604*

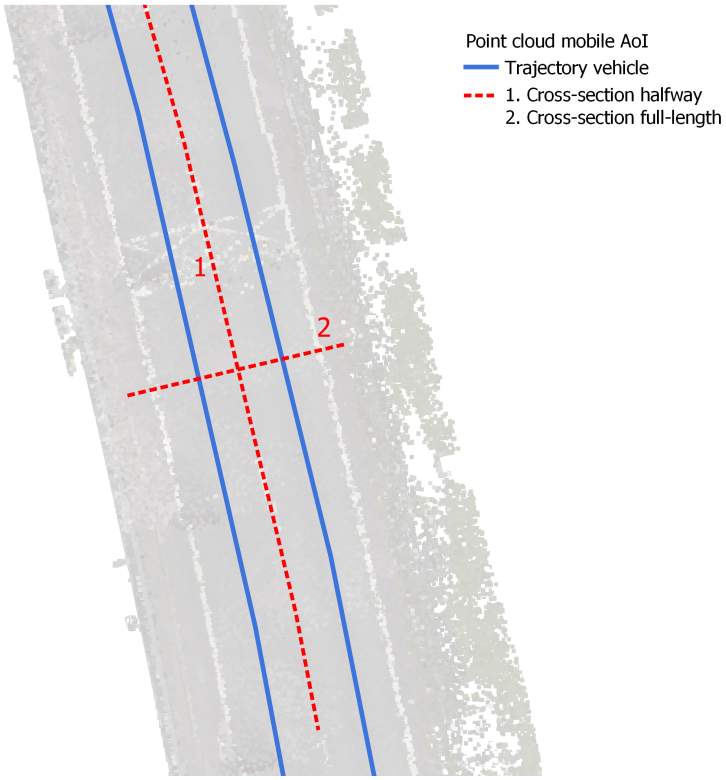

(b) *Location of cross-section for mobile point cloud*

Figure 5.18. *Location of cross-section for mobile point cloud*

Selection of Surfaces within Overlapping Regions

The investigation focuses on the full-length cross-section spanning scans 105604 and 084755. Compared to the static point cloud previously analyzed, the mobile point cloud exhibits significantly lower point density. Consequently, a wider 50-centimeter strip is extracted using CloudCompare instead of the initially planned 30-centimeter strip.

The profile spans 6 meters in total length, capturing the right side of the guard rail. Upon inspection, the profile reveals a road under a slope that appears inconsistent, showing a slight inward bulge. Due to these varying surface conditions, estimating with a single plane is impractical. A plane is selected at the midpoint of the profile where the overlap is confirmed, focusing the investigation on a 2-meter section.

Figure 5.19 displays the top view (left) and side view (right) of the selected area. Scan 105604 (orange color) contains approximately 600 points, whereas scan 095755 (purple color) has over double the points, totaling 1400.

From the top view, the captured data pattern illustrates how the point cloud was acquired in motion, resulting in diagonal lines due to changing orientation and position relative to the scanned surface. This characteristic underscores the limitation of using point-to-point distances, as the points do not conform to a uniform grid.

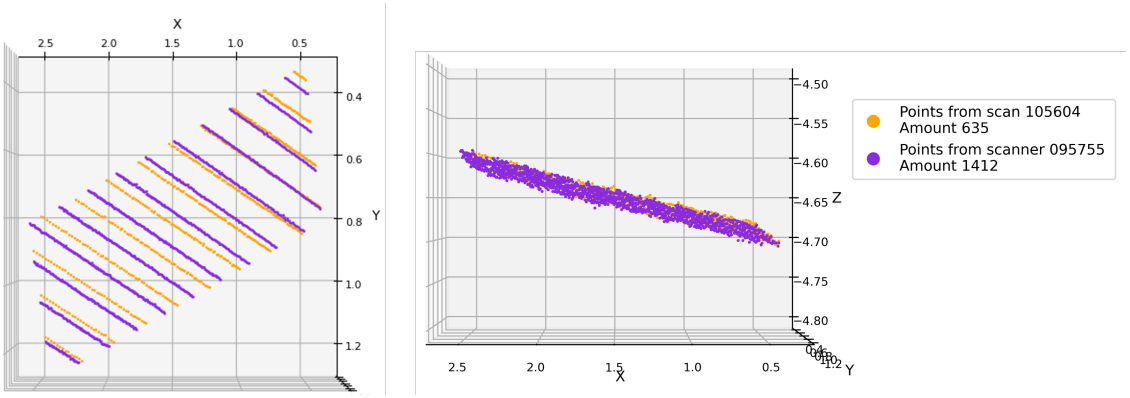

Figure 5.19. *Selected road surface area of full-length cross-section between scan 105604 and scan 095755 of mobile point cloud*

Comparing of Surfaces within Overlapping Regions

Figure 5.20a illustrates the fitted plane for **scan 105604**. Subsequently, Figure 5.22a displays the distances to this plane. The distances exhibit a normal distribution centered around 0, with a maximum distance of -6.5 mm. The RMSE of these distances is 1.79 mm. Within the surface, no discernible patterns can be identified; it appears as random noise.

According to specifications from the manufacturer of the LiDAR scanner used for the mobile point cloud scans (Riegl VMX450 Mobile Mapping System), the claimed precision is 5 mm (Riegl, 2015). Additionally, the IMU/GNSS typically provides a relative positioning accuracy of 10 mm. Given this, the RMSE is within an acceptable range.

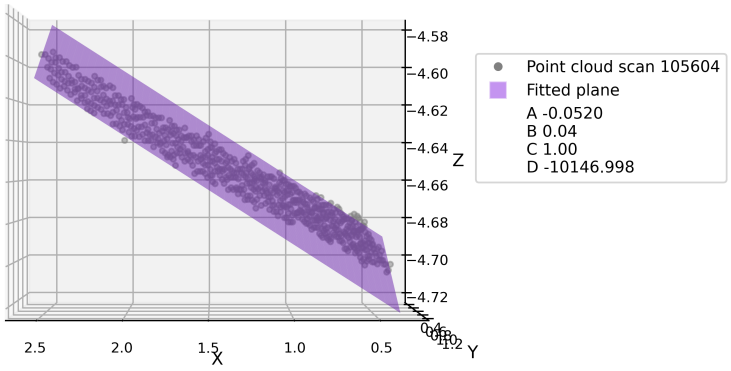

(a) *Fitted plane to **scan 105604** using PCA*

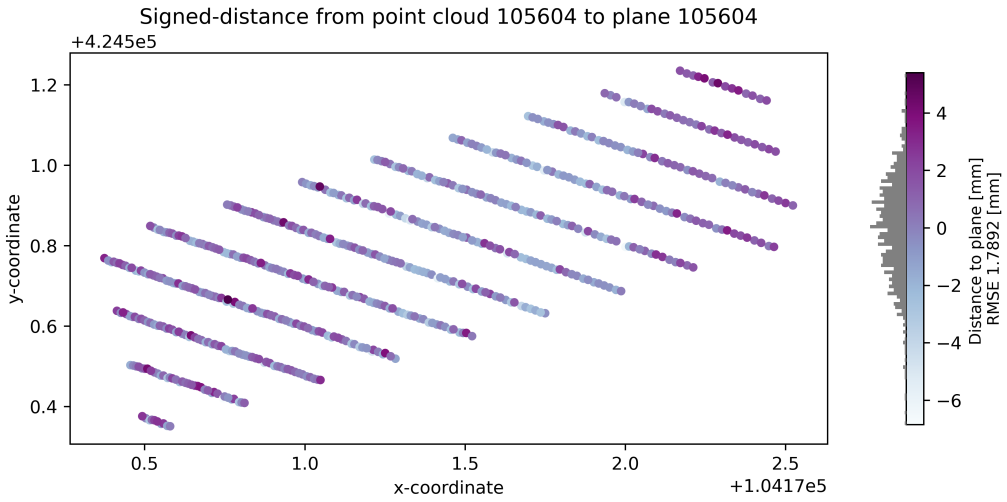

(b) *Point-to-plane signed distance from **scan 105604** to plane from **scan 105604***

Figure 5.20. *Evaluation plane fitted to **scan 105604***

Figure 5.21a presents the fitted plane to the point cloud from **scan 095755**. Figure 5.21b shows the distances from the scan to the plane. Similar to earlier findings, the distances are centered around zero. The distribution reveals that 95% of the distances fall within ±4.05 millimeters, and for 75%, this range narrows to ±1.39 millimeters. The RMSE of 2.06 millimeters falls within an acceptable range.

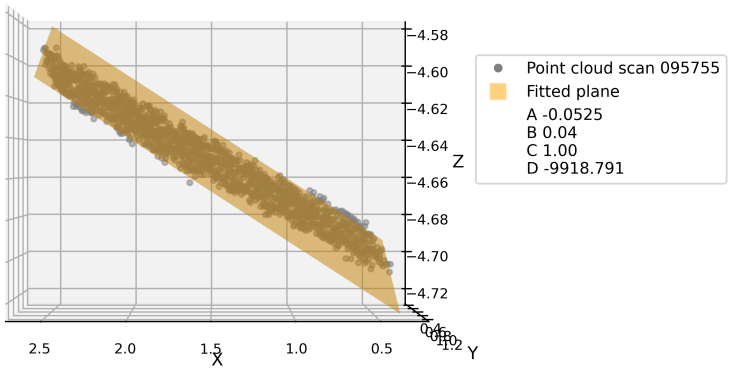

(a) *Fitted plane to **scan 095755** using PCA*

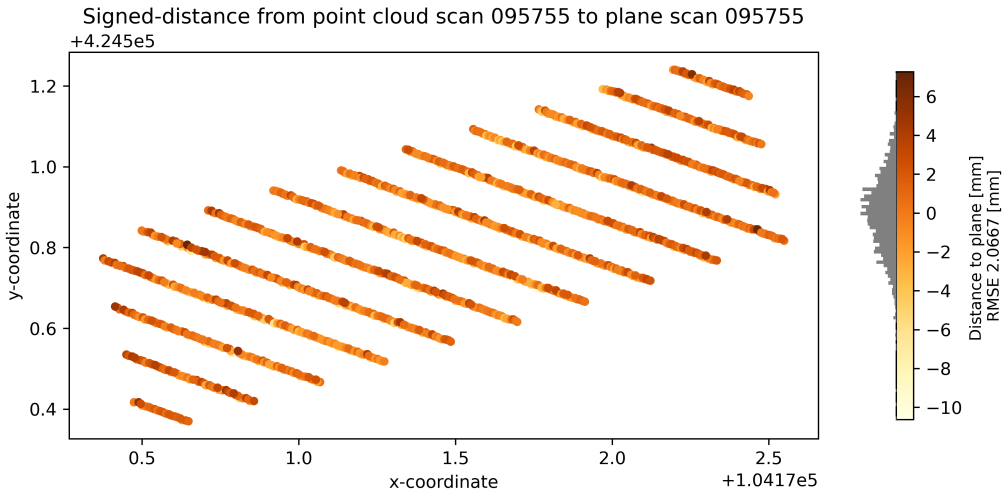

(b) *Point-to-plane signed distance from **scan 095755** to plane from **scan 095755***

Figure 5.21. *Evaluation plane fitted to **scan 095755***

Now that the representations are aligned, the point clouds are compared. Figure 5.22a shows the Point-to-plane signed distance from **scan 095755** to plane from **scan 105604**. Figure shows the other way around.

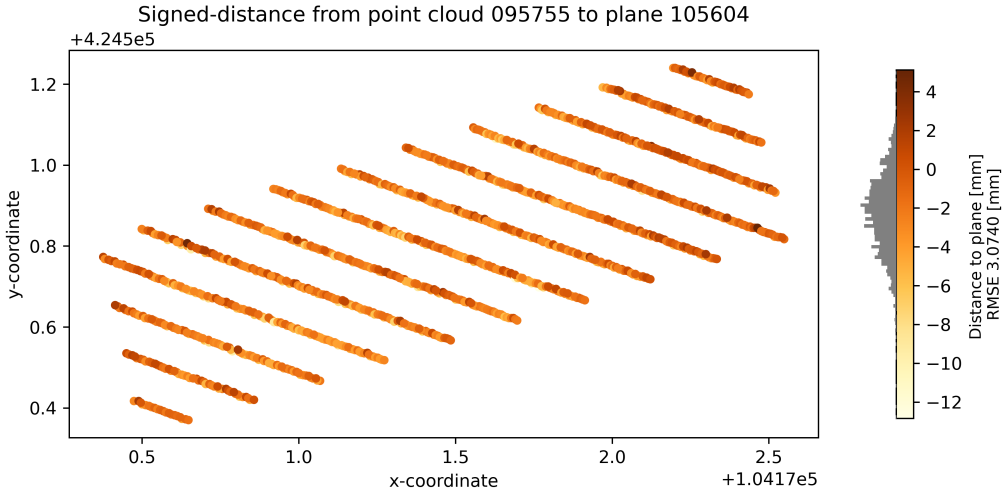

(a) *Point-to-plane signed distance from* ***scan 095755*** *to plane from* ***scan 105604***

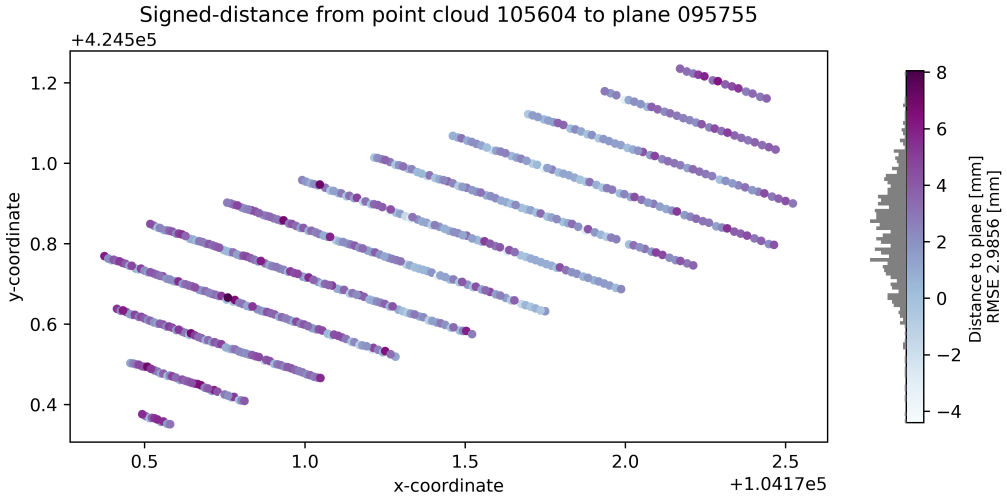

(b) *Point-to-plane signed distance from* ***scan 105604*** *to plane from* ***scan 095755***

Figure 5.22. *Comparison of distances in overlapping regions mobile scan*

From the figures, in both cases, the distances are not centered around 0. In the upper figure, the distances are centralized around -2.25 mm, while in the lower figure, they cluster around 2.37 mm. This systematic deviation suggests that the point clouds are offset by approximately 2 millimeters relative to each other rather than being perfectly aligned.

Assessing adherence to Relative Accuracy Requirement

For the mobile point clouds no relative accuracy requirement is determined. The same requirement is used as the static point clouds. Figure 5.23 illustrates the compliance to the relative accuracy requirement. The top figures show the adherence based on the plane fitted to the scan 105604 data, while the bottom figures are based on plane 095755.

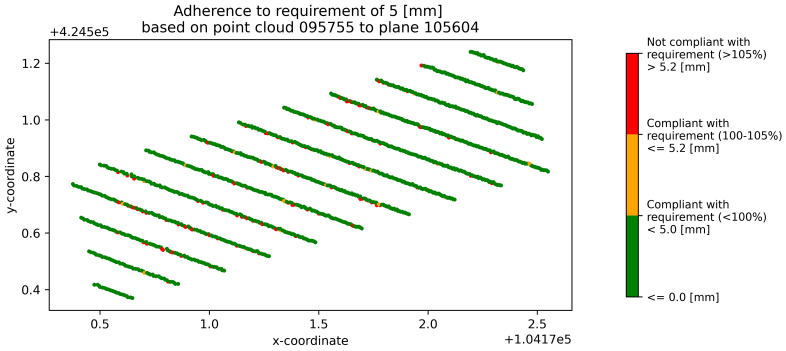

(a) *Adherence to relative accuracy requirement from* ***scan 095755*** *to plane from* ***scan 105604***

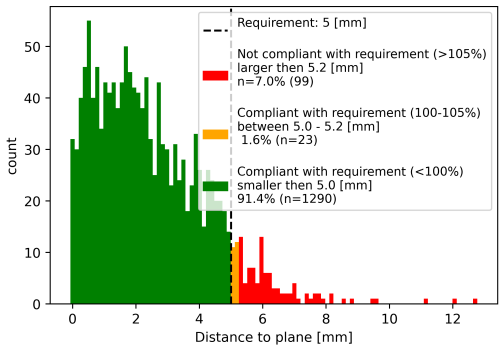

(b) *Histogram of distances* ***scan 095755*** *in relation to requirement*

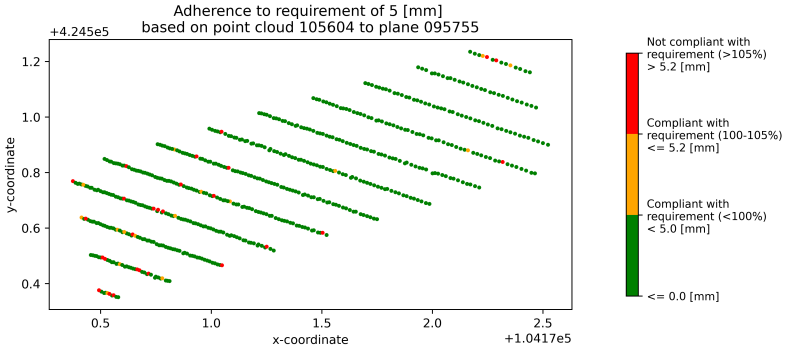

(c) *Adherence to relative accuracy requirement from* ***scan 105604*** *to plane from* ***scan 095755***

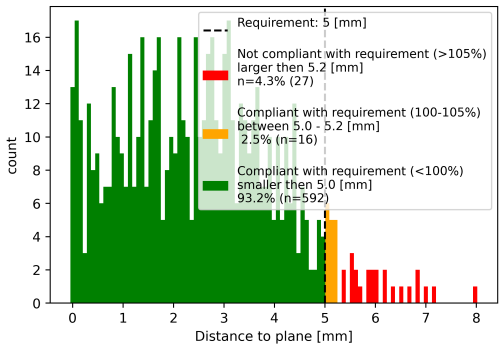

(d) *Histogram of distances* ***scan 105604*** *in relation to requirement*

Figure 5.23. *Resulting figures assessing adherence to relative accuracy requirement for mobile point cloud*

From the figures, it is evident that despite the observed systematic deviation of 2 millimeters, the majority of the area still meets the required specifications. Only 7.0% in the top figure and 4.3% in the bottom figure exceed the specified tolerance. In the histograms, this systematic deviation is less visible when considering absolute distances, making it challenging to pinpoint where the central tendency lies and interpret its significance.

5.3 Results Validation of Absolute Accuracy

The method of using the alignment of the spherical benchmarks to assess the absolute accuracy is only applicable to the static-derived composite point cloud of the PTZ project.

5.3.1 Absolute Accuracy of Static Point Cloud

Within the method, the Figures present the results for a single benchmark. The assessment of the absolute accuracy goes into the combined results of the benchmarks within the AoI[28].

Extract Points corresponding to the Spherical Targets

To evaluate the absolute accuracy, the alignment between the known positions of benchmarks and their estimated locations within the point cloud is examined. The spheres are extracted using the proposed multi-step process. The subsequent paragraphs present the results of the spatial-, intensity-, clustering-, and curvature filters.

1. Spatial filter: The assumption that the target is within half a meter of the known coordinate proved accurate. It has been demonstrated that a search radius of 0.5 meters adequately retrieves the points corresponding to all benchmarks.

2. Intensity filter: The areas around the benchmarks exhibit varying intensity distributions. Some adhere to the normal distribution (as previously described in the method) as shown in Figure 5.24 (left), while others correspond to the distribution depicted in Figure 5.24 (right). The latter distribution displays two distinct peaks: one at lower intensity values and another at higher intensity values.

Variations in intensity distribution stem from the positioning in relation to the tunnel wall. Notably, the middle area of the tunnel wall exhibits higher intensity levels than its upper and lower sections, owing to the diverse reflective properties of the materials involved. Thus, the positioning of benchmarks in relation to the wall directly impacts the prevalence of high-intensity points. As a consequence, the intensity threshold displays significant variance.

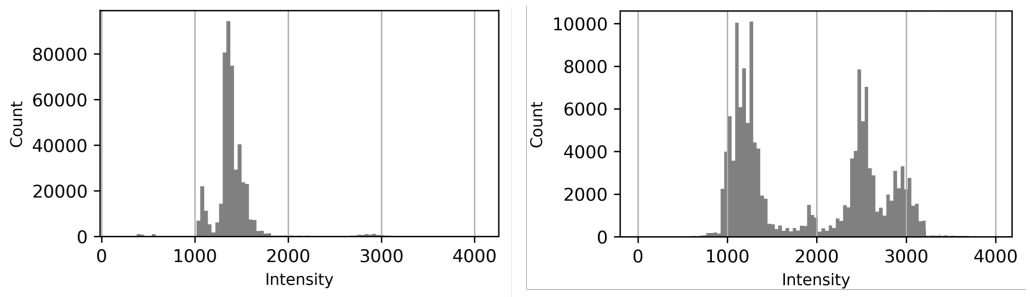

Figure 5.24. *Intensity distributions of area around benchmarks*

Nevertheless, determining the intensity threshold and consequent application of the threshold filter yields the anticipated outcome, effectively eliminating background points.

[28]Presented in Section 3.2, this concerns 8 benchmarks located in the tunnel for the static point cloud.

3. *Clustering*: The DBSCAN parameters need to be tailored to the high density of the static point clouds. Setting $\epsilon = 0.02$ and min_sample $= 10$ accordingly yields satisfactory performance. In instances where only the single sphere is to be filtered out, the algorithm correctly identifies and returns only a single cluster. For other benchmarks, multiple clusters are accurately clustered.

4. *Curvature*: As expected, clusters containing points representing flat areas (like the tunnel wall) exhibit curvature values nearing 0. The anticipation that the cluster exhibiting the highest curvature represents the sphere proves accurate. Across all benchmarks, the algorithm correctly extracts the sphere cluster.

Estimate Center Coordinate of Sphere

The workflow involves using RANSAC for outlier removal, LS sphere fitting on inliers, and centralized RMSE adjustment for each sphere. RANSAC effectively removed outliers across all 8 benchmarks, as indicated by the estimated radius of the LS sphere fitting being close to the expected value. However, the LS fitting consistently overfitted by a few millimeters. Centralized RMSE adjustment then compensated for the average deviation of points from the sphere surface. Using the adjusted radius, more accurate RMSE values were obtained, with minimum and maximum distances significantly reduced. This adjustment centralized the distances around 0, meaning most points were exactly on the estimated sphere surface. As shown in Table 5.3, all final RMSE values are close to 1 mm, with the largest being 1.36 mm.

Benchmark	**RMSE [mm]**	**Benchmark**	**RMSE [mm]**
PV7017	0.93	*PV8017*	1.11
PV7018	0.80	*PV8018*	1.10
PV7019	1.16	*PV8019*	0.99
PV7020	1.22	*PV8020*	1.36

Table 5.3. *Results final RMSE of benchmarks*

Table 5.4 presents the final estimated coordinates of the benchmarks.

Benchmark	**x-coordinate**	**y-coordinate**	**z-coordinate**
PV7017	104076.01	42472.89	-13.93
PV8017	104084.86	424728.93	-13.64
PV7018	104119.04	424640.66	-11.06
PV8018	104127.86	424644.68	-10.83
PV7019	104147.73	424565.64	-7.28
PV8019	104156.96	424568.39	-7.02
PV7020	104158.09	424531.01	-4.94
PV8020	104166.78	424536.28	-5.47

Table 5.4. *Results final estimated coordinates of benchmarks*

Results Validation of Absolute Accuracy Requirement

In Subsection 3.1.2, it was specified that the absolute measurement accuracy of the exterior areas, exits and entrances, and road surveys from the sky must adhere to $\sigma < 2,5$ cm. The RMSE is used as the value for evaluating against the requirement. Figure 5.25 shows the adherence of the RMSE to the absolute accuracy requirement using the specified color scale.

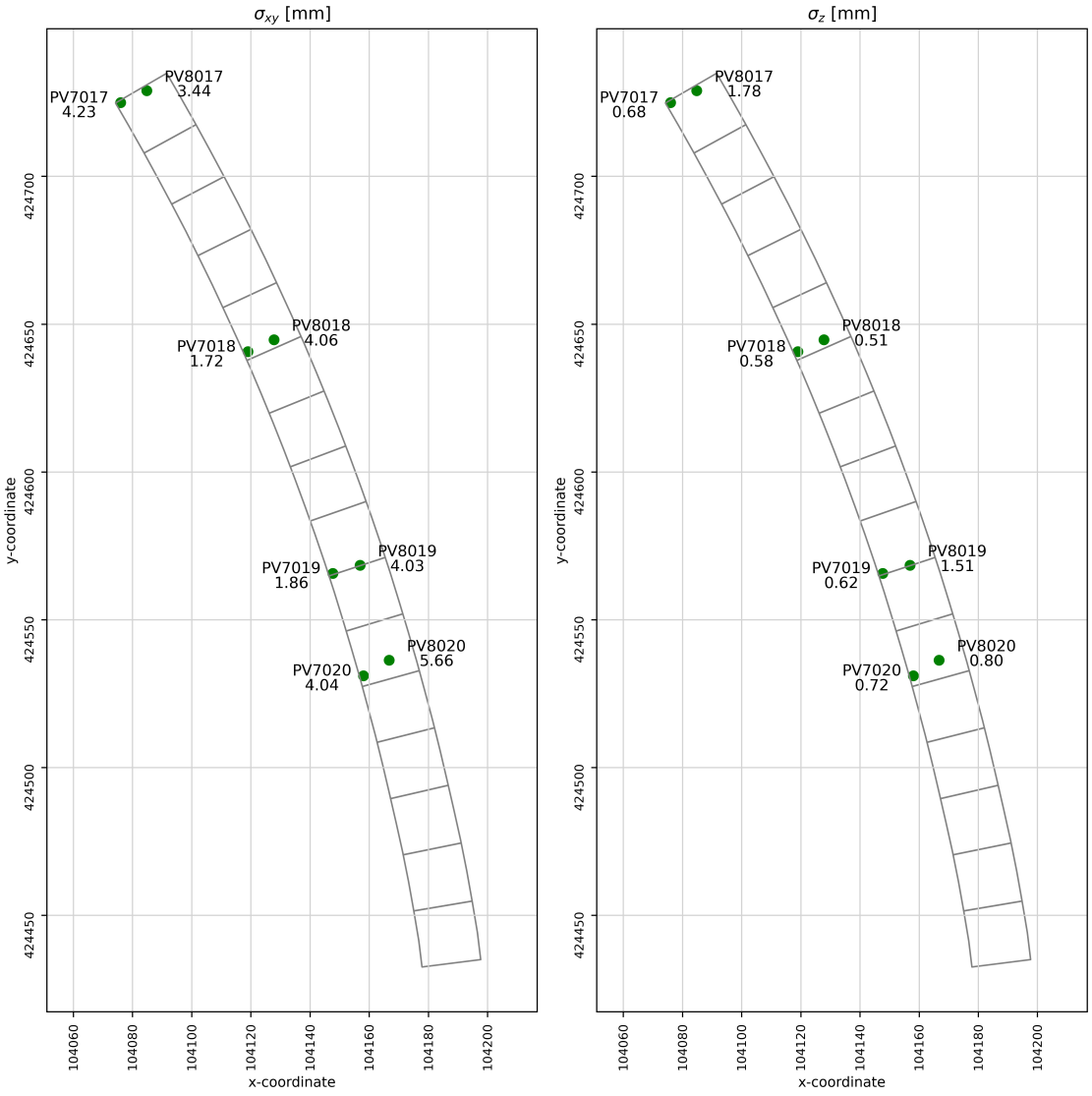

Figure 5.25. *Results adherence to absolute accuracy requirement of static dataset. Left shows compliance in the XY-drection, right shows compliance in the Z-direction*

All benchmarks are uniformly colored green in Figure 5.25, indicating total compliance to the specified requirement within this area. In the XY-direction, the discrepancy with the actual coordinates remains under 6 millimeters. Notably, in the Z-direction, the discrepancy is even smaller, with the maximum deviation being 1.78 millimeters. The results indicate that the point cloud absolute accuracy adheres to the specified requirement.

6 Discussion

6.1 Effectiveness Point Cloud Density Method

Density Requirement
The method to determine the point cloud density fundamentally relies on the coordinates (*x*,*y*,*z*) of the points. By dividing and analyzing the point clouds in cells, it can be assessed how densely packed the points are within a given spatial region. The method is adaptable to accommodate different density requirements and cell sizes.

To further enhance flexibility, the method can include an interactive feature for dynamic density requirement adjustments. For example, incorporating a slider mechanism enables users to modify the density threshold in real-time, as demonstrated in Figure 6.1. This interactive approach allows tailoring the density assessment to specific needs and exploring various scenarios, addressing issues found in the results of the static point cloud in Section 5.1.1.

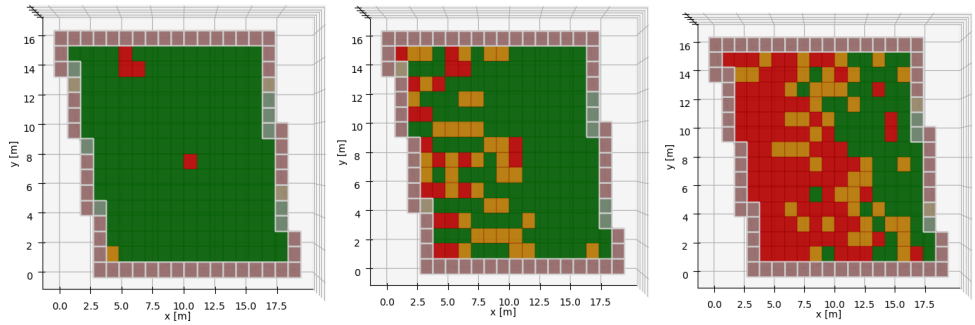

(a) *Requirement 100 pts/m*^{2} (b) *Requirement 110 pts/m*^{2} (c) *Requirement 120 pts/m*^{2}

Figure 6.1. *Incorporation of flexible point cloud density requirements*

Runtime
The runtime hinges mainly on two factors: the number of points and the chosen cell size. Processing larger point clouds, especially those exceeding 100 million points, requires more computational time in the determination of the alpha size. Initializing the cells at the meter level is efficient, but smaller cell sizes increase the processing time.

To address the runtime issues, the point cloud data can be ordered in octrees as described in (Y. Wang et al., 2024). Alternatively, an exploratory approach involves thinning the data and then investigating, which helps identify areas with high point density. Another option is to re-design the point cloud density tool so that coordinates are not read and stored if, within a cell, a certain threshold (the requirement) is exceeded.

6.2 Border Cell Misrepresentation

Within the method, the assumption is that grid cells are uniform in size and shape, with each cell covering an area of 1 m^2. However, in practice, grid cells may vary, particularly near the edges of the point cloud. Border cells might not be completely filled with points, leading to potential misrepresentation of density in these regions. An example is shown in Figure 6.2 where a zoom-out is presented of cells around the borders that are partially filled.

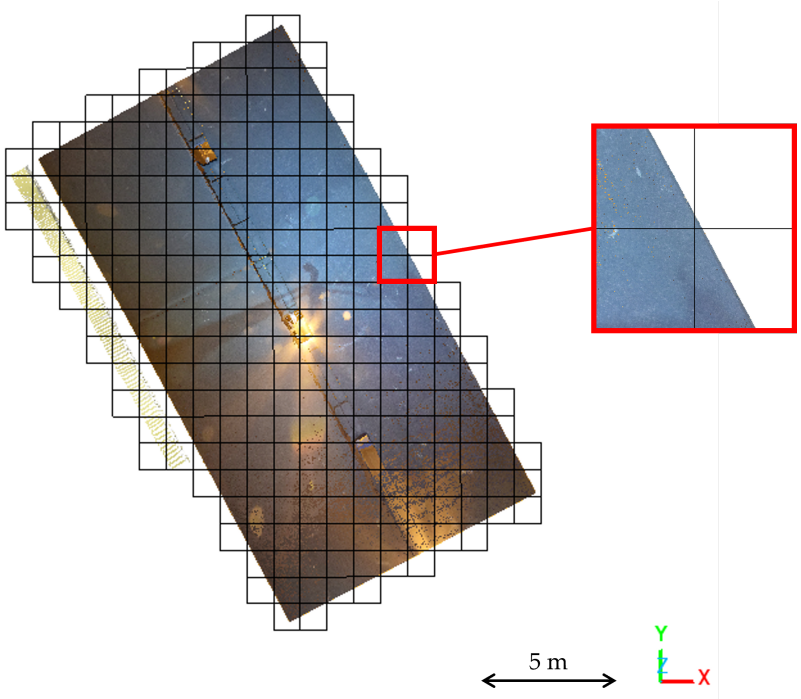

Figure 6.2. *Misrepresentation of point cloud density around the borders*
Zoom-out shows border cells that are only partially filled with points

The necessity of investigating border cells depends on whether there are significant structures of interest, such as tunnel walls. If these structures are present, it is crucial to consider how the grid is constructed to ensure accurate representation. One solution to mitigate the misrepresentation of border cells is employing an adaptive grid. Unlike a fixed grid, an adaptive grid dynamically adjusts cell sizes based on the density and distribution of points near the borders, such as the approach in (Zhou et al., 2021).

Furthermore, the method incorporates alpha shapes to define the outer boundary of the point cloud, introducing the alpha parameter that determines the hull's concavity. Selecting an appropriate alpha value is crucial and may require iterative testing, particularly in areas with complex geometries or irregular point distributions. Also, if the point density varies across the point cloud, the result may be satisfactory in some regions and poor in others, as is confirmed by (Mineo et al., 2019).

6.3 Evaluation of Point Cloud Density Requirement

2D Density Requirement
Analysis of the density requirement for the static point cloud in Section 5.1.1 indicates that the current requirement is not feasible for practical acquisition. Also, here it was underscored that the same density requirement across varied environments, such as roads and tunnels, is unsuitable. In contrast, the airborne point cloud exhibits significantly higher density. Therefore, it is essential to re-evaluate the requirement in relation to the application and the feasibility of the acquisition method.

Using an average density across the entire point cloud can be misleading for extensive areas, as it may not accurately reflect the true density. This was demonstrated in the static point cloud analysis, where including road tiles distorted the overall representation. Despite this challenge, averaging remains necessary due to the impracticality of assessing each tile individually. Instead, focus on predefined areas for density assessment. For instance, analyze the density of each individual tile rather than aggregating all tiles.

The level of non-compliance was investigated for the static point cloud and should be implemented within the specifications. For the non-compliance cells, introduce an acceptance criterion in the specifications where a maximum allowable deviation is set. For example, 5%; if the requirement is 100,000 points per tile, stipulate that no tile should fall below 95,000 points. This criterion is already implemented in the method, identifying non-compliant cells through orange coloring.

3D Density Requirement
Assessing density requirements in flat environments like roads within a partial-3D space yielded limited insights, as points typically cluster within a uniform height range, reducing the effectiveness of 3D analysis.

Conversely, environments with height variations, such as tunnels or 3D objects like lampposts, demonstrated more significant effects in the analysis. The results highlighted scenarios where the overall cell adheres to the 2D density requirement but fails to comply at individual heights within the cell. It is essential that density requirements ensure uniformity across all surfaces of objects. These findings underscore the necessity of transitioning from 2D to 3D requirements for environments with varying dimensions. Validating each height increment individually in 3D environments is crucial for accurately capturing density variations.

Moving forward, adopting a complete 3D approach is recommended for assessing such environments. One effective method involves using voxels, which are three-dimensional pixels that grid the space into cubes, enabling a detailed and precise analysis of point density across all dimensions, including height. Such an approach is introduced in (Hinks et al., 2013) and visualized in Figure 6.3.

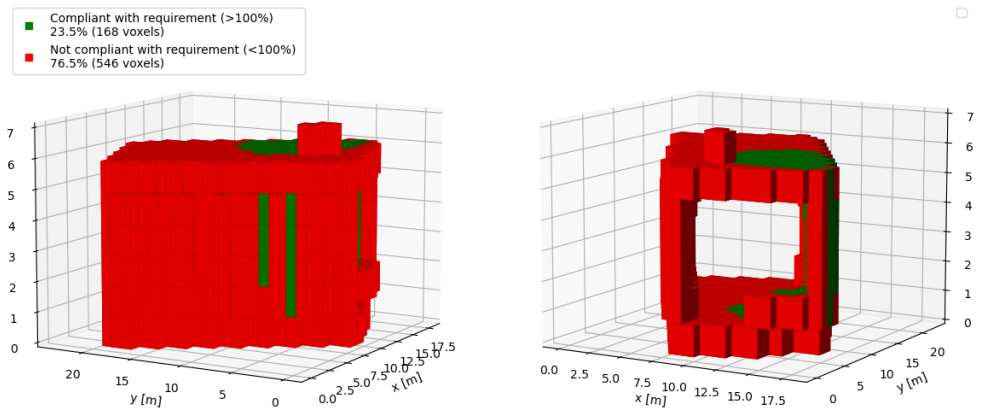

Figure 6.3. *Validation of point cloud in 3D using voxels*

6.4 Effectiveness Overlapping Regions Alignment Method

The approach of using overlapping regions can be employed to assess the relative accuracy, provided that the point cloud can be accurately represented by a plane. The method has limitations in assessing relative accuracy in the presence of 3D objects. Similar limitations can be found in research such as (Huang et al., 2018). For example, while planes can represent simple geometric shapes like street lamps, more complex shapes, such as curved guard rails, necessitate alternative geometric representations to avoid inaccuracies. Accurate relative accuracy assessment, especially on a millimeter scale, requires methods that account for these specific shapes and complexities.

The plane estimation is only effective for areas with minimal height variations. For longer cross-sections, a single plane is inadequate as a representation. For example, Figure 6.4 shows a 50-meter road cross-section where a single plane was fitted. The single plane fails to accurately represent the road, as evidenced by the clear pattern of distances and the distribution of these distances across the area.

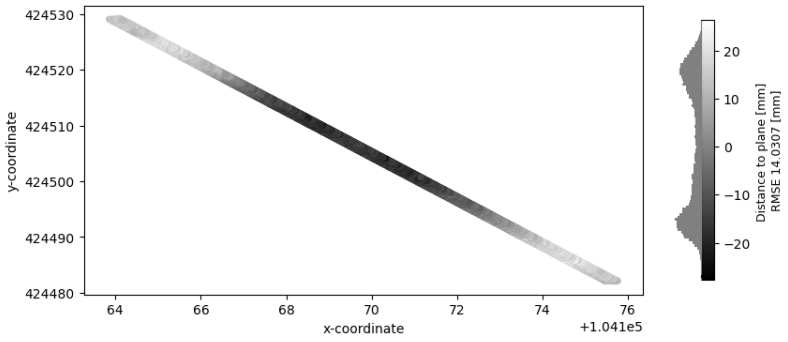

Figure 6.4. *Point-to-plane signed distance of full-length cross-section of 50 meters*

Therefore, to create an accurate representation, it is necessary to employ multiple planes or consider other more dynamic representations. B-splines, for instance, offer a versatile alternative by allowing flexible adjustments to the curve or surface based on control points and knot vectors (Yuwen et al., 2005). Such a method accommodates complex geometries and varying levels of detail. It is crucial that the representation captures the overall trend of the data without fitting the noise.

Steps toward Automated Surface Extraction
Currently, surfaces are manually extracted in the study, but automation is feasible. The following steps are proposed to move towards a more automatic and encompassing workflow:

- *Automatic detection of overlapping regions*: One option is to use the locations of the scans and subsequently employ determinants to locate the specific points belonging to the overlaps (such as described in (Kaltofen and Villard, 2004)). Another option is to utilize the point cloud attribute Point Source ID to find the points in overlapping regions.
- *Region-based segmentation for surface selection*: Implement region-based segmentation techniques, such as the one proposed by (Vo et al., 2015), which uses an octree-based region growing method. This approach segments the point cloud into regions based on spatial coherence and surface normals, aiding in the automated identification of relevant surfaces. In this process, include the RMSE so that if the representation is not deemed adequate, the surface is selected smaller.
- *Multi-plane analysis within cross-sections*: Fit multiple planes within a cross-sections to capture varying surfaces. This approach ensures that different features, such as roads, walls, and other structures, are accurately represented. Include the results of multiple planes within one cross-section to assess the adherence to the relative accuracy requirement.

6.5 Attributes of Point Cloud to determine Overlap

To determine the overlap within a point cloud, it is crucial that the origin of each point is identified — whether it comes from a specific scanner, lane, or flight path. The limitation of such information in the study underscores the significance of including attributes that help to determine the overlapping region. In static point clouds, the primary attribute used to determine origin is often the *Source ID*. For mobile point clouds, factors such as the *scan direction flag* and *scan angle rank* are crucial in trajectory determination. Meanwhile, for airborne point clouds, knowledge of flight lines is essential.

In conclusion, it is imperative that the *Point Source ID* attribute, indicating the point's origin regardless of the configuration, is included. To address this need, it is recommended that clients refer to the LAS specifications version 1.4 of the American Society for Photogrammetry and Remote Sensing (ASPRS) (ASPRS, 2013) which include this attribute.

6.6 Generalization of Benchmark Alignment Method

The primary limitation of the method is the exclusive focus on spherical benchmarks. Although the overall objective remains the same, the specific methodologies for extracting the benchmark coordinate from the point cloud will change heavily when other types of benchmarks are utilized. As a result, while the proposed method offers a structured approach, the generalization is constrained by the diversity of target types.

To address this limitation from a client perspective, several options can be considered. Firstly, extending the current method to include scripts for the automatic extraction of different target types could enhance its versatility. However, this approach requires additional time and resources for development and implementation. Secondly, opting to have targets extracted and delivered by the subcontractor offers a convenient solution for the client. This approach allows for independent comparison while potentially reducing the burden of method development on the client's end. However, it introduces a reliance on external sources, which impacts project timelines and increases costs. Lastly, the client could express a preference for the type of targets to be used or even impose constraints on available choices. Given the substantial influence and scale of RWS, choices, and requirements can greatly impact practices adopted by others. However, while this approach can lead to standardization and consistency within the industry, it may also introduce limitations, such as overlooking alternative solutions or innovations that could enhance flexibility and adaptability in diverse scenarios.

Feasbility of Indirect Co-registration Benchmarks
Investigate the feasibility of using indirect co-registration benchmarks, such as road markings, for validating absolute accuracy. As presented in Section 2.4.3, road markings can be extracted from point cloud data and can potentially serve as benchmarks for the alignment method. First, evaluate the accuracy of the extraction process. If accuracy levels are within the millimeter range, consider utilizing road markings as validation benchmarks.

6.7 Uncertainty of Benchmark Coordinate Measurement

In the proposed method for validating the absolute accuracy, the RMSE is directly compared with the benchmark coordinate provided by subcontractors or third parties. The approach overlooks a critical factor: the uncertainty inherent in the measurement of the benchmark coordinates. Assuming that benchmark measurements are free of errors is unrealistic. Similar to what is described in Subsection 2.1 about the error budget of laser scanners, the uncertainty in the measurements of the coordinates arises from the precision of the equipment, the calibration of the machine (Franco and Jodar, 2021) (Takamasu et al., 2008), and environmental noise (Mohammadi et al., 2022). Any errors present in the benchmark coordinates will propagate through the analysis, leading to misleading conclusions about the absolute accuracy of the point cloud.

Therefore, the inherent uncertainty associated with benchmark coordinates first needs to be acknowledged and accounted for to ensure a more accurate and complete validation process. The subcontractor should be responsible for conducting such analysis and ensuring it is documented in the quality report. The contractor must specify requirement for the absolute accuracy of the benchmark coordinates and subsequently has the option to independently validate the analysis.

6.8 Relative and Absolute Accuracy Assessment

The study examines only a single surface within one cross-section to evaluate the vertical **relative** accuracy. However, this single surface does not represent the relative accuracy of the entire point cloud; it merely examines the relationship between two scans in a localized area. To assess the overall relative accuracy of a point cloud, multiple surfaces within cross-sections and multiple cross-sections themselves must be taken into account. The findings from the mobile point cloud revealed a systematic deviation that is unfavorable and needs to be addressed to prevent its recurrence.

When assessing the overall **absolute** accuracy of a point cloud, the alignment of all benchmarks must be assessed collectively rather than focusing solely on individual reference points. Similarly, the absolute accuracy is assessed across both the vertical and horizontal components, aligning with common practices documented in the literature and by the subcontractor.

6.9 Requirements of Point Clouds

This final section discusses the previously outlined user requirements for point clouds in Subsection 2.2.3. Some aspects align with the initial descriptions, while others may require further specification based on the results of the proposed method to assess the quality.

6.9.1 Primary (Quality) Requirements

In current specifications, such as the specifications from Rijkswaterstaat as presented in Subsection 2.3.4, the focus is on accuracy rather than quality. In Subsection 2.2.3, the study has shown that quality is influenced by primary components, which additionally include coverage. The additional component of coverage is confirmed by its presence in the quality standards regarding point clouds as in Subsection 2.3.4 and the existing literature in Section 2.4. Therefore, it is advised to shift the focus from accuracy to quality by including the point cloud density.

To enhance clarity for subcontractors, the primary components should be referred to as quality components in the specification. Definitions for coverage, relative accuracy, and absolute accuracy should be explicitly included, ideally using the definitions provided in Subsection 2.3.4. It is also recommended that specifications start with the quality components and then proceed with the secondary components.

Coverage
The point cloud density requirement is discussed in Section 6.3. In conclusion, the point density should be specified as the number of points per area, typically measured in meters (m^2 or m^3). Instead of requiring the point cloud density to be uniform across the entire project area, specify it for each environment (e.g., 3D for tunnel and 2D for road).

All specifications should adopt an acceptance criterion. This criterion should mandate that a minimum percentage of points (e.g., 95%) meet the specified threshold. Additionally, criteria should be defined for the remaining points that do not meet the requirement, specifying a maximum allowable deviation. Table 6.1 presents an example of how the density requirements can be presented.

Density	Requirement	Acceptance criterion	Max allowable deviation
Tunnel	4000 pts/m^3	95% for each tile	5% or 200 pts/m^3
Road	200 pts/m^2	95% for each tile	5% or 10 pts/m^2

Table 6.1. *Example of specification of density requirements*

Relative and Absolute Accuracy
Instead of establishing a single accuracy requirement, it is advisable to define tolerances for vertical (Z) and planimetric (XY) measurements. For the accuracy requirement, random (noise) and systematic errors should each have their own specifications. Additionally, the acceptance criterion and maximum allowable deviation have to be specified. Furthermore, specifications for the coordinate measurements of benchmarks should be established as discussed in Section 6.7. Table 6.2 presents an example of how the relative- and absolute accuracy requirements can be presented.

Accuracy	Requirement xy	Requirement z	Acceptance criterion	Max allowable deviation
Relative	5 mm	5 mm	99%	1σ
Absolute	25 mm	15 mm	99%	1σ
Benchmarks	10 mm	10 mm	99%	1σ

Table 6.2. *Example of specification of accuracy requirements*

Assessment of Quality Components
To assess the quality components, the subcontractor should provide an evaluation that includes (at least) the following:

- Description of scanners and their claimed accuracy: This allows the validation of relative accuracy based on the specifics of the scanner, similar to the details presented in Sections 5.2.1 and 5.2.2.
- Description of the setup: e.g., for static setups, specify the locations and names of the scanners, and for mobile, specify the trajectory of the vehicles.
- Description and validation of the assessment method as presented in Chapter 4 (less detailed).
- Evidence supporting the fulfillment of specified requirements.
- Description of deviations where the requirements were not met.
- Summary of errors and identification of uncertainties observed during the project, including the errors mentioned in Subsection 2.1.

Additionally, the contractor can specify how they will verify these assessments independently and communicate this in the specifications. Such an approach is similar to the AHN, where control measures are specified.

6.9.2 Secondary (General) Requirements

Earlier Subsection 2.2.3 presented the secondary quality components. While this study primarily focused on the primary components, the secondary requirements are also evaluated. The secondary requirements should be referred to as general requirements as they do not directly impact quality.

- *Calibration*: The contractor must demonstrate that the scanner has been calibrated within the past year. Additionally, the contractor should supply specifics of the scanner for proper evaluation, including claimed accuracy numbers.
- *Environmental Impact*: The data should be free from disruptive interference caused by weather and natural conditions (e.g., snow, rain, etc.). Specific requirements can be detailed for other relevant factors affecting measurement conditions (e.g., foliage). Ideally, subcontractors should provide a brief description of the day's conditions during data acquisition in the quality report. Conditions like extreme wind or sunlight can influence scanner performance, which helps explain discrepancies in the point cloud data.
- *Coordinate System*: Specify the desired coordinate system and transformation.
- Noise and outliers: Maximum amount of outliers allowed in the data. Additionally, define in the specifications what is considered an outlier and what is considered noise.
- *Gaps*: Maximum amount of gaps allowed in the data (e.g., no gaps are permitted). Exemptions may be considered in specific circumstances (e.g., occlusion). Additionally, define what qualifies as a gap. In cases involving point clouds with lower densities, gaps may become ambiguous. Also, specify the method for identifying gaps, such as whether visual inspection is sufficient.
- *RGB coloring*: Specify the existence of RGB data and include details on the color encoding scheme and encoder parameters (bit depth).
- *Classifications*: Specify whether the project necessitates point classification. If classification is not required, assign all points as class 0. For projects requiring classification, adhere to the (ASPRS, 2013) LAS 1.4 specifications detailed in Table 6.3.

Value	**Class**
0	Never classified
1	Unclassified
2	Ground
6	Building
7	Noise
9	Water
12	Overlap points
13 - 31	Specific ASPRS definitions

Table 6.3. *ASPRS standard LiDAR point classes according to (ASPRS, 2013)*

Additionally, segmentation could be considered as an option within the classification process. For instance, in the classification of the static point cloud, there has already been segmentation of the tunnel (distinguishing between tunnel walls, top, and bottom as shown in Figure 3.3c), which could be integrated into the classification approach. Furthermore, include how many need to be classified correctly (e.g., 95%). Additionally, specify the methodology or algorithm used for classification.

- *Data removal*: Detail the criteria and method for removing outlying data points. Contractor should deliver the project boundaries to the subcontractor.

Additionally, a section would be added in the general requirements about the specification of the targets as introduced in Section 6.6.

Format Requirements
Considering the handling of large data files, .laz is generally preferred for its ease of use. As discussed in Section 6.5, clients are encouraged to consult the LAS specifications version 1.4 by (ASPRS, 2013). The attributes outlined in the specification are detailed in Table 6.4.

Item	**Item**
X, Y, Z	Return Number
Intensity	Number of Returns
Scan Direction Flag	Edge of Flight Line
Classification	Scan Angle Rank
User Data	Point Source ID
GPS Time	*RGB*
Scanner Channel	

Table 6.4. *ASPRS point data record*
Intensity and RGB are to be specified if required

7 Conclusion and Recommendations

This chapter will conclude the study. In Section 7.1, the research questions from Section 1.2 are answered. Section 7.2 presents recommendations for future research.

7.1 Conclusion

In Section 1.2, the main question for the study was defined as:

> **How to assess the quality of LiDAR point clouds acquired for infrastructure projects?**

The main question will be answered by answering the sub-questions below.

1. *What components contribute to the quality of a point cloud?*

As described in Subsection 2.2.3, primary and secondary factors are specified as requirements for point clouds. **Primary components** significantly influence quality and can alter the type and usage of the point cloud. These include *coverage*, which refers to the distribution of points within the cloud with a common metric density; *absolute accuracy*, which measures how closely point cloud features correspond to true geographic positions; and *relative accuracy*, which measures local differences within a point cloud.

Secondary components exert less influence on overall quality or are unrelated to it, but they remain important to consider. These include *calibration*, *environmental impact*, *coordinate system*, *noise and outliers*, *gaps*, *RGB coloring*, *classifications*, and *data removal*. All these factors must be considered when formulating requirements for a point cloud.

2. *What quality standards are specified during the acquisition of openly available national point cloud datasets?*

Section 2.3 presents quality standards specified during the acquisition of openly available national point cloud datasets. To address the quality standards for national point cloud on the European level, the INSPIRE directive from the European Union is investigated. INSPIRE, relevant to global DTMs, provides technical guidelines on elevation themes, covering completeness (equivalent to data removal), logical consistency (interpreted as relative accuracy on a larger scale), and positional accuracy (other words for absolute accuracy).

In Europe, the Danish Height Model and French Lidar HD use airborne-acquired point clouds, defining quality by relative accuracy (precision in DHM) and accuracy. Similarly, the AHN and Prorail point clouds of the Netherlands specify height and planimetric accuracy, point density, absolute positioning, and relative precision.

Rijkswaterstaat in the Netherlands specifies quality standards for products, including point clouds as source data. The DTB defines accuracy by object recognizability with absolute and relative tolerances, the DTM specifies precision for soft and hard topography, and the DRP details relative accuracy and reliability. Also, RWS has created specifications regarding point clouds where the requirements are categorized into general, accuracy, format, and delivery specifications.

Subsection 2.3.4 provides an overview of the various terms related to point cloud quality. It is observed that the terms are being used interchangeably. Key quality components consistently identified are **relative and absolute accuracy** (often split into height and planimetric aspects) and **density**, with secondary components also frequently mentioned.

3. *What workflow can be used for the assessment of quality components?*

Current relevant literature on the quality assessment of point clouds has been consulted in Section 2.4. For density, assessing point cloud density in 2D is standard practice, with established metrics for assessment. A shift from standard 2D metrics to 3D methods like voxel-based analysis is established. Relative accuracy assessment is done by comparing points within overlapping regions of adjacent scans and varies by laser scanning type (static, mobile, or airborne) due to different capture positions. Absolute accuracy is evaluated by comparing point cloud features to known reference sources such as *direct co-registration benchmarks* (targets) or *in-direct co-registration benchmarks* (features from data such as road markings).

A workflow is developed to assess the point cloud quality based on primary components in Chapter 4. The workflow includes the follow:

- **Coverage Assessment**: The density of points per cell is quantified, followed by the assessment of density requirements. Furthermore, density exploration extends into a partially-3D space, analyzing histograms and cumulative histograms that incorporate cell heights to verify adherence in these dimensions.
- **Relative Accuracy Assessement**: The alignment of points within overlapping regions is utilized to assess relative accuracy. Surfaces within these regions are extracted and compared to evaluate adherence to relative accuracy requirements.
- **Absolute Accuracy Assessment**: Benchmark positions are compared with estimated locations within the point cloud to evaluate absolute accuracy. Coordinates discrepancies indicate alignment levels. Spherical target points are extracted, their center coordinates estimated, and absolute accuracy requirements validated for each sphere.

4. *What variations are present in the outcomes of the quality assessment for infrastructure point clouds acquired through different acquisition methods?*

Chapter 3 introduced the PTZ project used in this study. The data for the PTZ project is acquired with static, mobile, and airborne methods, each producing a point cloud.

The coverage assessment of point clouds from static, mobile, and airborne methods revealed varying quality outcomes. A specific density requirement was set for the static dataset, allowing for compliance evaluation. In the 2D analysis, it was found that the densities did not comply with the requirement, with 48.4% of the total point cloud falling short. In 3D, particularly with tunnel tiles, while overall compliance was observed, individual 1-meter segments often fell short. Mobile and airborne datasets lacked specific density requirements. The 3D analysis results for the mobile and airborne datasets showed similar behavior to those of flat road surfaces in static datasets, suggesting limited additional insights due to limited height variations. These findings highlight the need for tailored quality standards: static datasets benefit from detailed 3D analysis in complex environments like tunnels, whereas mobile and airborne datasets, with minimal height variations, are effectively evaluated in 2D.

Relative accuracy assessment was conducted for static and mobile datasets in the PTZ project, excluding the airborne dataset due to time constraints. For static point clouds, a 30-centimeter strip extracted from overlapping regions sufficed given their high density. The RMSE values derived from plane-fitted distances adhered to scanner specifications, resulting in 99.1% to 99.7% of points falling within the required relative accuracy tolerances. On the other hand, mobile scans presented challenges stemming from their lower density, which led to higher RMSE values and slightly lower compliance percentages. To accommodate this, mobile point clouds were evaluated using 50-centimeter strips. Despite observing a systematic deviation of approximately 2 mm, the mobile datasets generally met relative accuracy requirements. RMSE values remained within acceptable limits according to manufacturer standards. As a result, 4.3% to 7.0% of points exceed specified tolerances, indicating slightly higher variability than static scans.

The absolute accuracy assessment was exclusively conducted on the static-derived composite point cloud of the PTZ project, utilizing the alignment of spherical benchmarks. The benchmarks were extracted using a multi-step process involving spatial, intensity, clustering, and curvature filters. In estimating the sphere centers RANSAC effectively removed outliers, and although LS fitting overfitted by a few millimeters, centralized RMSE adjustment corrected this, yielding accurate RMSE values. All final RMSE values for benchmarks were close to 1 mm, with the largest being 1.36 mm. The static dataset met the absolute accuracy requirements, with discrepancies under 6 mm in the XY-direction and a maximum deviation of 1.78 mm in the Z-direction.

5. *How should the requirements be specified for point clouds to validate the quality?*

As discussed in Section 6.9, distinguish the requirements for points clouds between primary (quality) and secondary (general) to ensure clarity and focus in specifications.

For **primary (quality) requirements**, the focus should be on coverage, relative- and absolute accuracy. Point density should be defined in accordance with the environment, such as 3D for tunnels and 2D for roads, with clear acceptance criteria and allowable deviations. For accuracy, separate tolerances for vertical (Z) and planimetric (XY) should be used. Clear acceptance criteria and maximum deviations need to be specified.

Specify the **secondary (general) requirements** including the calibration, environmental impact, coordinate system, noise and outliers, gaps, RGB coloring, classifications, and data removal. It is recommended that clients refer to the LAS specifications version 1.4 of the ASPRS for the attributes.

7.2 Recommendations

Shift from Coverage to Consistency

To enhance the quality of point clouds, it is recommended to shift the focus from merely assessing coverage to ensuring consistency. This involves an additional assessment of whether objects or environments are scanned from multiple perspectives. Thus, develop and standardize metrics that quantify consistency, going beyond the basic measure of coverage and point cloud density.

Requirements

Building upon specifications such as those from Rijkswaterstaat, as presented in Subsection 2.3.4, the following enhancements are recommended:

- Focus on quality rather than accuracy by incorporating point cloud density as a requirement.
- Define point density separately for different environments (e.g., 3D for tunnels, 2D for roads). To achieve this, it is recommended to explore specific density and dimensional requirements based on application needs and feasibility, as discussed in Section 6.3.
- Establish tolerances for vertical (Z) and planimetric (XY) measurements. Include clear acceptance criteria and maximum allowable deviations for all requirements. Specify accuracy standards for benchmark coordinate measurements.
- Require subcontractors to provide a detailed quality assessment, including methods, evidence, error summaries, uncertainties, and deviations from requirements.
- Specify adherence to ASPRS LAS 1.4 standards.

Point Cloud Density

To address runtime inefficiencies, optimize the point cloud density method by refining the Python code, as discussed in Section 6.1. Explore strategies such as organizing point clouds into octrees, thinning data selectively, or terminating processing upon meeting specified requirements. Investigate the use of dynamic density assessment, for instance by adopting a slider for assessing flexible requirements. As detailed in Section 6.2, incorporate an adaptive grid system that dynamically adjusts cell sizes based on point density near borders. Additionally, consider adopting voxel-based analysis methods for comprehensive 3D density assessments (Section 6.3).

Overlapping Regions Alignment

Automate and enhance the assessment of relative accuracy requirements (Section 6.4). Investigate alternatives to plane representations, such as B-splines, for aligning overlapping regions. Implement automated detection of overlapping regions, employ region-based segmentation for surface selection, and analyze multiple planes within cross-sections to improve alignment accuracy.

Benchmark Alignment

In Section 6.6, several strategies are presented to generalize benchmark alignment methods. The options are (1) extend the current method to automatically extract additional target types, (2) consider having targets extracted and provided by subcontractors or (3) specify constraints for the types of targets used. It is recommended that contractors internally discuss these options, considering the advantages and challenges outlined in the section, to assess feasibility effectively.

Additionally, explore the feasibility of using indirect benchmarks like road markings for absolute accuracy validation. If accuracy levels are within the millimeter range, consider utilizing road markings as validation benchmarks. Develop a validation process to automatically verify benchmark coordinate measurements (Section 6.7).

Bibliography

AHN. (2023a). *Besteksvoorwaarden inwinning landsdekkende dataset AHN2023-2025* (tech. rep.).

AHN. (2023b). *Kwaliteitsbeschrijving*. https://www.ahn.nl/kwaliteitsbeschrijving

Alhasan, A., Younkin, K., White, D. J., et al. (2015). *Comparison of roadway roughness derived from LIDAR and SFM 3D point clouds.* Iowa State University. Institute for Transportation. https://rosap.ntl.bts.gov/view/dot/29591

Altyntsev, M. (2022). Relative Adjustment of Mobile Laser Scanning Data in Different Scenes. *ISPRS Annals of the Photogrammetry, Remote Sensing and Spatial Information Sciences*, *1*, 111–120. https://isprs-annals.copernicus.org/articles/V-1-2022/111/2022/

ASPRS. (2013, July). *LAS specification version 1.4 – R13*. https://www.asprs.org/wp-content/uploads/2010/12/LAS_1_4_r13.pdf

ASPRS. (2015). ASPRS positional accuracy standards for digital geospatial data. *American Society for Photogrammetry and Remote Sensing*, *81*(3), 1–26. https://doi.org/10.14358/PERS.81.3.A1-A26

Benedek, C., Majdik, A., Nagy, B., Rozsa, Z., & Sziranyi, T. (2021). Positioning and perception in LIDAR point clouds. *Digital Signal Processing*, *119*, 103193. https://doi.org/10.1016/j.dsp.2021.103193

Christodoulides, C., & Christodoulides, G. (2017). Measurement errors. In *Analysis and presentation of experimental results: With examples, problems and programs* (pp. 39–56). Springer International Publishing. https://doi.org/10.1007/978-3-319-53345-2_2

CloudCompare. (2015, October). *Cloud-to-cloud distance*. https://www.cloudcompare.org/doc/wiki/index.php/Cloud-to-Cloud_Distance

CloudCompare. (2022, February). *Density*. https://www.cloudcompare.org/doc/wiki/index.php/Density

Dai, F., Rashidi, A., Brilakis, I., & Vela, P. (2013). Comparison of image-based and time-of-flight-based technologies for three-dimensional reconstruction of infrastructure. *Journal of construction engineering and management*, *139*(1), 69–79. https://doi.org/10.1061/(ASCE)CO.1943-7862.0000565

Danish Agency for Data Supply and Efficiency. (2020). *DHM product specification v1.0.0*. https://dataforsyningen.dk/asset/PDF/produkt_dokumentation/dhm-prodspec-v1.0.0.pdf

Danish Agency for Data Supply and Efficiency. (2022). *The Danish Elevation Model (DK-DEM)*. https://eng.sdfi.dk/data/the-danish-elevation-model-dk-dem

Department of Transport and Main Roads State of Queensland. (2023, March). *Mobile Laser Scanning Technical Guideline*. www.tmr.qld.gov.au/-/media/busind/

techstdpubs/Surveying/Surveying-support-documents/MLS-Guideline/MLSGuideline.pdf

Dewberry. (2022, February). *Puerto Rico and US Virgin Islands Topobathy Final Report of Survey*. https://noaa-nos-coastal-lidar-pds.s3.amazonaws.com/laz/geoid18/9390/supplemental/PR1801_VI1801_TB_C_Topobathy_Lidar_Project_Report_Final.pdf

Edelsbrunner, H., Kirkpatrick, D., & Seidel, R. (1983). On the shape of a set of points in the plane. *IEEE Transactions on information theory*, *29*(4), 551–559. https://doi.org/10.1109/TIT.1983.1056714

Elaksher, A., Ali, T., & Alharthy, A. (2023). A Quantitative Assessment of LIDAR Data Accuracy. *Remote Sensing*, *15*(2). https://doi.org/10.3390/rs15020442

El-Halawany, S., Moussa, A., Lichti, D. D., & El-Sheimy, N. (2012). Detection of road curb from mobile terrestrial laser scanner point cloud. *The International Archives of the Photogrammetry, Remote Sensing and Spatial Information Sciences*, *38*, 109–114. https://doi.org/10.5194/isprsarchives-XXXVIII-5-W12-109-2011

Forbes, A. B. (1989). *Robust circle and sphere fitting by least squares*. National Physical Laboratory Teddington.

Franco, P., & Jodar, J. (2021). Theoretical analysis of straightness errors in coordinate measuring machines (CMM) with three linear axes. *International Journal of Precision Engineering and Manufacturing*, *22*, 63–72. https://doi.org/10.1007/s12541-019-00264-0

Gargoum, S. A., & El-Basyouny, K. (2022). Impacts of point cloud density reductions on extracting road geometric features from mobile LiDAR data. *Canadian Journal of Civil Engineering*, *49*(6), 910–924. https://doi.org/10.1139/cjce-2020-0193

Harvey, L., & Green, D. (1993). Defining quality. *Assessment & Evaluation in Higher Education*, *18*(1), 9–34. https://doi.org/10.1080/0260293930180102

Hinks, T., Carr, H., Truong-Hong, L., & Laefer, D. F. (2013). Point cloud data conversion into solid models via point-based voxelization. *Journal of Surveying Engineering*, *139*(2), 72–83. https://doi.org/10.1061/(ASCE)SU.1943-5428.0000097

Hofmann, S., & Brenner, C. (2016). Accuracy assessment of mobile mapping point clouds using the existing environment as terrestrial reference. *The International Archives of the Photogrammetry, Remote Sensing and Spatial Information Sciences; XLI-B1*, *41*, 601–608. https://doi.org/10.5194/isprs-archives-XLI-B1-601-2016

Huang, R., Zheng, S., & Hu, K. (2018). Registration of Aerial Optical Images with LiDAR Data Using the Closest Point Principle and Collinearity Equations. *Sensors*, *18*(6). https://doi.org/10.3390/s18061770

IGN. (2023, October). *LiDAR HD- Descriptif de contenu*. IGN Institut national de l'information géographique et forestière. https://geoservices.ign.fr/sites/default/files/2023-10/DC_LiDAR_HD_1-0_PTS.pdf

INSPIRE. (2024, January). *D2.8.II.1 Data Specification on Elevation – Technical Guidelines*. INSPIRE Maintenance and Implementation Group (MIG). https://knowledge-base.inspire.ec.europa.eu/publications/inspire-data-specification-elevation-technical-guidelines_en

Kaltofen, E., & Villard, G. (2004). Computing the sign or the value of the determinant of an integer matrix, a complexity survey [Proceedings of the International Conference on Linear Algebra and Arithmetic 2001]. *Journal of Computational and Applied Mathematics*, *162*(1), 133–146. https://doi.org/10.1016/j.cam.2003.08.019

Kalvoda, P., Nosek, J., Kuruc, M., & Volarik, T. (2020). Accuracy Evaluation and Comparison of Mobile Laser Scanning and Mobile Photogrammetry Data. *IOP Conference Series: Earth and Environmental Science; IOP Publishing: Bristol, UK*. https://doi.org/10.1088/1755-1315/609/1/012091

Kim, M., Stoker, J., Irwin, J., Danielson, J., & Park, S. (2022). Absolute Accuracy Assessment of Lidar Point Cloud Using Amorphous Objects. *Remote Sensing*, *14*(19). https://doi.org/10.3390/rs14194767

Kjorsvik, N. (2022). *Mathematical and statistical modelling in multi-sensor mapping systems*. Terratec AS.

Kodors, S. (2017). Point Distribution as True Quality of LiDAR Point Cloud. *Baltic Journal of Modern Computing*, *5*(4). https://doi.org/10.22364/bjmc.2017.5.4.03

Kregar, K., Grigillo, D., & Kogoj, D. (2013). High precision target center determination from a point cloud. *ISPRS annals of the photogrammetry, remote sensing and spatial information sciences*, *2*, 139–144. https://doi.org/10.5194/isprsannals-II-5-W2-139-2013

Latypov, D. (2002). Estimating relative lidar accuracy information from overlapping flight lines. *ISPRS Journal of Photogrammetry and Remote Sensing*, *56*(4), 236–245. https://doi.org/10.1016/S0924-2716(02)00047-3

Leica. (n.d.). *Leica CityMapper-2*. https://leica-geosystems.com/nl-nl/products/airborne-systems/hybrid-sensors/leica-citymapper-2

Lemmens, M. (2011). Terrestrial Laser Scanning. In *Geo-information: Technologies, applications and the environment* (pp. 101–121). Springer Netherlands. https://doi.org/10.1007/978-94-007-1667-4_6

Lindenbergh, R., Pfeifer, N., & Rabbani, T. (2005). Accuracy analysis of the Leica HDS3000 and feasibility of tunnel deformation monitoring. *Proceedings of the ISPRS Workshop, Laser scanning*, *36*, 3.

Martínez Sánchez, J., Fernández Rivera, F., Cabaleiro Domínguez, J. C., López Vilariño, D., & Fernández Pena, T. (2020). Automatic Extraction of Road Points from Airborne LiDAR Based on Bidirectional Skewness Balancing. *Remote Sensing*, *12*(12). https://doi.org/10.3390/rs12122025

Meinderts, J. P., Lindenbergh, R., van der Heide, D. H., Amiri-Simkooei, A., & Truong-Hong, L. (2022). Clearance measurement validation for highway infrastructure with use of lidar point clouds. *The International Archives of the Photogrammetry, Remote Sensing and Spatial Information Sciences*, *XLVIII-2/W2-2022*, 69–76. https://doi.org/10.5194/isprs-archives-XLVIII-2-W2-2022-69-2022

Mineo, C., Pierce, S. G., & Summan, R. (2019). Novel algorithms for 3D surface point cloud boundary detection and edge reconstruction. *Journal of Computational Design and Engineering*, *6*(1), 81–91. https://doi.org/10.1016/j.jcde.2018.02.001

Mohammadi, F., Mirhashemi, M., & Rashidzadeh, R. (2022). A coordinate measuring machine with error compensation in feature measurement: Model development and experimental verification. *The International Journal of Advanced Manufacturing Technology*, 1–11. https://doi.org/10.1007/s00170-021-08362-y

Njambi, R. (2021). *LiDAR accuracy, explained—and when to use stereo satellite imagery for elevation modeling*. https://up42.com/blog/lidar-accuracy-explained-and-when-to-use-stereo-satellite-imagery

Pan, Y., Yang, B., Li, S., Yang, H., Dong, Z., & Yang, X. (2019). Automatic road markings extraction, classification and vectorization from mobile laser scanning data. *The International Archives of the Photogrammetry, Remote Sensing and Spatial Information*

Sciences, *42*, 1089–1096. https://doi.org/10.5194/isprs-archives-XLII-2-W13-1089-2019

Prorail. (2017). *Bijlage b - bestek inwinning terreinopnamen* (tech. rep.).

Prorail. (2022). *Het spoorwegnet tot in de puntjes in beeld*. https://www.prorail.nl/nieuws/spoorinbeeld-het-spoorwegnet-tot-in-de-puntjes-in-beeld

Rebolj, D., Pučko, Z., Babič, N. Č., Bizjak, M., & Mongus, D. (2017). Point cloud quality requirements for Scan-vs-BIM based automated construction progress monitoring. *Automation in Construction*, *84*, 323–334. https://doi.org/10.1016/j.autcon.2017.09.021

Riegl. (2015). *Riegl VMX-450*. http://www.riegl.com/uploads/tx_pxpriegldownloads/DataSheet_VMX-450_2015-03-19.pdf

Rijkswaterstaat. (n.d.-a). *Data en Informatievoorziening - Voorspelbaar, veilig en betrouwbaar dankzij data*. https://rwsinnoveert.nl/focuspunten/data-iv/

Rijkswaterstaat. (n.d.-b). *Drechttunnel (A16)*. https://www.rijkswaterstaat.nl/wegen/wegenoverzicht/a16/drechttunnel-a16

Rijkswaterstaat. (2020, November). *Projectspecificatie 3D - Het maken van 3D scans, KL grondradar onderzoek, het vervaardigen van 3D modellen en het verwerken van civiele areaal gegevens in de 3D modellen ten behoeve van de planfase van Project Tunnelrenovatie Zuid-Holland (PTZ).* (tech. rep.).

Rijkswaterstaat. (2021). *Productspecificaties Digitaal Terrein Model (DTM)*. https://standaarden.rws.nl/link/standaard/6068

Rijkswaterstaat. (2022a). *Productspecificaties Digitaal Topografisch Bestand (DTB)*. https://standaarden.rws.nl/link/standaard/6058

Rijkswaterstaat. (2022b). *Productspecificaties Doorrijprofielen*. https://standaarden.rws.nl/link/standaard/6067

Rijkswaterstaat. (2023). *Productspecificaties puntenwolken* (tech. rep.).

Rijkswaterstaat. (2024). *Tunnelrenovaties in Zuid-Holland*. https://www.rijkswaterstaat.nl/wegen/projectenoverzicht/tunnelrenovaties-in-zuid-holland

Rijkswaterstaat CIV. (2023, September). *Nota het nationaal 3d geo-datafundament*. Geo overleg RWS.

Soudarissanane, S. (2016, January). *The geometry of terrestrial laser scanning; identification of errors, modeling and mitigation of scanning geometry* [Doctoral dissertation]. Delft University of Technology; Geoscience and Remote Sensing Department. https://doi.org/10.4233/uuid:b7ae0bd3-23b8-4a8a-9b7d-5e494ebb54e5

Soudarissanane, S., Ree, J., Bucksch, A., & Lindenbergh, R. (2007). Error budget of terrestrial laser scanning: Influence of the incidence angle on the scan quality. https://doi.org/10.13140/RG.2.1.1877.6404

Stanley, M. H., & Laefer, D. F. (2021). Metrics for aerial, urban lidar point clouds. *ISPRS Journal of Photogrammetry and Remote Sensing*, *175*, 268–281. https://doi.org/10.1016/j.isprsjprs.2021.01.010

Takamasu, K., Takahashi, S., Abbe, M., & Furutani, R. (2008). Uncertainty estimation for coordinate metrology with effects of calibration and form deviation in strategy of measurement. *Measurement Science and Technology*, *19*(8), 084001. https://doi.org/10.1088/0957-0233/19/8/084001

Tiberius, C. C., Van der Marel, H., Reudink, R., & van Leijen, F. (2021). *Surveying and Mapping*. TU Delft Open. https://doi.org/10.5074/T.2021.007

Toschi, I., Remondino, F., Rothe, R., & Klimek, K. (2018). Combining airborne oblique camera and lidar sensors: Investigation and new perspectives. *The International*

Archives of the Photogrammetry, Remote Sensing and Spatial Information Sciences, *42*, 437–444.

Trimle. (n.d.). *Trimble TX8 Laser scanner*. https://www.laserscanning-europe.com/sites/default/files/redakteur_images/Data_sheet_Trimble_TX8.pdf

Truong-Hong, L., & Lindenbergh, R. (2022). Automatically extracting surfaces of reinforced concrete bridges from terrestrial laser scanning point clouds. *Automation in Construction*, *135*, 104127. https://doi.org/10.1016/j.autcon.2021.104127

van der Heide, D., van Natijne, A., Alkemade, I., & Hulskemper, D. (2024). *WP1: Inventarisatie van puntenwolken in Nederland* (tech. rep.). Rijkswaterstaat, Het Waterschapshuis, Kadaster TU Delft.

Vo, A.-V., Truong-Hong, L., Laefer, D. F., & Bertolotto, M. (2015). Octree-based region growing for point cloud segmentation. *ISPRS Journal of Photogrammetry and Remote Sensing*, *104*, 88–100. https://doi.org/10.1016/j.isprsjprs.2015.01.011

Vosselman, G., & Maas, H.-G. (2010). *Airborne and terrestrial laser scanning*. CRC Press (Taylor & Francis).

Wang, Q., Tan, Y., & Mei, Z. (2020). Computational Methods of Acquisition and Processing of 3D Point Cloud Data for Construction Applications. *Archives of Computational Methods in Engineering*, *27*, 479–499. https://doi.org/10.1007/s11831-019-09320-4

Wang, Y., Li, X., Zhao, F., Jin, Z., Tang, Y., & Zhao, H. (2024). Design of point cloud data structures for efficient processing of large-scale point clouds. *International Conference on Optical and Photonic Engineering (icOPEN 2023)*, *13069*, 85–98. https://doi.org/10.1109/ICAT.2011.6102102

Wang, Y., Cheng, L., Chen, Y., Wu, Y., & Li, M. (2016). Building Point Detection from Vehicle-Borne LiDAR Data Based on Voxel Group and Horizontal Hollow Analysis. *Remote Sensing*, *8*(5). https://doi.org/10.3390/rs8050419

Winiwarter, L., Anders, K., & Höfle, B. (2021). M3C2-EP: Pushing the limits of 3D topographic point cloud change detection by error propagation. *ISPRS Journal of Photogrammetry and Remote Sensing*, *178*, 240–258. https://doi.org/10.1016/j.isprsjprs.2021.06.011

Wu, J., Yao, W., Chi, W., & Zhao, X. (2011). Comprehensive quality evaluation of airborne lidar data. *International Symposium on Lidar and Radar Mapping 2011: Technologies and Applications*, *8286*, 30–37. https://doi.org/10.1117/12.912588

Yang, R., Li, Q., Tan, J., Li, S., & Chen, X. (2020). Accurate road marking detection from noisy point clouds acquired by low-cost mobile lidar systems. *ISPRS International Journal of Geo-Information*, *9*(10). https://doi.org/10.3390/ijgi9100608

Yu, Y., Guan, H., & Mi, W. (2015). Automated Detection of Urban Road Manhole Covers Using Mobile Laser Scanning Data. *IEEE Transactions on Intelligent Transportation Systems*, *16*, 1–12. https://doi.org/10.1109/TITS.2015.2413812

Yuwen, S., Dongming, G., Zhenyuan, J., & Weijun, L. (2005). B-spline surface reconstruction and direct slicing from point clouds. *Int J Adv Manuf Technol*, *27*, 918–924. https://doi.org/10.1007/s00170-004-2281-6

Zhang, Y., Li, C., Guo, B., Guo, C., & Zhang, S. (2021). KDD: A kernel density based descriptor for 3D point clouds. *Pattern Recognition*, *111*, 107691. https://doi.org/10.1016/j.patcog.2020.107691

Zhou, H., Feng, Y., Fang, M., Wei, M., Qin, J., & Lu, T. (2021). Adaptive graph convolution for point cloud analysis. *Proceedings of the IEEE/CVF international conference on computer vision*, 4965–4974. https://doi.org/10.48550/arXiv.2108.08035

Zhu, J., Li, H., Wang, S., Wang, Z., & Zhang, T. (2023). i-Octree: A Fast, Lightweight, and Dynamic Octree for Proximity Search. *arXiv preprint arXiv:2309.08315*. https://doi.org/10.48550/arXiv.2309.08315

For the purpose of this study, ChatGPT (OpenAI, 2023) was employed to enhance the clarity of the research writing.